ENERGY TRANSFER AND MECHANISM OF CAROTENOID TRIPLET FORMATION / EFFECTS OF MAGNETIC FIELDS. H. KINGMA

# REDOX STATES OF THE REACTION CENTER IN RELATION TO ENERGY TRANSFER AND MECHANISM OF CAROTENOID TRIPLET FORMATION IN PHOTOSYNTHETIC BACTERIA.

## EFFECTS OF MAGNETIC FIELDS

H. Kingma

# REDOX STATES OF THE REACTION CENTER IN RELATION TO ENERGY TRANSFER AND MECHANISM OF CAROTENOID TRIPLET FORMATION IN PHOTOSYNTHETIC BACTERIA.

## EFFECTS OF MAGNETIC FIELDS

# REDOX STATES OF THE REACTION CENTER IN RELATION TO ENERGY TRANSFER AND MECHANISM OF CAROTENOID TRIPLET FORMATION IN PHOTOSYNTHETIC BACTERIA.

## EFFECTS OF MAGNETIC FIELDS

**Proefschrift** ter verkrijging van de graad
van Doctor in de Wiskunde en Natuurwetenschappen
aan de Rijksuniversiteit te Leiden, op gezag
van de Rector Magnificus Dr. A.A.H. Kassenaar,
Hoogleraar in de faculteit der Geneeskunde,
volgens besluit van het College van Dekanen te
verdedigen op woensdag 7 december 1983 te klokke
14.15 uur

door

**Hermanus Kingma**

geboren te Rotterdam in 1950.

Druk: NKB Offset bv - Leiden

PROMOTIECOMMISSIE:

| | |
|---|---|
| Promotor | : Prof. Dr. L.N.M. Duysens |
| Referent | : Dr. R. van Grondelle |
| Overige commissieleden | : Prof. dr. J.H. van der Waals |
| | Prof. dr. J. Schmidt |
| | Prof. Dr. L.H. van der Tweel |



Wie denkt dat hij het gevonden heeft,
ja, die heeft het pas echt verloren.

REMCO CAMPERT

*Voor Anneke*

*Voor mijn ouders*

CONTENTS

CHAPTER III has been published in Photosynthesis (Akoyunoglou, G., ed.), Vol. III, 981-988, Balaban Int. Science Services, Philadelphia, Pa.
CHAPTER VI has been accepted for publication in Biochim. Biophys. Acta.



# INTRODUCTION

## General

Photosynthesis is the process in plants and several bacteria, through which light energy absorbed by the photosynthetic pigments, such as chlorophylls and carotenoids, is converted into chemical energy and stored in organic substrates, that serve as energy sources for all life processes. The atmospheric oxygen, used for the most important and apparent bioenergetic process, respiration, is also produced by plant photosynthesis

In the following I shall focus on the photosynthetic apparatus in several photosynthetic bacteria. For a more detailed introduction to the early excitation energy and electron transfer processes, the reader is referred to the introductions of Chapter III, IV, V and VI.

The photosynthetic apparatus of the purple bacteria Rhodospirillum rubrum and Rhodopseudomonas sphaeroides is situated in the invaginations of the cytoplasmic membrane [1]. In these "chromatophores", which can be isolated from whole cells by disruption, both a so-called antenna, which consists of an assembly of photosynthetic pigments non-covalently bound to proteins, and reaction centers, where the primary photochemistry occurs are present. The antenna system consists, depending on the bacterial strain, mostly of 40 - 200 bacteriochlorophyll molecules [1 - 8] and a somewhat smaller number of carotenoid molecules per reaction center; 10-20 of these photosynthetic units form a "domain" [9,10]. In R. rubrum only one antenna bacteriochlorophyll species is present (B880), whereas in Rps. sphaeroides three antenna bacteriochlorophyll species can be distinguished (B800, B850 and B880). After absorption of a light quantum by the antenna molecules, the excitation energy is transferred to the reaction center, which can be considered as the smallest entity which is capable of performing primary photochemistry. During the transfer process the singlet excitation energy may be lost by fluorescence, intersystem crossing to a lower lying triplet state or internal conversion. The reaction center protein, where

the primary photochemical reaction, a charge separation takes place, contains four molecules of bacteriochlorophyll a, two molecules of bacteriopheophytin a, one carotenoid molecule and an iron-quinone complex [1,11-13]. Two of the bacteriochlorophyll molecules form a dimer P880, whereas the two other molecules are monomers and both are designated as P800. The charge separation involves electron transfer from P880 to one of the bacteriopheophytins (I) within less than 5 ps. One of the P800 molecules may participate during the first few ps in the primary electron transport process. although its role has not been established unambiguously[14-23].
The reaction center protein can be separated from the membrane using detergents. This complex remains photochemically active, although the electron transport towards a secondary quinone electron acceptor is often inhibited. Several light harvesting complexes have been isolated and are designated as the B800/850, the B850 and the B880 complex. All these isolated antenna and reaction center pigment complexes have been characterized by a variety of biochemical and spectroscopic methods [1,2,23-27].

In the green bacterium Prostecochloris aestuarii no extensive membrane structure is present to incorporate the photosynthetic apparatus. Instead, the antenna complex which contains about 1500 bacteriochlorophyll c, 80 bacteriochlorophyll a and several carotenoid molecules per reaction center, is located in chlorosomes, oblong bodies of about 30 x 100 nm, appressed to the innerside of the cell membrane [1,28]. The reaction center is situated in the cytoplasmic membrane [29,30]. The smallest photoactive reaction center preparation that has been isolated, the so-called RCPP complex, contains about 35 bacteriochlorophyll a molecules, 4-6 bacteriopheophytin molecules, several carotenoid molecules and one photo-oxidizable cytochrome c-553 per reaction center [30-35]. After absorption of a light quantum by the antenna complex, mainly bacteriochlorophyll c, the excitation energy is transferred to the reaction centers via the antenna-bacteriochlorophyll a molecules, which are arranged in a crystalline-like baseplate situated between the chlorosome and the cytoplasmic membrane [1,29,35-37].



This work

The effectsof a magnetic field on the bacteriochlorophyll emission yield and the bacteriochlorophyll or carotenoid triplet yield have been studied to gain more insight in the mechanisms of triplet formation and energy transfer in both the reaction center and the antenna complex. A long time ago [38,39] it was observed that in several species of purple bacteria only 30 - 50% of the light energy absorbed is transferred to bacteriochlorophyll and used for "normal photosynthesis". Up to now, very little is known about the function of the remaining energy. By following the paths of energy flow, I tried to find an answer to this question.

In addition, a number of early studies [40-44] , dealing with the magnetic field effects in various photosynthetic preparations, showed conflicting results with respect to the magnitude of the effectsand exact magnetic field dependencies as a function of the preparation, the temperature and the redox state of the reaction center, and therefore a more detailed study of these phenomena was needed.

In Chapter III I describe the magnetic field induced emission changes (MFE) as a function of the redox state of the reaction center by applying various redox-compounds.

In Chapter IV I have extended the study of the MFE, and measured the emission and excitation spectra and in addition the temperature dependence of the MFE.

In Chapter V I have studied the process of triplet formation, which is partly related to the MFE.

In Chapter VI I studied the MFE as a function of the fraction of reaction centers in a specific redox state in order to gain insight in the type of energy transfer processes between reaction centers in a quantitative way and moreover, to obtain a new method to determine the fractions of the reaction centers in a specific redox state under various steady state conditions.

REFERENCES


1. Clayton, R.K. and Sistrom, W.R. (1978) The Photosynthetic Bacteria, Plenum Press, New York
2. Olson, J.M. and Thornber, J.P. (1979) in Membrane Proteins in Energy Transduction (Capaldi, R.A., ed.), pp. 279-340, Marcel Dekker, New York
3. Jensen, S.L., Cohen-Bazire, G., Nakayoma, T.O.M. and Stanier, R.Y. (1958) Biochim.Biophys. Acta 29, 477-498
4. Aagard, J. and Sistrom, W.R. (1972) Photochem. Photobiol. 15, 209-225
5. Clayton, R.K. and Clayton, B.J. (1972) Biochim.Biophys. Acta 283, 492-504
6. Slooten, L. (1973) Thesis, University of Leiden.
7. Richards, W.R., Wallace, B.R., Tsao, M.S. and Ho, E., (1975) Biochemistry 14, 5554-5561
8. Feick, R. and Drews , G. (1978) Biochim. Biophys. Acta 501, 499-513.
9. Den Hollander, W.Th.F., Bakker, J.G.C. and van Grondelle, R., (1983), in the press
10. Bakker, J.G.C., van Grondelle, R. and den Hollander, W.Th.F., (1983), in the press
11. Straley, S.C., Parson, W.W., Mauzerall, D. and Clayton, R.K. (1973) Biochim. Biophys. Acta 305, 597-609
12. Prince, R.C., Cogdell, R.J. and Crofts, A.R. (1974) Biochim. Biophys. Acta 347, 1-13
13. Vermeglio, A. and Clayton, R.K. (1976) Biochim. Biophys. Acta 449, 500-515
14. Dutton P.L., Kaufmann, K.J., Chance, B. and Rentzepis, P.M. (1975) FEBS Letters 60, 275-280
15. Rockley, M.G., Windsor, M.W., Cogdell, R.J. and Parson, W.W. (1975) Proc. Natl. Acad. Sci. U.S. 72, 2251-2255
16. Parson, W.W., Clayton, R.K. and Cogdell, R.J. (1975) Biochim. Biophys. Acta 387, 265-278
17. Holten, D., Hoganson, C., Windsor, M.W., Schenk, C.C., Parson, W.W., Migus, A., Fork, R.L. and Shank C.V. (1980) Biochim. Biophys. Acta 592, 461-477





18. Shuvalov, V.A., Klevanik, A.V., Sharkov, A.V.,Matveetz , Yu.A. and Krukov, P.G. (1978) FEBS Lett. 91, 135-139
19. Shuvalov, V.A. and Parson, W.W. (1981) Proc. Natl. Acad. Sci. U.S.A.
20. Van Grondelle, R. (1978) Thesis, University of Leiden
21. Van Bochove, A.C.,van Grondelle, R., Hof, R.M. and Duysens, L.N.M. (1983) Proc. VIth Int. Congr. Photosynth. Brussels.
22. Shuvalov, V.A. (1983), proceedings of the VIth Int. Congr. Photosynth. Brussels, in the press
23. Reed, P.W. and Clayton, R.K. (1968) Biochim. Biophys. Res. Comm. 30, 471-475
24. Gingras, G. and Jolchine, G. (1969) Proc. Int. Congr. of Photosynth. Res. (H. Mentzner ed.), Vol. 1, 209-216 Freudenstadt
25. Feher, G. (1971) Photochem. Photobiol. 14, 373,387
26. Slooten, L. (1972) Biochim. Biophys. Acta 256, 452-466
27. Romijn, J.C. and Amesz, J. (1977) Biochim. Biophys. Acta 461, 327-330
28. Staehelin, A., Golecki, J.R., Fuller, R.C. and Drews, G. (1978) Arch. Microbiol. 119, 269-277
29. Olson, J.M. and Romano, C.A. (1962) Biochim. Biophys. Acta 59, 728-730
30. Swarthoff, T. (1982) Thesis, University of Leiden
31. Swarthoff, T. and Amesz, J. (1979) Biochim. Biophys. Acta 548, 427-432
32. Olson, J.M., Philipson, K.D. and Sauer, K. (1973) Biochim. Biophys. Acta 292, 206-217
33. Olson, J.M., Prince, R.C. and Brune, D.C. (1977) Brookhaven Symp. Biol. 28, 238-246
34. Swarthoff, T.,van der Veek-Horsley, K.M. and Amesz, J. (1981) Biochim. Biophys. Acta 635, 1-12
35. Olson, J.M. (1966) in The Chlorphylls (Vernon, L.P. and Seely, G.R., eds.) pp 413-425, Academic Press, New York, London
36. Thornber, J.P. and Olson, J.M. (1968) Biochemistry 7, 2242-2249
37. Olson, J.M., Koenig, D.F. and Ledbetter, M.C. (1969) Arch. Biochem. Biophys. 129, 42-48

38. Duysens, L.N.M. (1951) Nature 168, 548
39. Duysens, L.N.M. (1952) Thesis, University of Utrecht
40. Blankenship, R.E., Schaafsma, T.J. and Parson, W.W. (1977) Biochim. Biophys. Acta 461, 297-305
41. Hoff, A.J., Rademaker, H., van Grondelle, R. and Duysens, L.N.M. (1977) Biochim. Biophys. Acta 460, 547-554
42. Rademaker, H., Hoff, A.J., van Grondelle, R. and Duysens, L.N.M. (1980) Biochim. Biophys. Acta 592, 240-257
43. Voznyak, W.M., Jelfimov, J.I. and Proskuryakov, I.I. (1978) Doklady Akad. Nauk. 242, 1200-1203
44. Rademaker, H. (1980) Thesis, University of Leiden.



## MATERIALS AND METHODS

### Bacterial cultures

Table 1 shows the various species and the type of preparations of the photosynthetic bacteria used for the experiments described in this thesis.
Cells of the purple bacteria, R. rubrum and Rps. sphaeroides. were grown in a continuous culture to obtain a good reproducibility. Fig. 1 is a schematic representation of the culture vessel and the feed back system used for growth control. The extinction of the bacterial suspension was measured at 880 nm and kept constant at an optical density of 0.5. The pulsed measuring light was provided by a light emitting diode (L) and detected

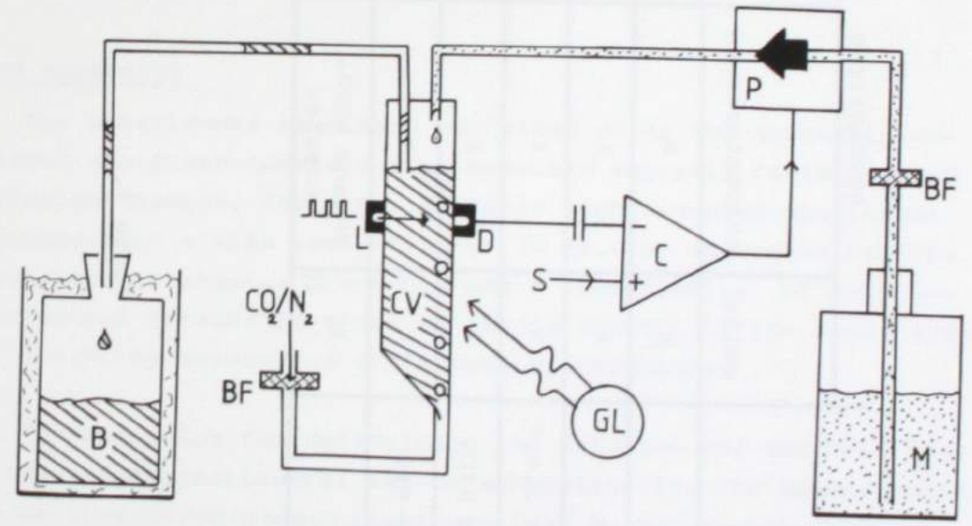


*Fig. 1. Schematic representation of the continuous culture. CV is culture vessel with bacterial suspension, M is culture medium, B is vessel for harvesting of the cells, BF is bacterial filter, GL is growing light, L is light emitting diode, D is photodiode, P is pump, C is comparator, S is preset-value of the optical density required. See text.*

| | PREPARATION | | | | |
|---|---|---|---|---|---|
| | cells | chromatophores | antenna complexes | RC's | major carotenoid composition |
| Rhodospirillum rubrum S1 | X | X | X | X | spirilloxanthin |
| Rhodospirillum rubrum FR1 VI | X | X | | | none |
| Rhodopseudomonas Sphaeroides 2.4.1 | X | X | X | | Sphaeroidene |
| Rhodopseudomonas Sphaeroides G1C | X | X | X | X | neurosporene |
| Rhodopseudomonas Sphaeroides R26 | X | X | | X | none |
| Prostecochloris aestuarii | X | PP and RCPP-complex | | X | |

Table 1.

by a photodiode (D). The photodiode current was fed into a current-voltage converter, amplified and via a high pass filter fed into a comparator (C). The reference signal (S) was used to set the optical density of the culture required. The pump (P) of the culturing medium (M) was controlled by the comparator output and switched on if the optical density exceeded the set-value. The continuous growing light (GL) (5 - 12 mW/cm$^2$ incandescent light) did not affect the setting of the comparator. A constant nitrogen / $CO_2$ flow forced the access of the bacterial suspension out of the culturing vessel into a container (B), which was kept in the dark at 0$^o$C. Cells were either directly used for the experiments or harvested for preparation of chromatophores or isolated pigment protein complexes. The additional culture conditions and preparation techniques are described in each section.

The apparatus

The experiments have been performed using two specially designed spectrophotometers. One measured magnetic field induced emission changes, the other measured light induced absorbance changes with a time resolution of 30 ns. The apparatus, briefly described in chapter III and VI, was a combination of both experimental set-ups in order to relate the MFE to the redox state of the RC by absorbance difference spectroscopy.

a. The apparatus for determining the emission and the MFE. Fig. 2 shows the experimental set-up schematically. The sample could be excited by continuous light provided by two tungsten-iodine lamps (W1,W2 250 Watt, 24 V), either through a monochromator (MON) or through narrow-band interference filters ($F_3$). The emission is detected by a photomultiplier (PM) through a cut-off filter $F_2$ (Schott, KV 550) and a field lens system ($L_1$-$L_3$) in order to increase the distance between the magnet and the photomultiplier tube (S1-type) to prevent a direct influence of the magnetic field on the photomultiplier current. The emission wavelength is selected by narrow band interference filters and/or cut-off-filters. The PM-current is converted to a voltage (I → V), which is preamplified (PA) and buffered. To prevent the pick-up of

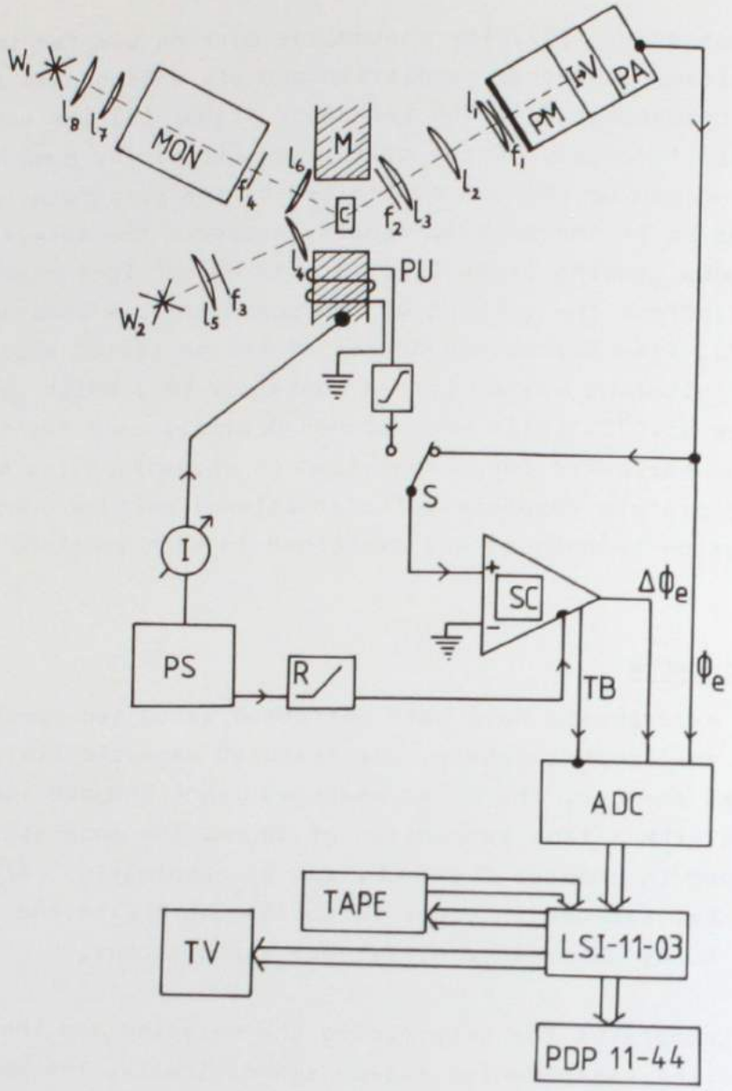


*Fig. 2. Schematic representation of the experimental set-up for measuring emission changes, $\Delta\phi_e$, in magnetic field. $W_1$ and $W_2$ are tungsten-iodine lamps (250 W-24V), $F_1$-$F_4$ are optical filters, $L_1$-$L_8$ are lenses. MON is monochromator, M is magnet, C is cuvette, PM is photomultiplier, I→V is current to voltage converter, PA is preamplifier, PU is pick-up-coil, S is switch, SC is oscilloscope TB is time-base output signal, I is current meter, PS is power supply for the magnet, R is rectifier, ADC is analog to digital converter. See text*



electrical noise, the photomultiplier and the current-to-voltage converter and the preamplifier are mounted in one shielding. The output signal of the preamplifier is fed into a two channel 12 bits AD-converter in order to sample the total emission $\phi_e$. Dependent on the position of the switch (S) either the preamplified photomultiplier signal, or the magnetic field strength (detected by a calibrated pick-up coil (PU) and electronically integrated) is fed into a Tektronix oscilloscope (SC) provided with a 3A9 operational amplifier (adjustable bandwidth and DC-compensation). The time base of the oscilloscope is externally triggered by the double phasic rectified 50 Hz sinus wave, provided by the AC-power supply of the magnet, resulting in a trigger frequency of 100 Hz. This results in an effective reduction of the electrical noise, that is in phase with the 50 Hz modulated magnetic field. The start of the time base of the oscilloscope generates the trigger pulse (TB) for the AD-converter. The output of the oscilloscope is fed into the AD-converter in order to determine small emission changes $\Delta\phi_e$ or the magnetic field strength. After each trigger pulse, 100 points in both channels (alternating) are read in via the AD-converter into the local computer, LSI-11/03 (Direct Memory Access), with a sample frequency of 20500 Hz in order to allow some time (240 µs per sweep) to reset and initialize the ADC and LSI before the next triggerpulse. The LSI-11/03 is on-line connected with a PDP-11/44 computer system for further data processing. In addition local data storage, display and preliminary calculations are possible.

The magnet is provided with two coils, one to induce a stationary field up to 800 Gauss, the other to induce a 50 Hz sinusoidally modulated field with an amplitude of maximally 1600 Gauss. The inhomogenity of the magnetic field in the sample is less than 5%. The strength of the stationary field is measured by a calibrated current meter (I).

The sensitivity of the apparatus is calibrated using a calibrated band-lamp and the energy of the excitation light is measured using a calibrated thermopile . At each excitation and emission wavelength the false fluorescence of the cuvet is measured and subtracted from the total emission of the sample. By using dilute samples, straylight effects are minimal.

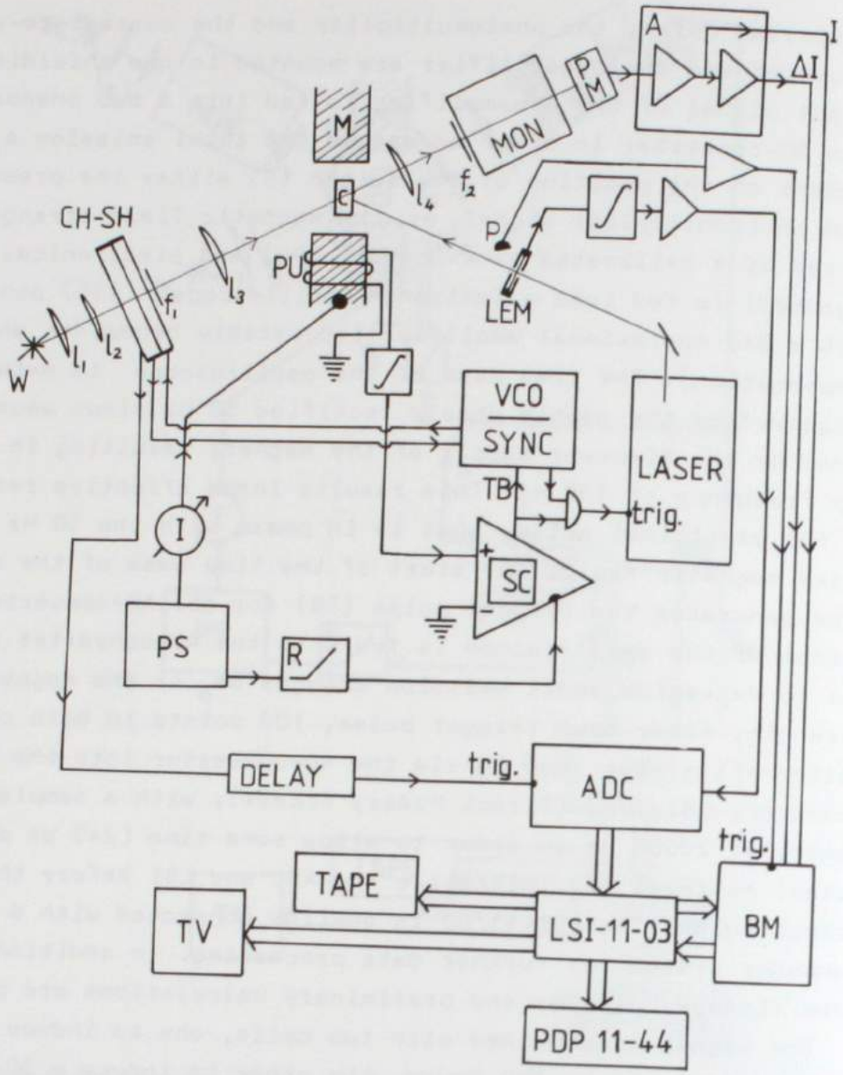


*Fig. 3. Schematic representation of the experimental set-up for measuring absorbance changes (ΔI) in magnetic fields. W is a tungsten iodine lamp (250W, 24V), $L_1$-$L_4$ are the various lens groups, $f_1$-$f_2$ are optical filters combinations, C is cuvette, M is magnet, MON is monochromator, PM is photomultiplier, A is current to voltage converter Sample and Hold amplifier, PU is pick-up-coil, LEM is laser energy monitor, P is photodiode, CH-SH is chopper-shutter combination, PS is power supply for the magnet, I is current meter, R is rectifier, SC is oscilloscope, VCO/SYNC is synchronizer and Voltage controlled oscillator, TB is timebase, ADC is analog to digital converter.*



b. The apparatus for determining absorbance changes. Fig. 3 shows the experimental set-up schematically. The excitation light is provided by a Q-switched frequency doubled Nd-YAG Laser System, generating a 532 nm pulse (full width at half maximum FWHM) of about 30 ns. The laser either directly excites the sample or is used to pump a home built tunable dyelaser (FWHM 15 ns). In some experiments a Phase-R dye laser is used to provide excitation light pulses in the blue region of the spectrum (FWHM ≈ 200 ns). The lasers are mounted in Faraday cages, triggered via opto-couplers and isolated from the main supply by RFI-filters to prevent electrical disturbances. The electrical noise, induced by the firing of the pockels cell and the flash lamps, is reduced by more than 110 dB. No significant electrical noise is detected within the accuracy of the measurements.

The measuring light, provided by a 250 Watt tungsten iodine lamp (W) reached the sample after passing through the chopper (CH), the shutter (SH) and narrow band interference filters ($F_1$). The transmitted light is detected by a specially wired photomultiplier (PM) for high output currents, through a Bausch and Lomb monochromator (MON) and additional interference filters and absorbance filters ($F_2$), to prevent scattered laser light and fluorescence from reaching the photomultiplier. The photomultiplier is connected via a current-voltage converter and a differential amplifier (A) to a Biomation 8100 transient digitizer (BM) (100 MHz). The amplifier (A) has been described elsewhere (H. Rademaker, (1981), Thesis University of Leiden.). A small modification is made to increase the bandwidth up to 15 MHz.

The whole timing system is synchronized by the sinusoidally modulated magnetic field. The time base of the oscilloscope is triggered by a double phasic rectified (R) sinuswave (i.e. 100 Hz) provided by the AC-power supply (PS) of the magnet (see the previous section). The trigger pulse, generated by the start of the timebase of the oscilloscope , is fed into a synchronizer (SYNC) in which a phase locked higher frequency is generated that controls the speed of a stepper motor, which drives the chopper

The trigger pulse for the laser is directly provided by the time base pulse of the oscilloscope. In this way the magnetic field, the laser pulse and the measuring light pulse, formed by the chopper, are synchronized. An adjustible delay time after the time base pulse of the synchronizer provides a time-shift of the chopperhole with respect to the actual time the laser is fired. An optical detector system, mounted in the chopper, generates a pulse, just before the chopper hole will be in line with the monochromator input slit, in order to open the shutter in time and to switch the sample and hold of the operational amplifier (OA) to the hold-mode just before the recording is started. At the same time the triggering of the laser is enabled and the transient recorder is armed. A photodiode (P) together with a 100 MHz amplifier detects the actual time at which the laser is fired and triggers the transient recorder, which is used in the pretrigger mode to prevent time jitter due to the intrinsic jitter of the laser system. The delay between the laser trigger pulse and the detection of the laser pulse by the photodiode is less than 30 µs. Therefore, if a 50 Hz sinusoidally magnetic field is applied, the setting of the magnetic field strength, actually present when the laser is fired, shows a systematical error of maximally 2%.

In order to obtain a high accuracy at low field and with long sweeptimes, the triggering is set at the maximum of the magnetic field and the strength of the field is adjusted by reducing the supply voltage. The laser energy is measured by a home built laser energy monitor (lineairity > 98%). The LEM is calibrated prior to each set of experiments, because of adjustments of the aligning of the laser often required to optimalize the laser output energy and spatial homogenity of the laser flash. The output of the LEM is fed into a 8 bits AD-converter, triggered 250 µs before the laser is fired and read into the LSI 11/03. The content of the output buffers of the transient recorder, containing the transmittance of the sample and/or the laser flash induced absorbance change, are read into the LSI-11/03 only, if the energy detected by the LEM fits in the energy window set with the data-registration program. To increase the signal to noise ratio, the experiments are averaged in the LS1 11/03. The



LSI 11/03 is on-line connected with a PDP 11/44 computer system for further data processing. Local display, data storage and simple data manipulation are possible.

c. Low temperature cuvette. The distance between the poles of the magnet is about 27 mm, which does not allow the use of most cryostates commercially available. A small cuvette (Fig. 4) is therefore designed, which together with a feed back system (Fig. 5) controls the temperature of the sample within 1 , down to 77K. The temperature of the sample is measured with a Cu-constantan thermocouple (D), extended into the sample. The tempera-

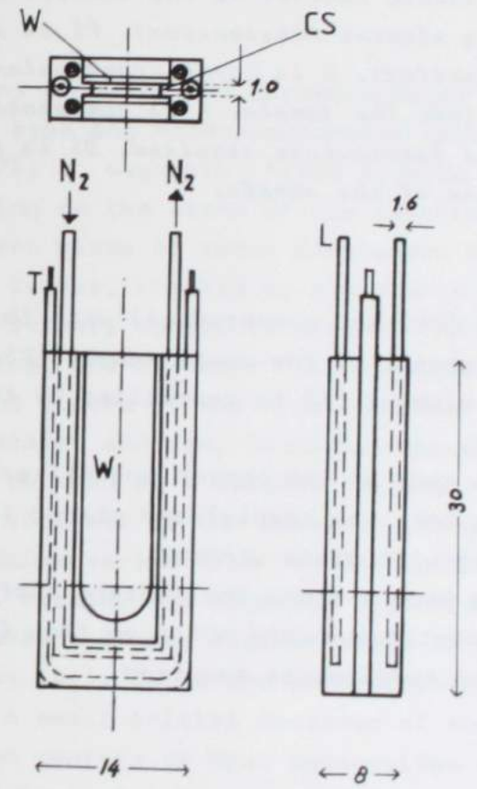


*Fig. 4. Low temperature cuvette made of silverised copper, optical pathlength 1 mm, W is glass window, L is an outlet for cold nitrogen flow, T is thermocoax, CS is contact surface at which heat exchange occurs.*

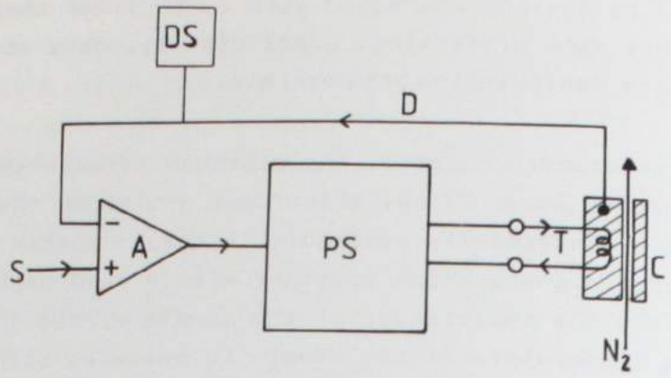


*Fig. 5. Schematic representation of the feed back system used for temperature control of the sample. C is cuvette, T is heating element (thermocoax), PS is powersupply (Current controlled), D is Copper-constantan thermocouple extended into the sample, A is comparator, S is set-value of the temperature required, DS is display of the temperature of the sample.*

ture is displayed (DS) and compared (A) with the preset-value (S). The output current of the power supply (PS), which is fed into the heating element (T) is controlled by the output signal of the comparator.

The cuvette is made of red copper and silverised (to prevent Cu-ions diffusing into the sample) and placed in a small perspex dewar provided with glass windows.
The heat exchange occurs along the contact surface (CS) indicated in Fig. 4. A continuous cold nitrogen flow ($N_2$) cools the sample down to the temperature required.



# THE RELATION BETWEEN THE MAGNETIC FIELD-INDUCED INCREASE IN BACTERIOCHLOROPHYLL EMISSION AND THE STATE OF THE REACTION CENTER IN RHODOSPIRILLUM RUBRUM AND RHODOPSEUDOMONAS SPHAEROIDES.

H. Kingma, L.N.M. Duysens en H. Peet
Department of Biophysics, Huygens Laboratory of the State University, P.O. Box 9504, 2300 RA Leiden, The Netherlands

SUMMARY

In suspensions of cells and chromatophores of Rhodospirillum rubrum wild type and Rhodopseudomonas sphaeroides wild type, G1C and R26, a magnetic field induces an increase in emission depending on the state of the reaction center. By applying different kinds of redox compounds, the redox state of the reaction center, checked by absorbance difference spectroscopy of the primary donor, is varied. The results of this study indicate that the magnetic field-induced increase in emission in light occurs if the first quinone acceptor $Q_1$ is in the reduced state, and can, in conjunction with the fluorescence yield, be used as a measure for the redox state of $Q_1$. The maximum increase of the emission change under strongly reducing conditions varies from 9 $^{o}/_{oo}$ to 26 $^{o}/_{oo}$ depending on the bacterial strain. The magnetic field-induced increase reaches fifty percent of its maximum value at magnetic fields of 270 $\pm$ 50 Gauss ($H_{\frac{1}{2}}$). Cells and chromatophores of Rps. sphaeroides G1C show a small initial decrease of the emission yield. Isolated reaction centers of Rps. sphaeroides R26 have the low value of 50 Gauss for $H_{\frac{1}{2}}$, suggesting a different environment of the primary reactants.

## INTRODUCTION

In the reaction centers of photosynthetic purple bacteria in which the quinone acceptor, $Q_1$, is reduced prior to illumination, a short flash produces a reaction center triplet with a yield of about 0.3 at 300 K and 1 at 77 K in intact systems [1]. In the past it has been observed that in a number of photosynthetic bacteria a magnetic field decreases the reaction center triplet yield [2,3,4] and stimulates the recombination emission yield [5,6]. This effect has been explained by a magnetic field-dependent steady state distribution between a singlet and triplet state of the radical pair $P^+I^-$ of the reaction center.

The absorbance changes of the acceptor $Q_1$, a quinone [7,8], due to light-induced oxidation or reduction, are mainly seen in the UV region of the spectrum and are rather small (extinction less than 10 $mM^{-1}$ $cm^{-1}$ [9,10]). Therefore they are difficult to determine, especially in preparations of bacteria where other compounds taking part in light-driven reactions also feature absorbance changes in the same range of wavelenghts (P880,other quinones, etc.). Because it is important to know the state of the acceptor while studying several properties of the photsynthetic apparatus, another method to measure $Q_1^-$ would be of general interest. Therefore we have studied the effect of an external applied magnetic field on the emission yield as a function of the state of the acceptor in different preparations of Rhodospirillum rubrum S1M and Rhodopseudomonas sphaeroides wild type, G1C and R26.

## EXPERIMENTAL SET-UP AND METHODS

To determine the saturation curves of the magnetic field-induced emission change, the experimental set-up in Fig. 1 has been used. By applying a 50 Hz modulated magnetic field (to prevent orientation effects) with an amplitude of maximally



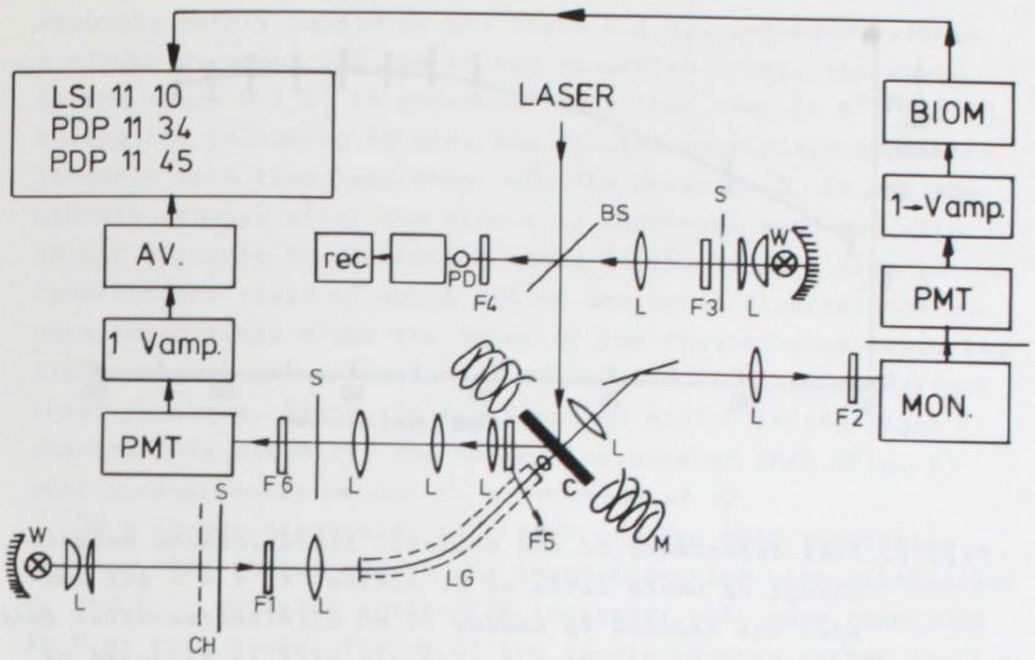


*Fig. 1. Experimental set-up. The measuring light for both emission and absorption measurements is provided by tungsten-iodine lamps W; L = lens; CH = chopper; S = shutter; F1 - F6 are filter combinations; LG = light guide; BS = beam splitter; PD = photodiode; rec. = recorder; c = cuvette; M = magnet; MON = monochromator; PMT = photomultiplier tube; I → V amp = current to voltage conversion and amplification; AV = averager; BIOM = transient recorder.*

2000 Gauss, itwas possible to compute the saturation curve from half a period, averaged up to 16384 times to increase the signal-to-noise ratio. The apparent change in emission due to magnetic disturbances on the photomultiplier (DUMONT KM 2290-S1) was smaller than the accuracy of the measurement.To check the state of the reaction centers, a 604 nm laser flash

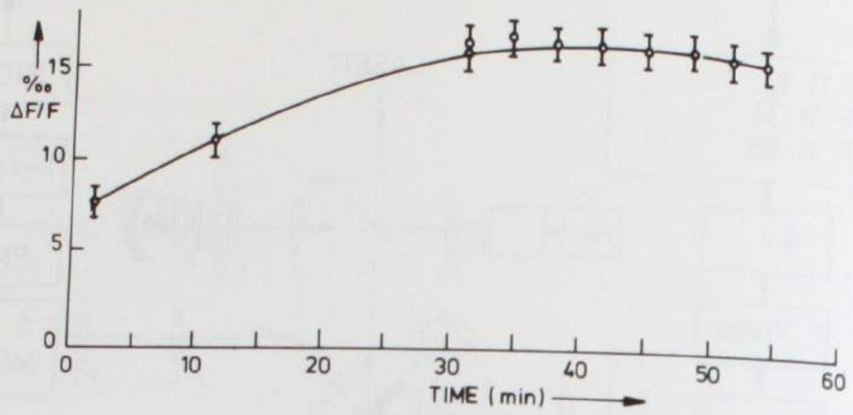


*Fig. 2. Time dependency of the magnetic field-induced emission change of whole cells of R. rubrum. At t = 0 all samples are reduced by adding 50 mM dithionite. After dark adaption varying from 0 - 40 min ΔF/F is measured of each sample.*

was used to observe the change in absorbance of P880 at 432 nm. The state of the primary reactants was controlled by the actinic light (which was also used to measure the fluorescence of the preparation) using a corning CS-5-61 broadband absorbance filter and by the addition of reductants, oxidants or inhibitors to accumulate either $P^+I\ Q_1$ or $P\ I\ Q_1^-$.

## RESULTS AND DISCUSSION

### General observations

In whole cells of R. rubrum the magnitude of $\Delta F_{max}/F = F_{max}(H = max) - F_{max}(H = 0)\ /F_{max}(H = 0)$ is a function of time and reaches a maximum in about 30 min after the addition of the reductant (see Fig. 2). After adding dithionite up to a high final concentration of 50 mM, the fluorescence yield,



probably mainly caused by the state $P^+I\ Q_1$, decreases within a minute by about 30% due to the reduction of $Q_1$. The yield in the state $P\ I\ Q_1^-$ is somewhat lower than that in $P^+I\ Q_1$[17]. During the following 40 min, the fluorescence yield decreases linearly with time (less than 8%). The acceptor $Q_1$ is not completely reduced after one minute in darkness; even not after 40 min exposure to dithionite since in the light a rise in fluorescence yield of about 20% of the total fluorescence occurs immediately after the onset of the fluorescence measuring light. Higher concentration of dithionite (1 M) do not affect these features. Since (in the first 40 min) F in the light F changes only slightly, the marked increase of ΔF/F (Fig. 2) will predominantly be due to an increase of ΔF.

On a longer timescale, both ΔF/F and the half saturation field $H_{\frac{1}{2}}$ are influenced by the incubation time with dithionite. $H_{\frac{1}{2}}$ and $F_{max}$ decrease while ΔF/F increases with more than 100% in 6 or more hours. The pH of the sample becomes rather low,i.e. pH = 4. Over the range of pH = 4 to 10, ΔF/F and $H_{\frac{1}{2}}$ vary within 20% if the time between the addition of dithionite and the experiment is about 20 min. This indicates that the large increase of ΔF/F may be due to deformation of the antenna. The value of $H_{\frac{1}{2}}$ is dependent on several reaction velocities [11,12] and may therefore be influenced by the long exposure to the low pH of 4. In all experiments ΔF/F and $H_{\frac{1}{2}}$ were determined after 30 min of incubation with the chemical reagentia used.

### ΔF/F and $H_{\frac{1}{2}}$ under strongly reducing conditions

After 30 min of incubation with dithionite (50 mM) maximum ΔF/F values were found and minimal $H_{\frac{1}{2}}$ values. As is shown in Fig. 3, the magnitude of $H_{\frac{1}{2}}$ and ΔF/F depends on the species, but no significant difference is observed between cells and chromatophores of the same bacterium. ΔF/F is varying ± 25% depending of the age, the growing conditions and the condition of the cells used for the preparation. This might be related to the bacteriochlorophyll and the carotenoid content of the cells, which also varies during bacterial growth [13] and in-

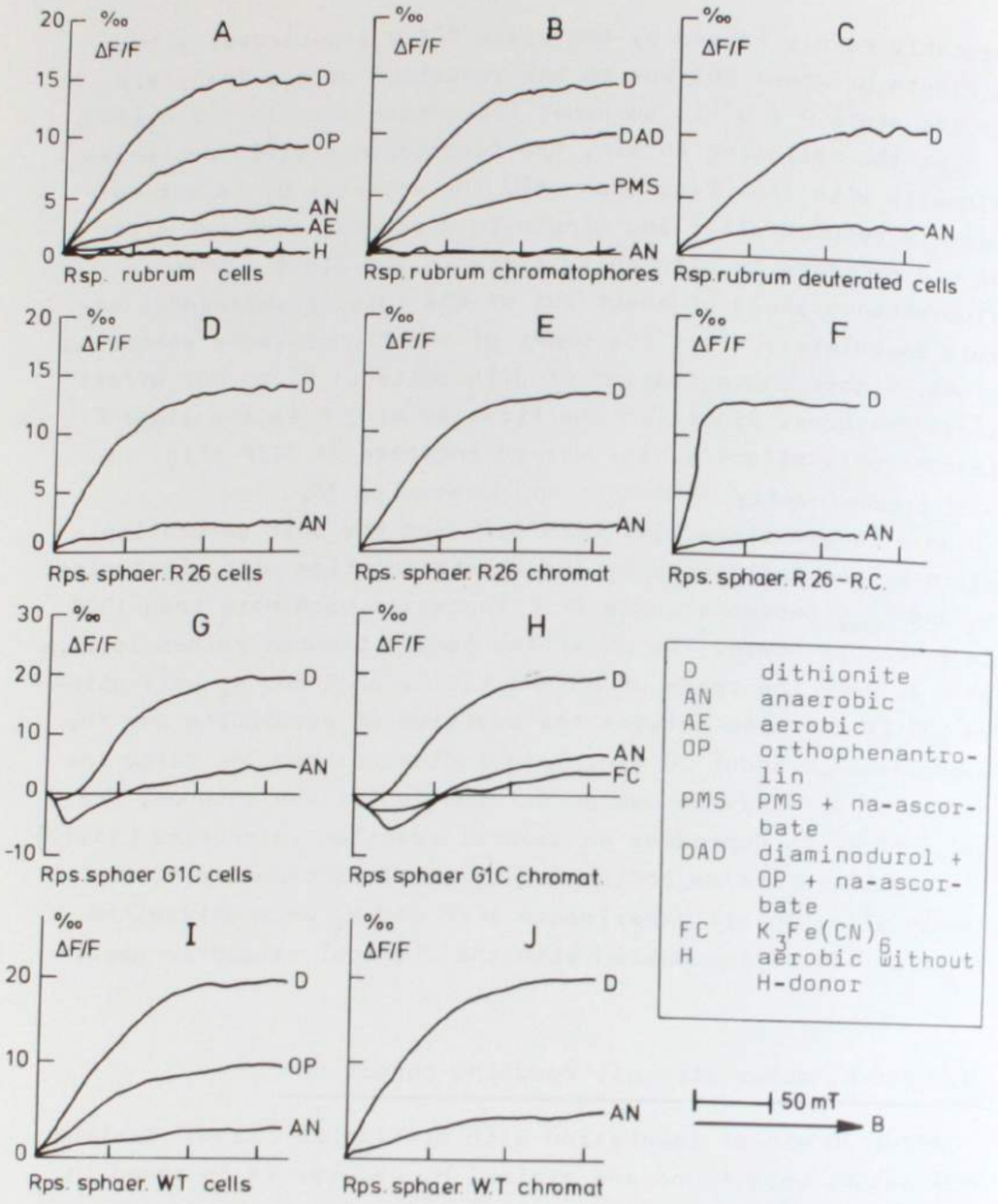


*Fig. 3. The magnetic field-induced fluorescence change as a function of the magnetic field strength. The fluorescence F per incident quantum does not change during the experiment.*



fluences $F_{max}$, as is suggested by the observation that ΔF/F in the carotenoidless mutant R26 of Rps. sphaeroides is significantly lower than in the two other carotenoid containing strains and shows less variation (± 5%). The magnitude of the ΔF/F value in cells and chromatophores of Rps. sphaeroides wild type and G1C (21 ± 5 ‰) is significantly higher than in R. rubrum (12 ± 3) and Rps. sphaeroides R26 (13 ± 0.5). This might be explained by the relatively low values for $F_o$ in Rps. sphaeroides wild type and G1C.

In Rps. sphaeroides G1C, which differs from the wild type because only one carotenoid is present, an initial decrease can be observed below values of 400 Gauss, which is more pronounced in partly reduced samples (Fig. 3 G/H). A similar effect is reported by others [6,11]. This decrease in emission yield is not observed in Rps. sphaeroides wild type. In reaction center preparations of Rps. Sphaeroides R26, $H_{\frac{1}{2}}$ is about 50 Gauss, small compared to the $H_{\frac{1}{2}}$-value observed in intact cells and chromatophores of the same mutant, in agreement with earlier reports on the change of the carotenoid triplet yield [4]. This suggests a large difference in magnetic properties of these isolated reaction centers compared to the intact cells and chromatophores. Possibly a different geometry of the primary reactants causes another orientation of the members of the radical pair which influences the sensitivity to a magnetic field [4]. The absence of the antenna in these isolated reaction center preparations may also influence the $H_{\frac{1}{2}}$-values.

To study the mechanism of the magnetic field-induced changes, cells of R. rubrum were deuterated, which resulted in a decrease of the hyperfine interaction by a factor of 6.5 [4]. In agreement with results obtained by determination of the triplet yield in a magnetic field, no significant change of ΔF/F and $H_{\frac{1}{2}}$ can be observed compared to the non-deuterated controls (Fig. 3 C) [4]. This indicates that the conversion frequency between the singlet and triplet state of the radical pair is not determined by the hyperfine interactions.

## $\Delta F/F$ and $H_{\frac{1}{2}}$ of partly light-reduced samples

During the fluorescence experiments, the samples are continuously illuminated by a tungsten-iodine lamp (see Fig. 1). In this relatively weak light the reaction centers are largely present in the state P I $Q_1^-$ or $P^+$I $Q_1$, depending on the preparation and experimental condition. In illuminated chromatophores of R. rubrum, without additions $\Delta F/F$ was smaller than the accuracy of our measurements and no flash-induced oxidation of P was observed, suggesting that the reaction centers are predominantly in the state $P^+$I $Q_1$. In the presence of PMS (10 µM) and Na-ascorbate (200 µM), an increase of $\Delta A$ in a flash is observed as well as a magnetic field-induced increase of F (Fig. 3B); the added donor system may be expected to reduce rapidly $P^+$ , so that state P I $Q_1^-$ accumulates. The reaction centers in cells of R. rubrum without artificial donors are in the states P I $Q_1$, P I $Q_1^-$ and/or $P^+$I $Q_1$, respectively, as was checked by absorbance spectroscopy. The donor system in chromatophores is less efficient than in cells of R. rubrum because of slower $P^+$ reduction. Thus in cells of R. rubrum, accumulation of P I $Q_1^-$ occurs causing a $\Delta F_{anaerobic}/F$ effect (Fig. 3A). $\Delta F/F$ is markedly decreased under aerobic conditions, presumably because of the (indirect?) oxidation of $Q_1^-$ by $O_2$.

To check the explanation that in whole cells of R. rubrum the donor system is responsible for the larger $\Delta F/F$ than in chromatophores, cells were incubated in 0.5% NaCl under aerobic conditions during two hours, resulting in a depletion of the H donor system [14]. The oxidation of the primary donor is maximal , but the reduction is extremely slow after a saturating flash in a dark-adapted sample. In light no P oxidation is seen, suggesting a similar situation as discussed for chromatophores of R. rubrum. $\Delta F/F$ decreased below the level of observability.

Ortho-phenanthroline is an inhibitor of the electron transport between the acceptor $Q_1$ and the following acceptor UQ [15,16]. In chromatophores of R. rubrum, $\Delta F/F$ can only be observed if artificial donors are applied in the presence of ortho-phenanthroline (Fig. 3B). The combination of 1 mM DAD and 250 µM Na-succinate (Na-s) appears to be an efficient donor system, as is indicated by P oxidation in a flash given to illuminated chromatophores and by the faster reduction of $P^+$ after a flash in dark-adapted samples.

In cells of R. rubrum and Rps. sphaeroides a marked increase of $\Delta F/F$ is apparent after the addition of ortho-phenanthroline (Figs. 3 A and I). Chromatophores of Rps. sphaeroides show a considerable modulation of the emission under anaerobic conditions, suggesting a more efficient donor system than in chromatophores of R. rubrum. Addition of $K_3Fe(CN)_6$ decreased $\Delta F/F$ (fig. 3H), which can be explained by the oxidation of the acceptor side.

The experiments described above all indicate that, within the accuracy of the measurements, in illuminated cells only the state P I $Q_1^-$ generates the magnetic field-induced emission but that $\Delta F/F$ is also affected by other parameters such as time of incubation of bacteria with dithionite. In Fig. 4 an example is given, introducing $\Delta F/F$ as a measure for the amount of P I $Q_1^-$ that is formed by a particularly chosen concentration of NAD and NADH. Determining the fraction of $Q_1^-$ is very difficult under steady state conditions if absorbance difference spectroscopy is used. Another problem is that NAD and NADH absorb in the same region as $Q_1/Q_1^-$. After determining $\Delta F/F$, $Q_1$ was completely reduced by adding ditionite up to a final concentration 50 mM. In this way $\Delta F/F$, caused by the addition of NAD or NADH, can be related to the maximum value for $\Delta F/F$ at strongly reducing conditions, which yields a relative measure for the amount of P I $Q_1^-$. This is consistent with the finding that the P oxidation, observed by means of absorption difference spectroscopy, yields, as a function of the NADH/(NAD total) ratio , a curve comparable to the difference of the curves shown in Fig. 4 (van der Wal, H.N. and Giménez-Gallego, G., unpublished results).

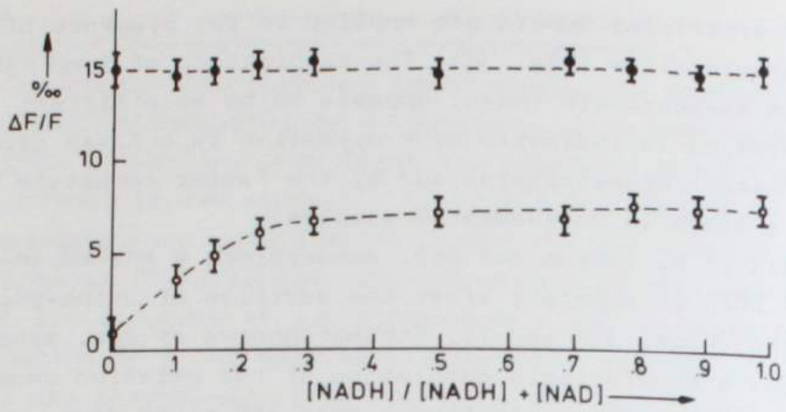


*Fig. 4. Chromatophores of R. rubrum are treated with glucose-oxidase, catalase and glucose for creating strictly anaerobic conditions. The concentration of NAD + NADH is 1 mM, while the ratio NADH/(NAD + NADH) is varied. Each sample is incubated during 20 min in the dark. After determining ΔF/F (o), dithionite is added to measure the maximum change in emission yield (o).*

Acknowledgement

We wish to thank Dr. R. van Grondelle and Ir. A. Sonneveld for suggestions during the experiments and for critically reading the manuscript.

REFERENCES

1 Holmes, N.G., van Grondelle, R., Hoff, A.J. and Duysens, L.N.M. (1976) FEBS Lett. 70, 96-101
2 Blankenship , R.E., Schaafsma, T.J. and Parson, W.W. (1977) Biochim. Biophys. Acta 461, 297-305
3 Parson, W.W. (1976) Conference in The Primary Electron Transport and Energy Transduction in Photosynthetic Bacteria, Brussels, abstr. MA 1
4 Hoff, A.J., Rademaker, H., van Grondelle, R. and Duysens L.N.M. (1977) Biochim.Biophys. Acta 460, 547-554
5 Rademaker, H., Hoff, A.J. and Duysens, L.N.M. (1979) Biochim. Biophys. Acta 546, 248-255
6 Voznyak, W.M., Jelfimov, J.I. and Proskaryakov, I.I. (1978) Doklady Akad. Nauk 242, 1200-1203
7 Bolton, J.R. (1978) in The Photosynthetic Bacteria (Clayton, R.K. and Sistrom, W.R., eds.), pp. 419-429, Plenum Press, New York
8 Wraight, C.A. (1979)Photochem. Photobiol.30, 767,775
9 Clayton, R.K. and Straley, S.C. (1972) Biophys. J. 12, 1221-1234
10 Slooten, L. (1972) Biochim. Biophys. Acta 275, 208-218
11 Rademaker, H. (1980) Thesis, University of Leiden
12 Werner, H.J., Schulten, K. and Weller, A. (1978) Biochim. Biophys. Acta 502, 255-268
13 Duysens, L.N.M. (1952) Thesis, Unversity of Utrecht
14 Duysens, L.N.M., Huiskamp, W.J., Vos, J.J. and van der Hart, J.M. (1956) Biochim. Biophys. Acta 19, 188-190
15 Prince, R.C. and Dutton, P.L. (1978) in The Photosynthetic Bacteria (Clayton, R.K. and Sistrom, W.R., eds.), pp. 439-453, Plenum Press, New York
16 Parson, W.W. (1978) in The Photosynthetic Bacteria (Clayton, R.K. and Sistrom, W.R. eds.), pp. 455-469, Plenum Press, New York
17 van Grondelle, R. (1978) Thesis, University of Leiden

# ON THE ORIGINS OF MAGNETIC FIELD INDUCED BACTERIOCHLOROPHYLL EMISSION CHANGES IN SEVERAL PHOTOSYNTHETIC BACTERIA.

H. Kingma*, R. van Grondelle+ and L.N.M. Duysens*.
*Department of Biophysics, Huygens Laboratory of the State University, P.O. Box 9504, 2300 RA Leiden, The Netherlands.
+Department of Biophysics, Physics Laboratory of the Free University, De Boelelaan 1081, 1081 HV Amsterdam, The Netherlands.

## SUMMARY

In cells/chromatophores, isolated antenna complexes and isolated reaction centers (RC's) of a number of photosynthetic bacteria we determined the magnetic field induced emission (MFE) as a function of the magnetic field strength, the redox state of the reaction center, the temperature, the emission and excitation wavelength. Two types of MFE were observed. Category I is closely associated with the charge recombination in the reaction center, decreases upon cooling, is found in reaction center containing preparations in which the first quinone acceptor $Q_1$ has been reduced and the relative MFE ($\Delta F/F$) does not depend on the excitation wavelength. Category II is associated with the energy transfer process in the antenna of the carotenoid containing bacteria , does not depend upon the temperature or the redox state of the reaction center, only occurs upon direct carotenoid excitation and is not found in isolated RC's. Upon carotenoid excitation of reduced cells/chromarophores, MFE of both categories is found. The MFE of the first category is discussed in terms of the radical pair mechanism and some suggestions are made to explain the descrepancies observed between cells/chromatophores and RC's. The activation energy for the luminescence, calculated from the measured temperature dependence of the relative MFE ($\Delta F/F$), is found to be in the range of 0.10 - 0.14 in purple bacteria and between 0.2 - 0.3 in the green bacterium Prosthecochloris aestuarii.The MFE of the second category is discussed in terms of singlet fission of the first excited singlet state of an antenna carotenoid molecule into a double triplet state of the carotenoid and another nearby molecule. A process of homofission explains very well our results but with some energetical restrictions a process of heterofission might also account for the MFE observed.



## INTRODUCTION

The study of magnetic field effects on excitation transfer and primary electron transport has been an important aspect of photosynthesis research during the last decade [1]. The phenomena observed involve magnetic field induced changes of the (bacterio)chlorophyll emission (MFE) (2,3,4,5,6,7,8, chapter III ) and triplet yields [7, 9, 10] and these results are mainly discussed in terms of the radical pair mechanism [11]. Some years ago Rademaker et al. [12] discovered in whole cells of the purple bacteria Rhodospirillum rubrum a strong magnetic field dependence of the antenna carotenoid triplet yield upon carotenoid excitation.
These authors pointed out that the change in triplet yield could be explained either by the mechanism of charge separation and subsequent recombination (radical pair mechanism) or by a magnetic field dependent fission reaction of a carotenoid excited singlet state into two triplet states (see ref. 13 for a review of the process of fission). The process of energy transfer, charge separation and charge recombination as proposed by us for R. rubrum is shown schematically in Fig. 1 [14, 15, 16, 17]. Two types of magnetic field effects occurred and will be discussed separately.

Upon excitation of antenna carotenoid or BChl molecules a fraction of the excitation energy is transferred to the BChl species absorbing at the longest wavelength (B880). The trans-

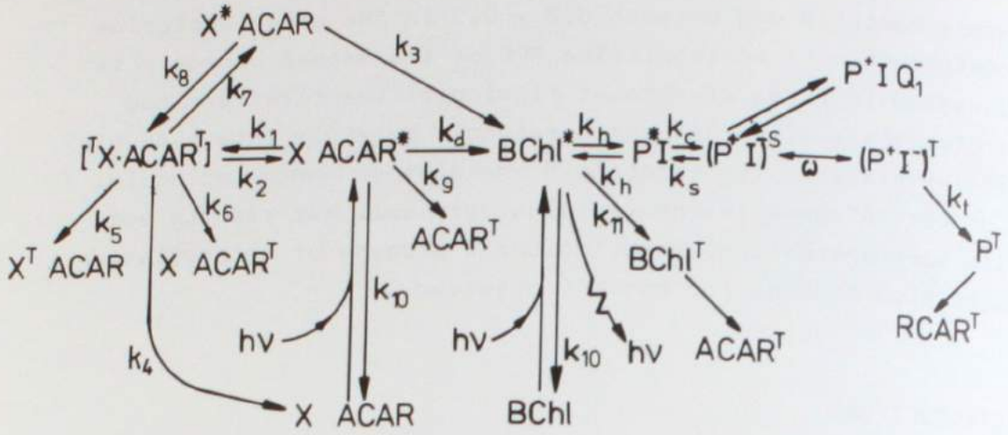


*Fig. 1. Scheme of energy and electron transfer in R. rubrum $S_1$. The superscripts °, T, S, +, - indicate respectively the lowest excited singlet state, the lowest excited triplet state, the singlet state, the radical cation and the radical anion. ACAR is antennacarotenoid; P is reaction center bacteriochlorophyll dimer (P880); I is bacteriopheophytin ; $Q_1$ is the first quinone acceptor; X is an unspecified molecule which is part of the triplet pair $[^T X.ACAR^T]$; RCAR is reaction center carotenoid. The K's are rateconstants. For explanation see text.*

fer efficiencies upon carotenoid excitation vary strongly between the various purple bacteria, i.e. 30% for transfer from spirilloxanthin to B880 in R. rubrum and close to 90% for transfer from neurosporene or sphaeroidene to B800, B850 or B880 in Rhodopseudomonas sphaeroides and Rhodopseudomonas capsulata [18]. Sofar no satisfactory explanation for these difference has been proposed.

Upon arrival of the excitation in the B880 bacteriochlorophyll network the excitation performs a diffusive type of transfer process among a large number of B880 molecules and visits several RC's before trapping takes place. The traps are not perfect i.e. excitations arriving at a trap have a high probability of escaping back into the surrounding antennae (90% for R. rubrum, 70% for Rps. capsulata [8,19].



## 1. Charge separation and recombination in the reaction center

Upon excitation of the RC bacteriochlorophyll dimer P880 or P, a charge separation may take place ($t_{\frac{1}{2}}$ 3-4 ps) resulting in the radical pair $P^+I^-$ (I is a bacteriopheophytin ), which after its formation oscillates between a singlet state $(P^+I^-)^S$ and a triplet state $(P^+I^-)^T$. The mixing of these states depends upon a magnetic field [20]. In a low field the energy difference between the singlet and triplet levels is 2 J (J = 3-8 gauss [21]), while anisotropic spin-spin dipole interactions split the triplet levels into three so-called zero field states. In principle, all three levels are available for S-T conversion of the radical pair. At high magnetic field, Zeeman splitting shifts the $m_s$ = +1 and $m_s$ = -1 levels of the triplet state far beyond reach of the singlet level and only the $m_s$ = 0 participates in S-T conversion. The reaction center triplet yield is thus lower in the presence of a magnetic field. When the primary quinone acceptor $Q_1$ is oxidized, the electron transfer from $I^-$ to $Q_1$ is so fast that these processes have no chance to become operative; only if $Q_1$ is reduced, the lifetime of the $P^+I^-$ is long enough (≈ 10 ns [20,22]) to allow marked S-T conversions. Under these reducing conditions the decay of the state $P^+I^-$ is mainly governed by recombination of $(P^+I^-)^S$ to the ground state (P I) or to the excited state $P^*I$ and of $(P^+I^-)^T$ to the RC-triplet state $P^FI$ which in carotenoid containing species rapidly decays into the RC-carotenoid triplet state ($RCAR^T$). The backreaction to $P^*$ followed by back transfer to the antenna is responsible for the observed MFE in this scheme. These processes and their associated rate constants are summarized in the right part of Fig. 1.

In earlier work we showed that in R. rubrum the RC-associated magnetic field dependent processes could be studied by using selective BChl-excitation light (see also Results) and concluded that these effects can qualitatively be explained in terms of a matrix model of energy transfer (chapter VI, [8,23])

## 2. Singlet fission and fusion in the antenna

Upon excitation of the antenna carotenoid molecule the energy may be transferred to an adjacent BChl molecule or the carotenoid excited state may form two triplet states involving either a secondidentical carotenoid molecule (homofission) or a different molecule, e.g. BChl, tyrosine or trytophan (heterofission). The occurrence of these processes with high efficiency in organic crystals has been well documented [13, 24-28]. The state of the thus formed triplet pair is described by 9 spin states, each of which may have some singlet, triplet or quintet character. The probability of triplet or singlet formation now dependsupon the fraction of the nine states, all of which are formed with various probabilities, that contain triplet or singlet character. As fission is a spin-conserving process, a single triplet state can only be formed from a singlet excited state if there exists a substate with a mixed singlet-triplet character. The rate constants of fission and fusion increase with the number of substates with some singlet character. The ratio of the rate constant for fission and fusion depends on the energy differences between the various excited states involved and therefore an effect of the temperature upon both emission and triplet yield may occur. Although the process of singlet-fission is the inverse of triplet-fusion, the explicit details of the process need not be identical. We nevertheless assume that the theory adopted for the fusion process is also valid in the case of fission [13]. If the BChl emission yield depends upon a magnetic field it will in principle show a dependence more or less complementary to that of the antenna triplet yield, if the transfer of excitations competes with the fission process (see Fig. 1 rate constants $k_d$ and $k_1$). If, however, fusion (rate constant $k_7$) follows fission (rate constant $k_1$) the effect of a magnetic field on the emission and triplet yield will depend on the values of $k_d$, $k_1$, $k_5$, $k_6$, $k_7$ and $k_8$. All these processes and their associated rate constants are shown in Fig. 1, (left side). Recent reports have shown the existence of magnetic field induced emission changes which may result from such fusion and fissionprocesses [29-31]. This work is an extensive study on the origin of magnetic field induced emission (MFE) changes in various purple



bacteria. The observations can be attributed to reaction center or antenna associated phenomena. A study dealing with the mechanism of triplet formation in the reaction center and the antenna complex is presented in chapter V.

## MATERIALS AND METHODS

R. rubrum (wild type and FR VI-mutant) and Rps. sphaeroides (wild type, G1C and R26-mutant) were grown anaerobically in the light on media described by Cohen-Bazire et al. [32] and Slooten [33] respectively, in a continuous culture described in chapter II (see Figure 1). Prosthecochloris aestuarii, strain 2 K was grown anaerobically in a mixed culture known as Chloropseudomonas ethylica [34] as described by Holt et al. [33]. The cells were harvested by centrifugation and resuspended in buffer containing 250 mM tricine, 5 mM $K_2H\ P\ O_4$, 5 mM $Mgcl_2$, pH = 8.0. Chromatophores of R. rubrum and Rps. sphaeroides were prepared using a French press or by 10 min. sonification at 273 K. After centrifugation for 20 min at 20,000 x g, the remaining supernatant was centrifuged for 2 ns at 110,000 x g. The pellet was resuspended in buffer containing 60% glycerol and stored in the dark at 240 K until use. RC's of R. rubrum (wild type and FR VI) and Rps. sphaeroides (wild type and G1C) were isolated as described by Slooten [36]. RC's of Rps. sphaeroides R-26 were isolated as described by Kendall-Tobias and Seibert [37]. The RC's showed normal P-oxidation and reduction kinetics. The PP and RCPP complexes were prepared as described by Swarthoff et al. [38]. The B800/B850 light-harvesting complexes of Rps. sphaeroides 2.4.1 and G1C were prepared using the method of Clayton and Clayton [39]. The antenna complexes have been extensively described by Van Grondelle et al. [18]. The B850 complex was isolated from the B800/B850 complex by dialysis against 1% LDS (Kramer, H.J.M. and Van Grondelle, R, results to be published). The B880 complex of R. rubrum wild type was isolated as described by Cogdell and Thornber [40] but instead of

a hydroxylapatite column we used a 10 - 40% continuous sucrose gradient (2 - 5 h, 200 000 x g). Samples of the isolated light-harvesting complex and reaction center preparations were suspended in 250 mM tricine buffer containing 5 mM $K_2HPO_4$, 5 mM $MgCl_2$ and 0.1% LDAO or 0.1% SDS, pH = 8.0. Samples were prepared by adding dithionite 1 mg/ml (5 mM) (reduced samples) or by adding $K_3Fe(CN)_6$ up to a final concentration of 1 - 2 mM (oxidized samples). In oxidized samples of whole cells or chromatophores the oxidized primary donor $P^+$ was accumulated in the light as was checked by absorbance spectroscopy. For measurements at temperatures below 273 K, glycerol (60% v/v) and 0.5 M sucrose were present to prevent crystallization upon cooling. The B800-B850 complex as well as the B880 complex were in some cases (see Results) oriented by pressing a polyacrylamide gel in a similar way as described by Abdourakhmanov et al. [41]. The magnetic field induced emission changes and the total bacteriochlorophyll emission was measured in an apparatus described in chapter II For some experiments two excitation light sources, both 250 Watt tungsten-iodine lamps, were used. The light excited the sample, placed between the poles of a home-built magnet, after passing a Schott Calflex-C and narrow band interference filters (Schott AL or Balzers-B40) and/or through a Bausch and Lomb monochromator(halfwidth 4.8 nm). The bacteriochlorophyll emission was detected by a S1-type photomultiplier (Dumont KM 2290) through a Kodak KV 550 and appropriate interference filters. By applying a sinusoidally 50 Hz modulated magnetic field with an amplitude of maximally 1300 Gauss, it was possible to compute the saturation curves of the magnetic field-induced emission changes from half a period, averaged up to 270,000 times to increase the signal to noise ratio. In the experiment to study the emission changes in dependence of the orientation of the triplet-pair members with respect to the magnetic field vector, an oriented sample was placed between the poles of the magnet with various orientations. In addition the sample was then excited and bacteriochlorophyll emission was detected through polarizing filters. For most other experiments a special designed cuvette was used, in which a heating element was mounted and through which continuously cold nitrogen flowed. Temperature was monitored by



a Cu-constantan thermocouple extended into the sample and controlled within 1 K by a feedback system. If not indicated otherwise, the experiments were performed at 18°C.

RESULTS

Upon excitation of cells or chromatophores of Rhodospirillum rubrum, Rhodopseudomonassphaeroides 2.4.1 and Rhodopseudomonas sphaeroides G1C, either in the presence of sodium dithionite to reduce the primary quinone $Q_1$ or in the presence of $K_3Fe(CN)_6$ to oxidize the primary donor P880 or at intermediate redox levels small magnetic field induced emission (MFE) changes are observed, typically of the order of a few percent or less. Part of these changes are due to reaction center associated phenomena and are therefore also observed in isolated reaction centers from these species and the observations are described in section I. A second type of MFE is associated with the light-harvesting antenna, are therefore also observed in isolated light-harvesting complexes from these species and occurs only upon carotenoid excitation. These phenomena are described in section II. In section III we will present the results concerning the temperature dependence of MFE for both types of phenomena.

To exclude that these small emission [illegible] are caused by orientational effects due to the magne[illegible] [22] sinusoidally modulated [illegible] field [illegible] used [illegible] nary magnetic field w[illegible] and [illegible] was s[illegible] ing the amplitude of [illegible] al[illegible] th[illegible] field. In addition [illegible] by adding various a[illegible] For all experiments re[illegible] not depend on the t[illegible] yield incre[illegible] shape of t[illegible] of the v[illegible] using [illegible] vide[illegible]

lack of remanent magnetism and is not sensitive to low frequency drift of amplifiers due to phaselocked detection.

For the experiments reported under reducing or oxidizing conditions, the relative MFE ($\Delta F/F$) did not depend upon the excitation light intensity for $I \leq 45$ MW/cm$^2$ ($\lambda$ = 603 nm) or the extinction of the sample ($OD_{880}$ = .1 - 1.0).

## I. The reaction center associated MFE

### a. R. rubrum S1

Fig. 2A shows the maximum relative MFE increase ($\Delta F_{max}/F$) in cells of R. rubrum, reduced by 5 mM dithionite, as a function of the emission wavelength upon 603 nm excitation. The magnetic field strength $H_{\frac{1}{2}}$ at which the emission change is half maximum measured 240 Gauss and was independent of the emission wavelength

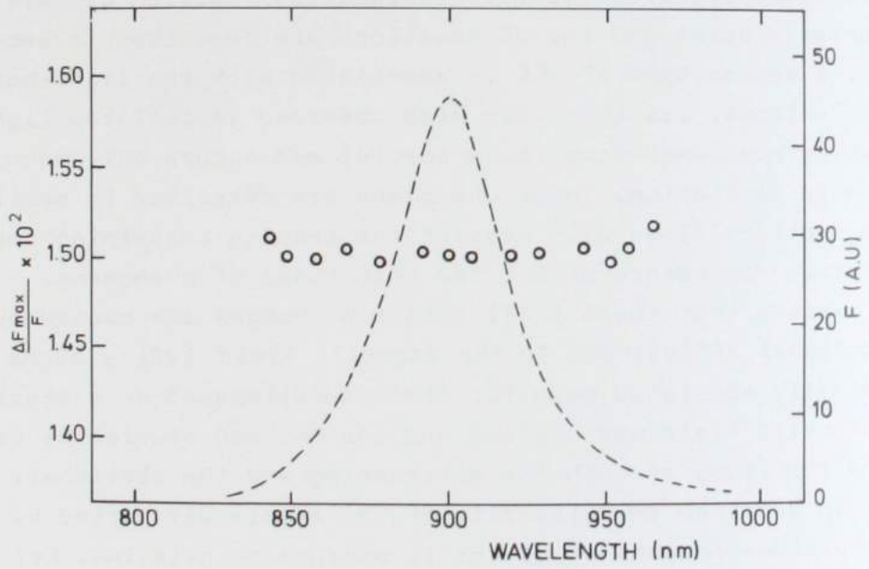


*Fig. 2A. Spectrum of the ratio $\Delta F_{max}/F$ (o) and the total emission F (broken line) in reduced cells of R. rubrum S1. 5 mM dithionite added. $A_{880\text{-}960\ nm}$ = .3; optical path length 1 mm. Excitation wavelength 603 nm.*



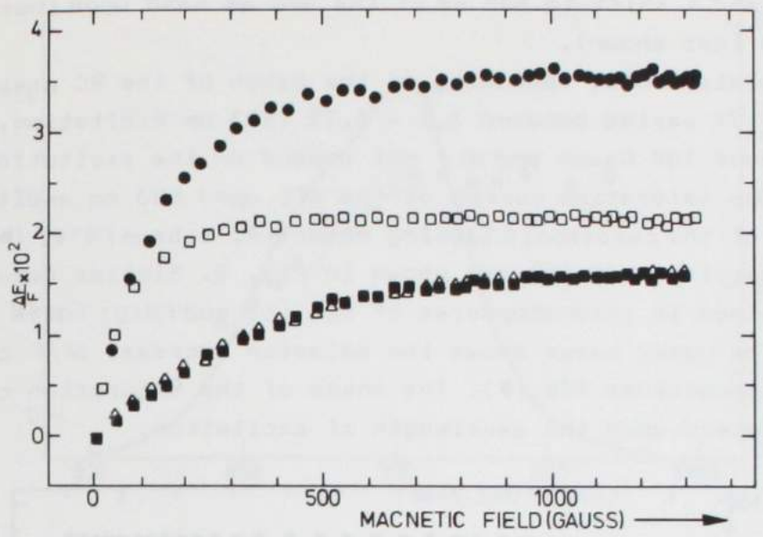


*Fig. 2B. The relative MFE ($\Delta F/F$) monitored at 905 nm as a function of the magnetic field strength in the presence of 5 mM dithionite in cells (■), chromatophores (Δ), cells at pH = 3 (□) and isolated RC's (●) of R. rubrum S1. $A_{880\text{-}960\ nm}$ = .3; optical path length 1 mm. Excitation wavelength 603 nm.*

between 840 - 970 nm. The broken line shows the total emission spectrum.

Fig. 2B shows $\Delta F/F$ detected at 905 nm as a function of the magnetic field strength in several preparations of R. rubrum reduced by 5 mM dithionite. The lower curves show the emission change upon 603 nm excitation in whole cells (□) and in chromatophores (Δ). Both saturation curves are dependent on the excitation wavelength (not shown). Upon direct excitation of the carotenoid between 420 and 570 nm, $H_{\frac{1}{2}}$ increased from 240 to maximally 290 Gauss and $F_{max}/F$ increased from 1.5 to 1.6%. If cells/chromatophores were incubated at low pH (< 3.5) $\Delta F_{max}/F$ increased and $H_{\frac{1}{2}}$ decreased (■). A similar change was observed if a suspension of whole cells in growth medium was kept in the dark for at least six hours. Upon lowering the pH the absorbance spectrum

showed a marked decrease, or even disappearance of the P800 absorbance and a shift to 885 nm of the 880 nm band upon lowering of the pH (not shown).

In isolated RC's, depending on the batch of the RC preparation $\Delta F_{max}/F$ varied between 2.1 - 3.7% (603 nm excitation, ●). $H_{\frac{1}{2}}$ was about 100 Gauss and did not depend on the excitation wavelength. The saturation curves of the MFE upon 603 nm excitation of cells of the carotenoid lacking mutants R. rubrum FR1VI (■) and Rps. sphaeroides R26 (o) are shown in Fig. 3. Similar results were obtained in chromatophores of R26 (Δ) and FR1VI (data not shown). The upper curve shows the emission increase ΔF/F of RC's of Rps. sphaeroides R26 (●). The shape of the saturation curve did not depend upon the wavelength of excitation.

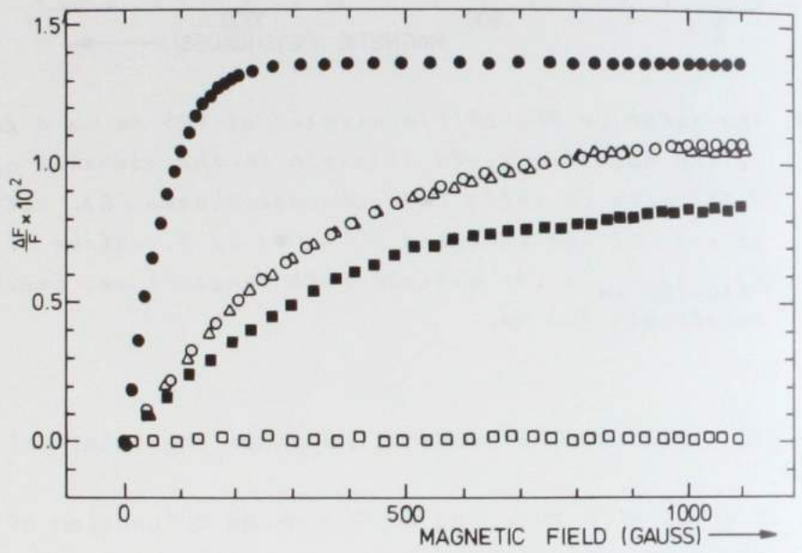


*Fig. 3. ΔF/F as a function of the magnetic field strength in cells (o), chromatophores (Δ) and RC'S (●) of Rps. sphaeroides R26 in the presence of 5 mM dithionite detected at 863 nm and in reduced cells (■) and in oxidized (1 mM $K_3Fe(CN)_6$) cells (□) of R. rubrum FRVI detected at 900 nm. Excitation wavelength 603 nm. $A_{880}$-$A_{960}$ (R. rubrum FRVI) = .3; $A_{850}$-$A_{960}$ (Rps Sphaeroides R26) = .25. Optical path length 1.0 mm.*



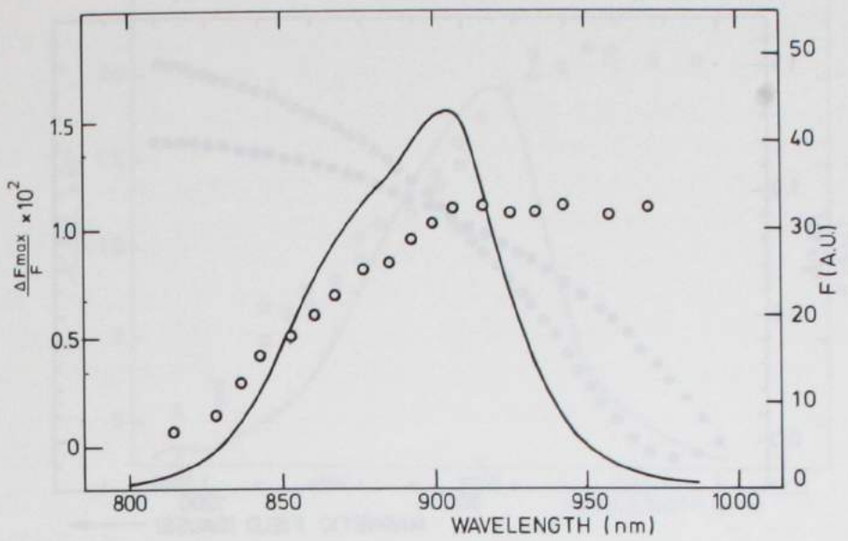


*Fig. 4A. Spectrum of the ratio $\Delta F_{max}/F$ (o) and the total emission F (solid line) in reduced cells of Rps. sphaeroides 2.4.1. 5 mM dithionite added, absorbance$_{850-960\ nm}$ = .3; optical pathlength 1.0 mm; 603 nm excitation.*

b. Rps. sphaeroides

Fig. 4A shows the ratio $\Delta F_{max}/F$ at various wavelengths in cells of Rps. sphaeroides 2.4.1 reduced by 5 mM dithionite upon 603 nm excitation. The broken line shows the spectrum of the total emission. $H_{\frac{1}{2}}$ did not depend upon the emission wavelength.

Fig. 4B shows $\Delta F/_F$ detected at 890 nm as a function of the magnetic field strength in reduced cells of Rps. sphaeroides 2.4.1 upon 603 nm excitation (●). The shape of the saturation curve was strongly dependent on the excitation wavelength. Excitation in the region of the absorbance spectrum where energy is mainly absorbed by the carotenoid sphaeroidene (430 - 530 nm) showed an initial decrease of the emission in low magnetic field followed by an emission increase in high magnetic field (o, excitation at 515 nm). $H_o$, the magnetic field strength at which no net emission change was observed, shifted as a function of the excitation wavelength. Similar results were obtained

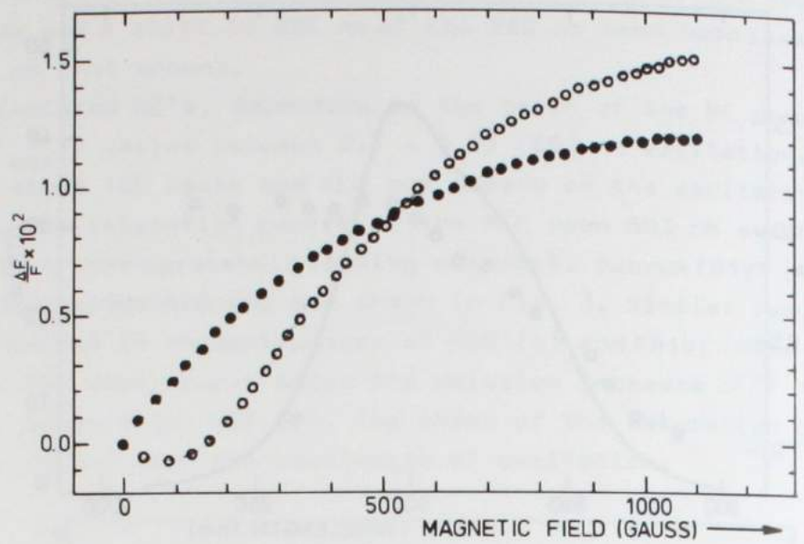


*Fig. 4B. $\Delta F_{max}/F$ detected at 890 nm as a function of the magnetic field strength in the presence of 5 mM dithionite in cells of Rps sphaeroides 2.4.1 upon 603 nm (●) and 510 nm (o) excitation; $A_{850-960\,nm}$ = .3; optical path length 1.0 mm.*

with chromatophores of Rps. sphaeroides 2.4.1.

Fig. 5A shows the ratio $\Delta F_{max}/F$ as a function of the emission wavelength in chemically reduced cells of Rps. sphaeroides G1C (o) and the spectrum of the total emission (solid line) upon 603 nm excitation. $H_{\frac{1}{2}}$ at 603 nm excitation did not depend on the emission wavelength.

Fig. 5B shows $\Delta F/_F$ detected at 890 nm in reduced cells of Rps. sphaeroides G1C as a function of the magnetic field strength upon 603 nm excitation (●) and 494 nm excitation (o). In chromatophores of Rps. sphaeroides G1C similar results were obtained. The upper curve (x) shows $\Delta F/_F$ versus the magnetic field strength in RC'S of G1C, which did not depend upon the excitation wavelength.



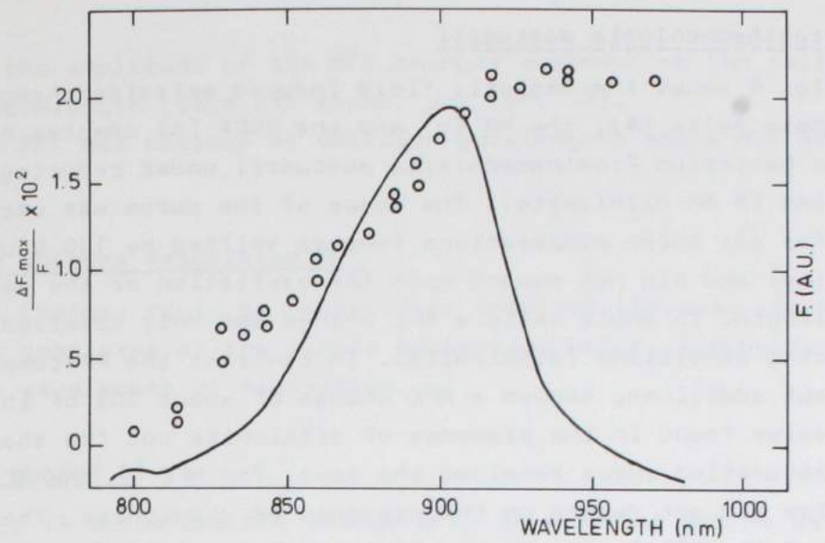


*Fig. 5A. Spectrum of $\Delta F_{max}/F$ (o) and the total emission F (solid curve) in reduced cells of Rps. sphaeroides G1C upon 603 nm excitation. 5 mM dithionite added; $A_{850-960\,nm}$ = 0.3; optical path length 1.0 mm.*

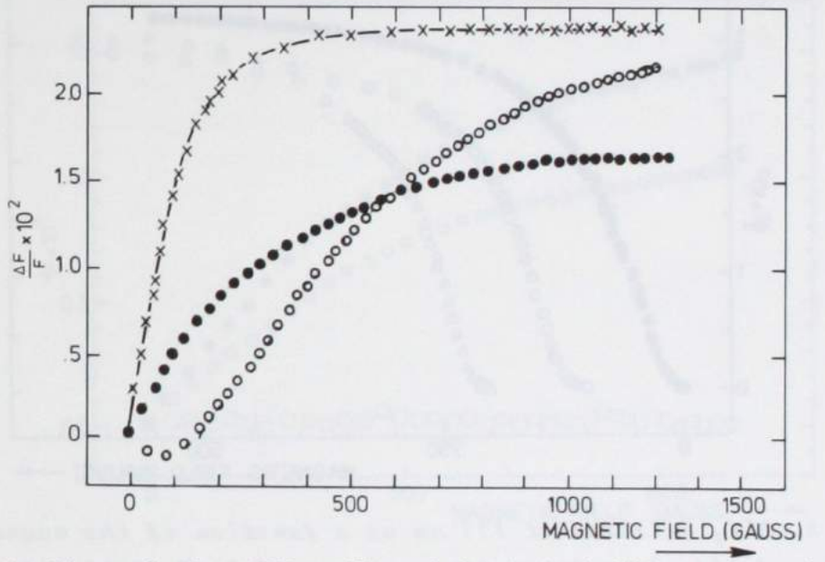


*Fig. 5B. The relative MFE, $\Delta F/_F$, detected at 890 nm as a function of the magnetic field strength in the presence of 5 mM dithionite in cells (●,o) and RC's (x) of Rps. shpaeroides G1C. (●,x) excitation at 660 nm; (o) excitation at 494 nm. $A_{850-960\,nm}$ = .3; optical path length 1.0 mm.*

c. Prosthecochloris aestuarii

Fig. 6 shows the magnetic field induced emission change ΔF/F in whole cells (●), the PP (o) and the RCPP (Δ) complex of the green bacterium Prosthecochloris aestuarii under reducing conditions (5 mM dithionite). The shape of the curve was very similar for all three preparations (curves shifted by 100 Gauss for clarity) and did not depend upon the excitation or the emission wavelength. In whole cells a MFE change was only observed under reducing conditions (dithionite). In contrast the PP-complex, without additions, showed a MFE change of about 30% of the maximum value found in the presence of dithionite but the shape of the saturation curve remained the same. The MFE in the RCPP-complex did not depend on the presence of dithionite. The amplitude of the MFE in the PP and RCPP complex varied from 2 to 6% depending on the preparation. In all preparations (cells, PP and

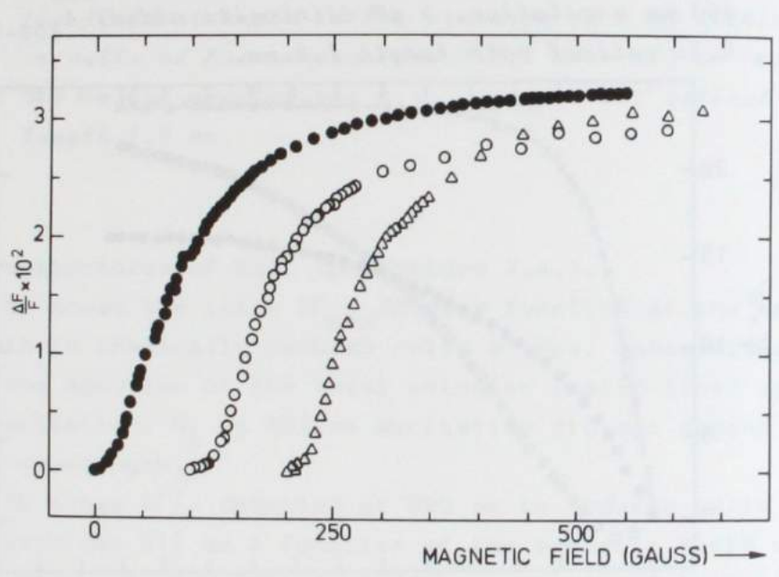


*Fig. 6. $\Delta F/_F$ detected at 853 nm as a function of the magnetic field strength in the presence of 5 mM dithionite in cells (●), the PP-complex (o) and the RCPP-complex (Δ) of Prost. aestuarii. (Curves shifted by 100 Gauss for clarity). $A_{810-960\ nm}$ = .3; optical path length 2.0 mm.*



RCPP) the amplitude of the MFE changes depended on the excitation wavelength (data not shown, see ref. 32).

The MFE was maximum at emission wavelengths above 850 nm.

II The antenna associated MFE

No MFE Changes could be detected in oxidized isolated reaction center complexes of the purple bacteria studied, independent of the wavelength of excitation.

a. R. rubrum S1

Fig. 7A shows the MFE change $\Delta F/_F$ detected at 905 nm as function of the magnetic field strength in oxidized cells (o) and in the isolated B 880 complex (●) of R. rubrum upon 510 nm excitation and 603 nm excitation (□). The dependence of the ratio

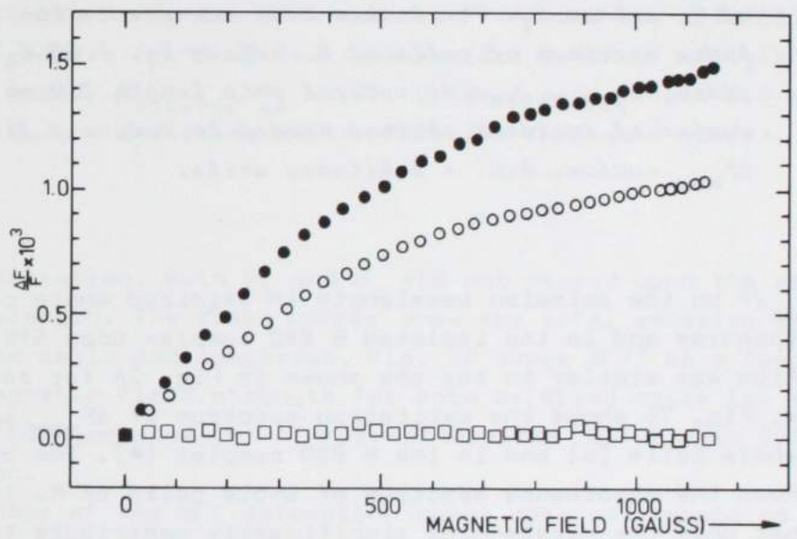


*Fig. 7A. $\Delta F/_F$ detected at 905 nm as a function of the magnetic field strength in oxidized cells (o,□) and in the B880-antenna complex (●) of R. rubrum S1 (●,o) 510 nm excitation.1 mM $K_3Fe(CN)_6$ added. $A_{880-960\ nm}$ = .4; optical path length 2.0 mm. (□) 603 nm excitation.*

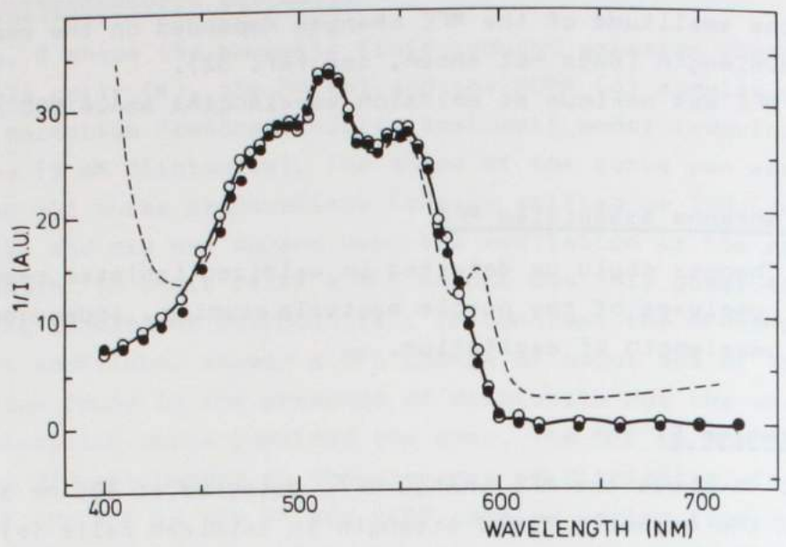


*Fig. 7B. Excitation spectrum of the maximum MFE($\Delta F_{max}$) detected at 905 nm in oxidized cells (o) and the B880 (●) complex of R. rubrum $S_1$. The broken line represents the absorbance spectrum of cells of R. rubrum $S_1$. 1 mM $K_3Fe(CN)_6$ added. $A_{880-960nm}$=.4; optical path length 2.0 mm. I = number of incident photons needed to induce a fixed $\Delta F_{max}$ -value. A.U. = arbitrary units.*

of $\Delta F_{max}/F$ on the emission wavelength in oxidized whole cells, chromatophores and in the isolated B 880 complex upon 510 nm excitation was similar to the one shown in Fig. 2A for reduced samples. Fig. 7B shows the excitation spectrum of $\Delta F_{max}$ in oxidized whole cells (o) and in the B 880 complex (●). The broken line shows the absorbance spectrum of whole cells of R. rubrum. Note that only the carotenoids significantly contribute to the excitation spectrum.

b. Rps. sphaeroides 2.4.1 and G1C

Fig. 8A gives the wavelength dependence of the ratio $\Delta F_{max}/F$ in oxidized cells (●), the isolated B800/B850 complex in LDAO (o) and the B850 complex in LDS (★) of Rps. shpaeroides 2.4.1 upon



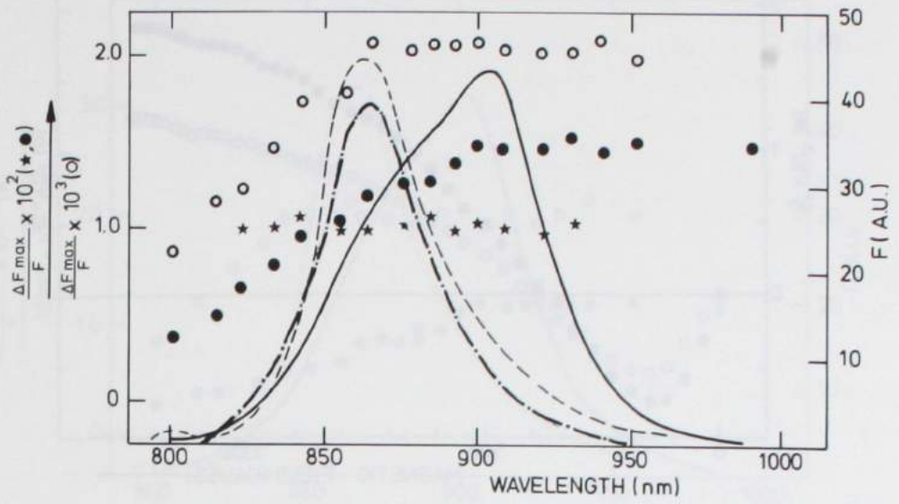


*Fig. 8A. Spectrum of the ratio $\Delta F_{max}/F$ upon 515 nm excitation in oxidized cells (●), the B850 complex (★) and the B800-B850 complex (o) of Rps. sphaeroides 2.4.1. The drawn curves show the total emission (F) spectrum of oxidized cells (—), the B850 complex (---) and the B800/B850 complex (-·-) of Rps. sphaeroides 2.4.1. 1 mM $K_3Fe(CN)_6$ added. $A_{850-960\ nm}$ = .35. Optical path length 2.0 mm. A.U. = arbitrary units. Note the different scales.*

515 nm excitation. Both $H_{\frac{1}{2}}$ and $H_o$ did not depend upon the emission wavelength. The drawn curves show the total emission spectra of the cells and complexes. Fig. 8B shows $\Delta F/F$ as a function of the magnetic field strength for both oxidized cells (o) and the B800/B850 complex (●) of Rps. sphaeroides 2.4.1 upon 515 nm excitation.

The shape of the MFE saturation curve does not depend on the excitation wavelength. The excitation spectrum of $\Delta F_{max}$ in oxidized whole cells is shown in Fig. 8C. The absorbance spectrum of whole cells of Rps. sphaeroides 2.4.1 is indicated by the broken line.

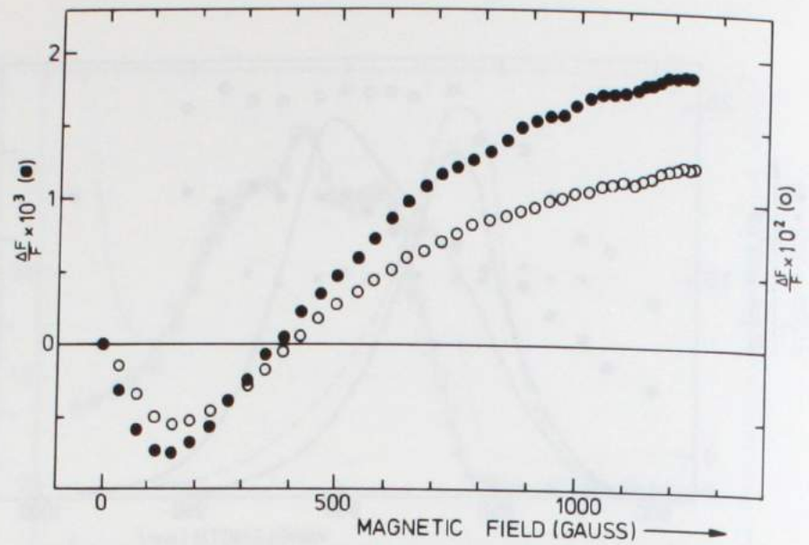


*Fig. 8B. $\Delta F/_F$ detected at 890 nm as a function of the magnetic field strength upon 515 nm excitation in oxidized cells (○) and the B800/B850 complex (●) of Rps sphaeroides 2.4.1 1mM $K_3Fe(CN)_6$ added. $A_{850-960nm}$=.35. Optical path length 2.0 mm. Note the different scales.*

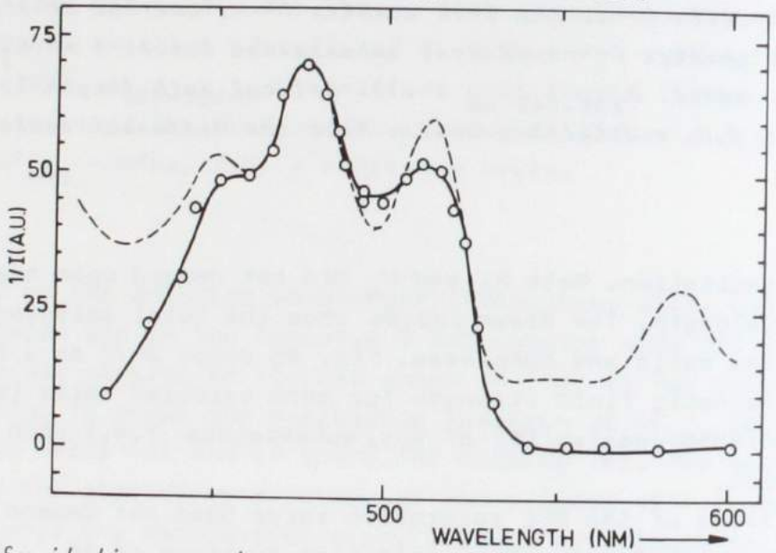


*Fig. 8C. Excitation spectrum of the maximum MFE ($\Delta F_{max}$) detected at 890 nm in oxidized cells (○) of Rps sphaeroides 2.4.1. The broken line indicates the absorbance spectrum of oxidized cells of Rps. sphaeroides 2.4.1. 1 mM $K_3Fe(CN)_6$ added. $A_{850-960nm}$=.35. Optical path length 2.0 mm. I = number of incident photons needed to induce a fixed $\Delta F_{max}$-value. A.U. = arbitrary units.*



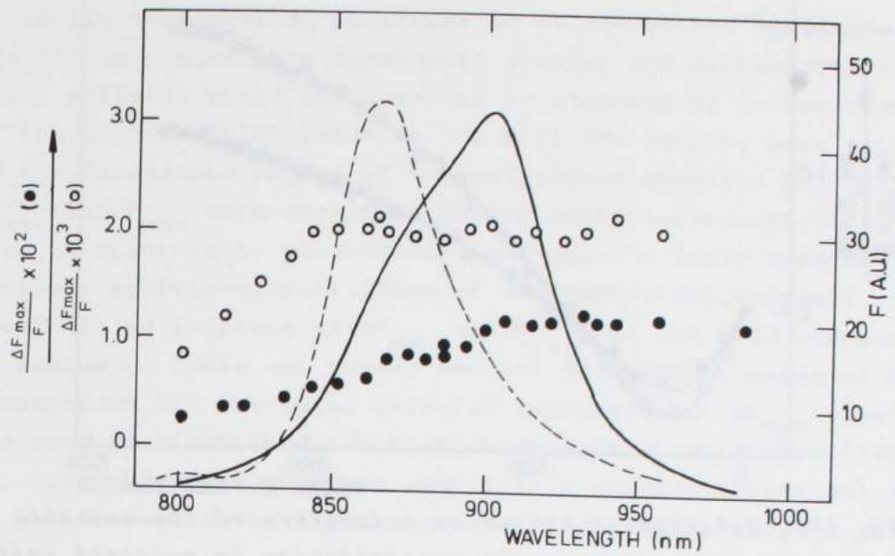


*Fig. 9A. Spectrum of $\Delta F_{max}/F$ upon 494 nm excitation in oxidized cells (●) and the B800/B850 complex(○) of Rps. sphaeroides G1C. The drawn curves show the total emission (F) spectrum of cells (—) and the B800/B850 complex (---) of Rps. sphaeroides G1C. 1 mM $K_3Fe(CN)_6$ added. $A_{850-960\ nm}$ = .33. Optical path length 2.0 mm. A.U. = arbitrary units. Note the different scales.*

The wavelength dependence of the ratio $\Delta F_{max}/F$ in oxidized cells ( ) and the B800/B850 complex (o) of the mutant Rps. sphaeroides G1C upon 494 nm excitation is given in Fig. 9A. The saturation curves show a similar shape as those of the wild type (Fig. 9B). In the carotenoid region of the spectrum, the excitation spectrum (Fig. 9C) follows the absorbance spectrum (broken line). $H_{\frac{1}{2}}$ and $H_o$ both do not depend on the excitation wavelength and the emission wavelength.

c. R. rubrum FR1VI, Rps. sphaeroides R26 and Prosthecochloris aestuarii

In the oxidized cells, chromatophores of R. rubrum FR1VI (Fig. 3), Rps. sphaeroides R26 and the various preparations of Prosthecochloris aestuarii no MFE could be detected.

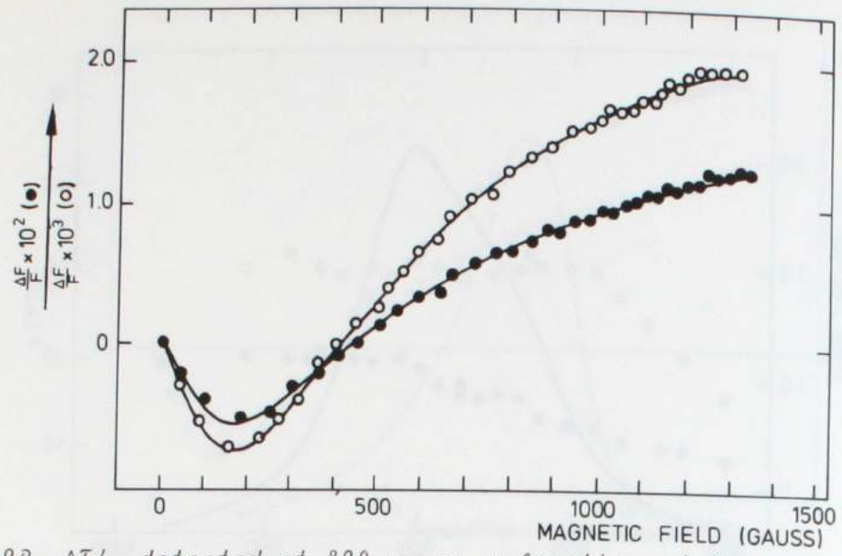


*Fig. 9B. $\Delta F/_F$ detected at 890 nm as a function of the magnetic field strength upon 494 nm excitation in oxidized cells (●) and the B800/B850 complex(○) of Rps.sphaeroides G1C 1 mM $K_3Fe(CN)_6$ added. $A_{850-960nm}$=.33. Optical path length 2mm. Note the different scales.*

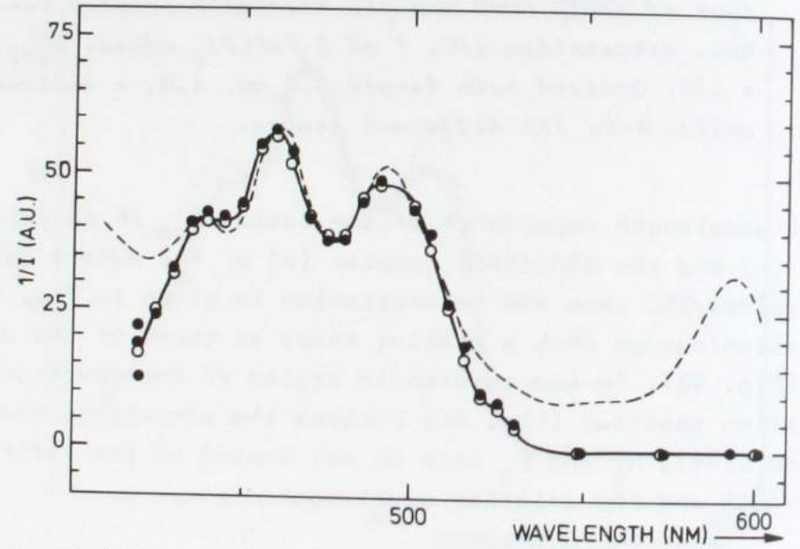


*Fig. 9C. Excitation spectrum of the maximum MFE detected at 890 nm in oxidized cells (●) and the B800/B850 complex (o) of Rps. sphaeroides G1C. The broken line indicates the absorbance spectrum of oxidized cells of Rps. sphaeroides G1C. 1 mM $K_3Fe(CN)_6$ added. $A_{850-960nm}$=.33. Optical path length 2mm. I = number of incident photons needed to induce a fixed $\Delta F_{max}$-value. A.U. = arbitrary units.*



In light-harvesting complexes of R. rubrum and Rps. sphaeroides G1C we checked the hypothesis whether the bacteriochlorophyll emission yield was quenched by products or intermediates of the process which leads to the MFE. The samples were excited in the carotenoid region of the absorbance spectrum and both $\Delta F_{max}$ and $F_{max}$ were detected. If the bacteriochlorophyll emission is quenched by products of the magnetic field dependent process, additional excitation of the bacteriochlorophyll would result in an increase of $\Delta F_{max}$ and $F_{max}$. In the B880 complex of R. rubrum S1 (data not shown) and the B800/B850 complex of Rps. sphaeroides G1C the total emission increases but $\Delta F_{max}$ remains the same upon additional bacteriochlorophyll excitation (Table 1). Upon orientation of the sample in a polyacrylamide gel and / or photoselection by excitation and/or detection through polarization filters, no change in the shape of the saturation curves of $\Delta F_{max}/F$ as a function of the magnetic field strength in the antenna complex of Rps. sphaeroides G1C was observed.

## III Temperature dependence of the MFE changes

In several preparations some crystallization or "cracks" were observed in the samples upon cooling. It is not clear what causes the crystallization or cracks of the samples. The temperature curves shown are the averaged result of 3 independent measurements in completely transparant samples.

### a. R. rubrum S1

In the oxidized samples and in the isolated antenna complexes of R. rubrum S1 the MFE increase did not depend on the temperature between 300 and 77 K. In contrast, $\Delta F_{max}/F$ decreased upon cooling in reduced cells, chromatophores and RC's (Fig. 10A-B). In the isolated reaction centers and in the reduced whole cells upon bacteriochlorophyll excitation, the temperature dependence did not vary with the emission wavelength (840 - 920 nm) and below 150 K no MFE changes clearly different from zero were detected (open symbols). In addition $H_{\frac{1}{2}}$ in these samples did not depend upon the temperature within 5%. However, upon direct caro-

| excitation wavelength (nm) | $\Delta F_{max}$ (a.u.) | $F_{max}$ (a.u.) |
|---|---|---|
| 494 | 5.6 | 2840 |
| 603 | 0 | 1683 |
| 494 + 603 | 5.6 | 4391 |

Table 1.
MFE ($\Delta F_{max}$) and the total emission $F_{max}$ upon 494 nm (16 mW/cm²) or 603 nm (12 mW/cm²) and 494 + 603 nm excitation in the B800-B850 complex of Rps. sphaeroides G1C in the presence of 1 mM $K_3 Fe(CN)_6$. $A_{850}$ = .2. a.u. = arbitrary units.

| | emission wavelength (nm) | | |
|---|---|---|---|
| temperature (K) | 853 | 898 | > 850 |
| 292 | 0.6 % | 1.1 % | 1.0 % |
| 250 | 0.5 % | 0.7 % | 1.1 % |
| 200 | 0.5 % | 0.5 % | 1.0 % |
| 150 | 0.4 % | 0.4 % | 1.0 % |
| 100 | 0.4 % | 0.4 % | 1.0 % |

Table 2.
$\Delta F_{max}/F$ as a function of the temperature and the emission wavelength in oxidized chromatophores of Rps. sphaeroides G1C. Samples ($A_{850}$ = .2) were excited at 494 nm (16 mW/cm²). 1 mM $K_3 Fe(CN)_6$ added. Shape of the saturation curves did not depend upon the temperature or the emission wavelength selected.



tenoid excitation (Fig. 10A, closed symbols) in reduced cells and chromatophores a substantial relative MFE was found below 150 K which remained constant down to 77K, while $H_{\frac{1}{2}}$ shifted from 240 Gauss at room temperature to more than 400 Gauss at 77 K. In the RC's the temperature dependence did not vary with the excitation wavelength between 420 - 650 nm (Fig. 10B).

b. Rps. sphaeroides 2.4.1 and G1C

As in the B880 antenna complex of R. rubrum the relative changes in the isolated B850 and B800/B850 complexes of both strains of Rps. sphaeroides did not depend upon the temperature between 300 and 77 K. In contrast, in oxidized cells of G1C (we did not check strain 2.4.1) the relative MFE decreased upon cooling depending on the emission wavelength (Table 2). The relative MFE in these cells did not depend on the temperature, if the emission was detected through a cut-off filter transmitting wavelengths above 850 nm (Kodak Wratten 87C). The shape of the saturation curves in both the antenna complexes and the oxidized cells did not depend on the temperature.

In reduced RC's $\Delta F_{max}/F$ decreased upon cooling, but $H_{\frac{1}{2}}$ remained constant within 5%, independent of the excitation wavelength. In reduced whole cells or chromatophores upon bacteriochlorophyll excitation $\Delta F_{max}/F$ decreased upon cooling (Figs.10C-D, open symbols) but again $H_{\frac{1}{2}}$ remained the same. Upon direct carotenoid excitation of reduced cells and chromatophores (Figs. 10C-D, closed symbols) the shape of the saturation curve changed drastically upon cooling. At room temperature the curve showed only a small initial emission decrease in low field (see Figs. 4B, 5B open symbols). Below 150 K down to 77 K the magnetic field dependence remained constant and was similar to the curves found in the oxidized samples and the antenna complexes. In the temperature range between 300 and 150 K a continuous change of the shape of the curve was observed.

c. R. rubrum FR1VI and Rps. sphaeroides R26

The temperature dependence of these carotenoid lacking mutants were similar to the dependences found for wild strains under reducing conditions upon selective bacteriochlorophyll

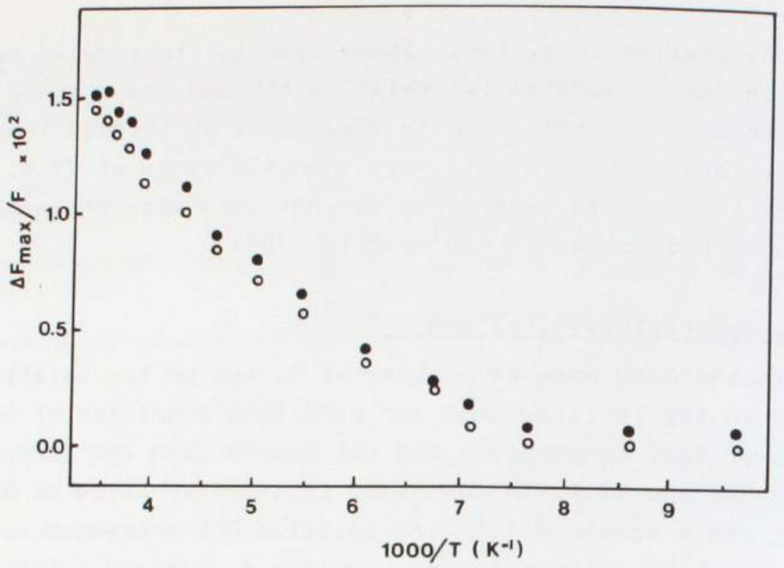


*Fig. 10A.* $\Delta F_{max}/F$ *as a function of the temperature under reducing conditions (5 mM dithionite added) of cells of R. rubrum S1 detected at 905 nm upon 603 nm (o) and 510 nm (●) excitation.*

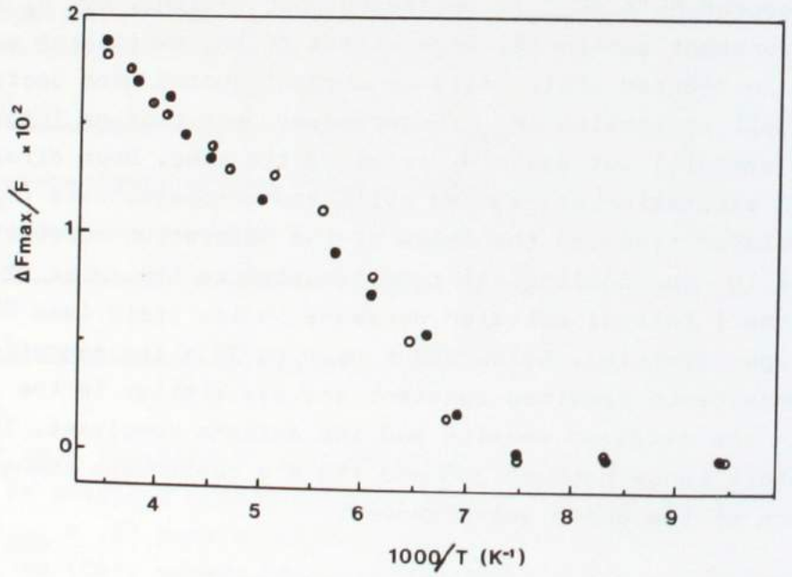


*Fig. 10B. Same as in Fig. 10A but now RC''s of R. rubrum S1 detected at 905 nm upon 603 nm (o) and 510 nm (●) excitation.*



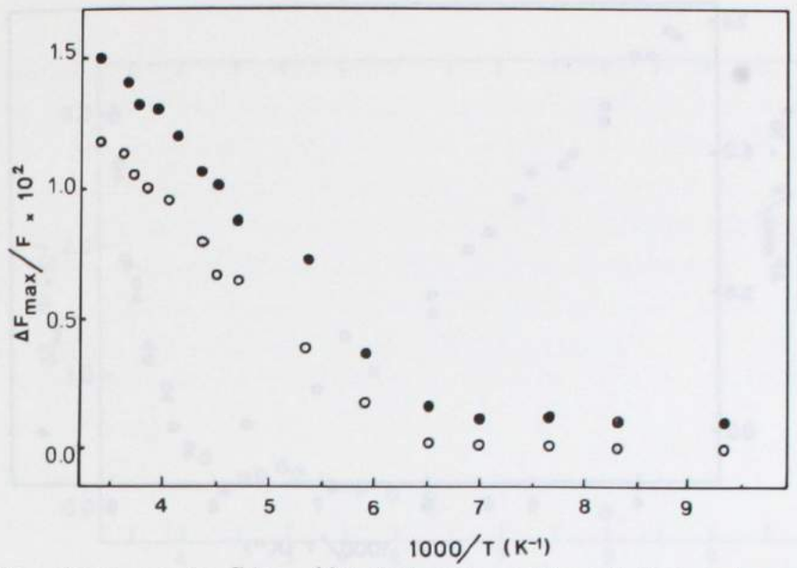


*Fig. 10C. Same as in Fig. 10A but now cells of Rps. sphaeroides 2.4.1 detected at 890 nm upon 603 nm (o) and 515 nm (●) excitation*

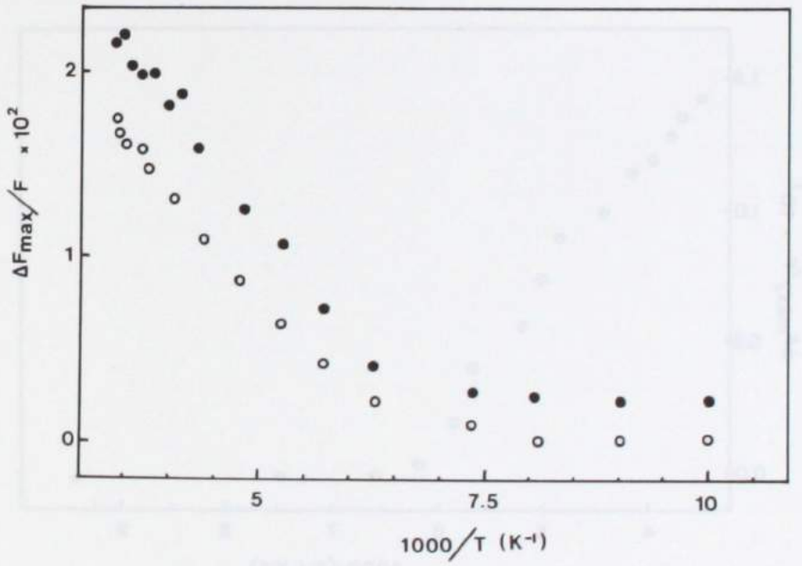


*Fig. 10D. Same as in Fig. 10A but not cells of Rps. sphaeroides G1C detected at 890 nm upon 603 nm (o) and 494 nm (●) excitation.*

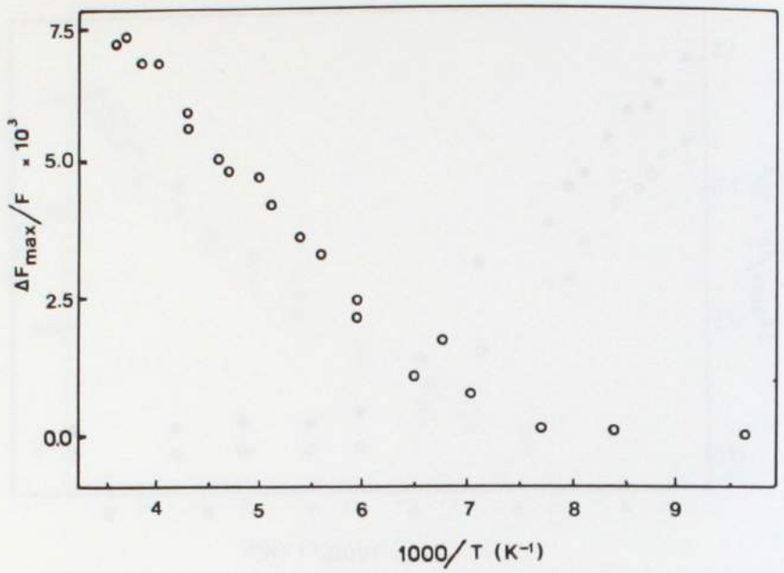


*Fig. 10E. Same as in Fig. 10A but now cells of R. rubrum FR1VI detected at 905 nm upon 603 nm (o) excitation.*

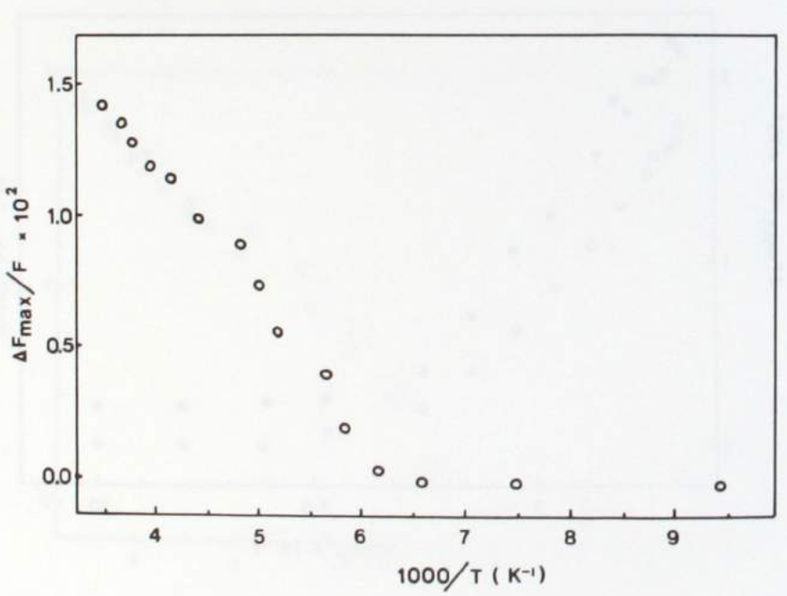


*Fig. 10F. Same as in Fig. 10A but now RC's of Rps. sphaeroides R26 detected at 890 nm upon 603 nm (o) excitation.*



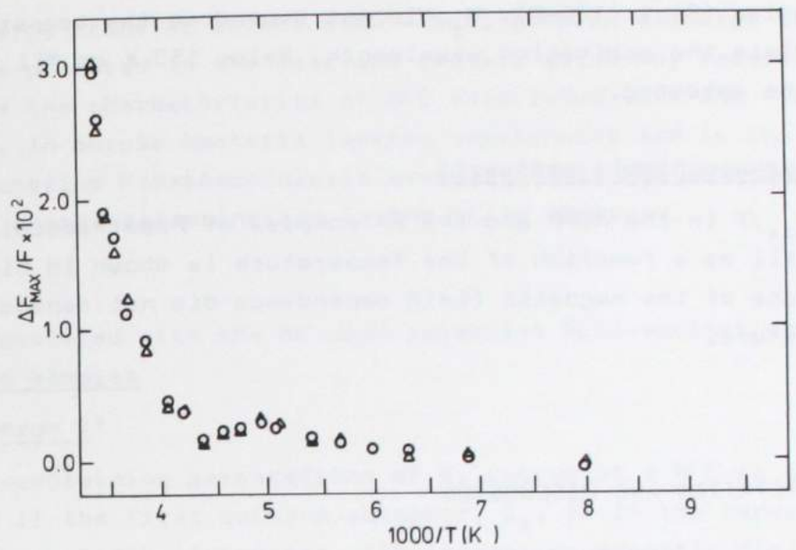


*Fig. 10G. Same as in Fig. 10A but now the PP-complex (Δ) and the RCPP-complex (o) detected at 853 nm upon 669 nm excitation.*

excitation (Figs. 10E-F). $H_{\frac{1}{2}}$ did not depend on the temperature regardless the excitation wavelength. Below 150 K no MFE changes could be detected.

d. Prosthecochloris aestuarii

$\Delta F_{max}/F$ in the RCPP and the PP complex of Prosthecochloris aestuarii as a function of the temperature is shown in Fig. 10G. The shape of the magnetic field dependence did not depend on the temperature.

## INTERPRETATION AND DISCUSSION

We propose that the MFE observed in bacterial photosynthetic systems in a number of preparations and under a variety of conditions can be divided into two categories i.e. reaction center and antenna associated phenomena.

The first category contains the observations of MFE increases in isolated reaction centers of R. rubrum S1, R. rubrum FRVI, Rps. sphaeroides G1C, Rps. sphaeroides R26 and the RCPP-complex of Prosthecochloris aestuarii, that do not depend on the excitation wavelength, are strongly temperature activated (Figs. 2B, 3, 4B, 5B and 6) and are only found if the first quinone acceptor $Q_1$ is reduced (see also ref. 8).

The second category consists of the observation of MFE in whole cells and chromatophores, in which the primary donor $P_{880}$ is oxidized, and in isolated light harvesting complexes of R. rubrum S1, Rps. sphaeroides 2.4.1 and Rps. sphaeroides G1C. MFE is only observed upon direct excitation of the carotenoids (Fig. 7A, 8B, 9B) and does not depend upon the temperature (see below).

In reduced carotenoid containing cells or chromatophores of purple bacteria, MFE usually shows contributions from both categories. Upon carotenoid excitation the excitation transfer process induces MFE changes associated with the second category.



After energy transfer to the B880 – BChl complex a charge separation is produced in the reaction center, which may recombine and shows the characteristics of MFE associated with the first category. In purple bacteria lacking carotenoids and in the green bacterium Prosthecochloris aestuarii only MFE associated with the charge recombination in the RC is observed.

I MFE associated with the RC upon selective BChl-excitation in reduced samples

a. R. rubrum S1

In RC-containing preparations of R. rubrum S1 a MFE is only observed if the first quinone acceptor, $Q_1$, is in the reduced state. The emission increases with increasing magnetic field strength. MFE decreases upon cooling, as does the recombination luminescence [19] and this supports the hypothesis that this category of MFE is correlated with the charge recombination in the RC.

The spectrum of the total emission (prompt plus variable fluorescence) in reduced cells shows a maximum near 905 nm (Fig. 2A) and most likely arises predominantly from the antenna bacteriochlorophyll $B_{880}$, due to a high rate of backtransfer from the excited RC to $B_{880}$ and the abundance of $B_{880}$ over RC's. The ratio $\Delta F_{max}/F$ was independent of the emission wavelength (Fig. 2A), which supports the notion that the antenna of R. rubrum is composed of one major bacteriochlorophyll species. In isolated RC's the emission yield is about 50 times lower as compared to that in cells/chromatophores but the amplitude of $\Delta F_{max}/F$ for RC's (2 - 4%) is of the same order of magnitude as that observed in cells/chromatophores (≃ 1.5%). These data show that rapid energy transfer among antenna molecules and RC's occurs.

The shape of the saturation curves (Fig. 2B) depends on the preparations, pH and time of darkadaptation. In cells/chromatophores a $H_{\frac{1}{2}}$ value of about 240 Gauss is observed while in isolated RC's $H_{\frac{1}{2}}$ is about 100 Gauss and this confirms earlier reports showing marked differences between RC-preparations and more intact systems [2, 3, 5, 8]. In spite of extensive theore-

tical studies concerning the origin of the magnetic field dependence of the charge recombination process [1, 7, 11, 20, 21, 43, 44] no satisfactory explanation for the observed $H_{\frac{1}{2}}$ values in RC's and cells/chromatophores is available. From ESR-data a relatively low exchange interaction of 1 - 5 Gauss has been estimated for the electron spins on $P_{880}^{+}$ and $I^{-}$ [45]
It has been argued therefore that,if the RC-pigment $P_{800}$ acts as an intermediate electron carrier between $P_{880}$ and I and if the electron is delocalized long enough over $P_{800}$ and I a large exchange interaction between $P_{800}$ and $P_{880}$ would prevent a fast dephasing of the electron spins of the radical pair into a triplet state [1, 46] . However indications for the role of $P_{800}$ as an electron carrier between $P_{880}$ and I have only been obtained in isolated RC's [46] , whereas in cells/chromatophores in which even larger $H_{\frac{1}{2}}$ values are obtained requiring even higher values for the exchange interaction or more effective delocalization of the electron on $P_{800}$, no evidence for $P_{800}$ as an electron carrier could be found [47].
Recently we have shown that in several cases a shortening of the $P^{+}I^{-}$ average lifetime either by studying the $P^{+}I^{-}Q_1^{-}$ decay time in the presence of a large number of open traps ($P\ I\ Q_1$) or by applying an electrical field across the membrane leads to a significant increase in observed $H_{\frac{1}{2}}$ [8, 48, 49]. Consequently one may speculate that the increase of the $P^{+}I^{-}$ lifetime in RC's (10 - 15 nS [50]) compared to cells/chromatophores (8 - 10 nS [47]) leads to a decreased $H_{\frac{1}{2}}$ in RC's although the observed decrease seems much toolarge.

However it is not al all clear if the lifetime of $P^{+}I^{-}$ in cells/chromatophores reflects the same mixture of decay processes as in RC's. In several studies we have extensively documented that in cells/chromatophores a significant fraction of the decay of $P^{+}I^{-}$ proceeds via loss processes in the antenna due to rapid back transfer from $P_{880}^{*}$ to $B_{880}$ [8, 19] . In isolated RC's this decay pathway will be about fourty times slower and may be represents only a minor contribution [50], Parson personal communication . The fact that the $P^{+}I^{-}$ lifetimes in the two systems are almost identical suggests that different decay processes operate in isolated RC's compared to cells/chromatophores and



make it therefore complicated to assign $H_{\frac{1}{2}}$ to any specific rate constant in the system (see below).

Upon lowering the pH of the samples of chemically reduced cells/chromatophores to pH = 3, $H_{\frac{1}{2}}$ decreases to about 50 Gauss, again indicating that the $H_{\frac{1}{2}}$ value may be related to some decay process at present not understood. The value $\Delta F_{-max}/F$ increases somewhat, which suggests that the fraction of $P^{+}I^{-}$ decaying via $P880^{*}$ and $B880^{*}$ has increased. In addition it was observed that in cells/chromatophores the P800 absorption band disappears upon lowering the pH to 3.0, making a correlation between the P800 and the reaction center associated MFE even more unlikely. These effects of pH will be fully discussed elsewhere. For the moment it suffices to remark that the $H_{\frac{1}{2}}$ value of 100 Gauss reported by Rademaker et al. for reaction center associated MFE([7],page 43) may be ascribed to the rather high concentration of dithionite (100 mM) in poorly buffering growth medium, which rapidly leads to a large decrease in pH [51] Kingma, H., unpublished results).

b. Rps. sphaeroides 2.4.1. and G1C

Similar to R. rubrum S1, in all reaction center containing preparations of Rps. sphaeroides 2.4.1 and G1C MFE is only found if $Q_1$ has been reduced. The emission increases with magnetic field strength (Figs. 4B and 5B, 603 nm excitation) and $\Delta F_{max}/F$ decreases upon cooling (Figs. 12 and 13, open symbols), again indicating that the observed MFE is closely related to the primary charge recombination in the reaction center.

The spectra of the total emission (Figs. 4A, 5A) show a maximum near 900 nm, a shoulder near 865 nm and a small peak at 800 nm. The antenna of these bacteria is composed of a B800/B850 complex and a B880 complex of which the latter is closely associated with the reaction center [18]. The wavelength dependence of the ratio $\Delta F_{max}/F$ (Figs. 4A, 5A) shows that the MFE is closely related to the B880 emission (neglecting the P880 emission). $\Delta F_{max}/F$ decreases at wavelengths where the B850 emission contributes to the total emission. This indicates that at room temperature energy transfer from the reaction center pigment P880 to the antenna mainly proceeds toward B880 and that only a small

fraction of this excitation energy is transferred to the BChl species emitting at shorter wavelengths. These findings agree with the fact that most of the variable emission observed upon closing the reaction centers ($P880^{+}I\ Q_1^{-}$) is due to B880 and argue against a rapid thermal equilibrium between excitations in B880 and B800/850.

Similar to what was observed for R. rubrum S1 $\Delta F_{max}/F$ is of the same order of magnitude in reaction centers and cells/chromatophores (Fig. 5). The low $H_{\frac{1}{2}}$ values in reaction centers of Rps. sphaeroides G1C may again be ascribed to the absence of energy transfer to the surrounding antenna or changes in conformation due to the isolation procedure, resulting in for example an increase of the effective lifetime of the radical pair state.

The magnetic field dependence of the emission in both Rps. sphaeroides 2.4.1 and G1C does not significantly differ from the one observed in R. rubrum S1, nor does the temperature dependence of $\Delta F/F$ and $H_{\frac{1}{2}}$. Apparently the carotenoid composition, sphaeroidene in 2.4.1 (wild type), neurosporene in G1C and spirilloxanthin in R. rubrum S1 does not affect MFE associated with the reaction center.

c. R. rubrum FR1VI and Rps. sphaeroides R26

In the various preparations of these carotenoid lacking mutants we observed MFE similar to those found in the wild strains (Fig. 3). Only under reducing conditions MFE is observed. Thus the presence of the carotenoid molecules is not required for MFE associated with the primary charge separation and the absence of carotenoids does not significantly affect the $H_{\frac{1}{2}}$ or $\Delta F_{max}/F$ values.

d. P. aestuarii

As in the carotenoidless purple bacteria discussed above, MFE in cells of P. aestuarii is only observed after reduction of the secondary electron acceptor. The presence of MFE in the non-reduced PP and RCPP complex is presumably caused by charge recombination due to a partially disturbed electron transport to secondary electron acceptors [42, 52]. Upon 600 nm excitation the



energy is transferred to the 815 nm emitting BChl species, probably a watersoluble light harvesting BChl a protein [53] and partly to the 838 nm emitting BChl species closely associated with the reaction center [42]. In contrast, upon 670 nm excitation only the 838 nm emission band is excited and no 815 nm emission is found. The maximum MFE is observed upon 670 nm excitation at emission wavelengths above 850 nm, where the 815 nm emission contribution can be neglected. This indicates that MFE is closely associated with the recombination luminescence in the reaction center.

In contrast to the purple bacteria studied, the saturation curves of the MFE are similar for whole cells and the PP and RCPP complex (Fig. 6). The RCPP complex contains about 40 BChl molecules per reaction center [53]. In this respect it resembles more the chromatophore preparations of the purple bacteria and not the isolated reaction center preparations of these species which show a clearly different magnetic field dependence as compared to the more intact preparations. In the PP and the RCPP complex the lifetime of the radical pair is about 30 ns (Van Bochove, A.C. et al, manuscript in preparation ) which is relatively long as compared to the lifetime observed in purple bacteria of about 8 - 10 ns [47]. It seems not unlikely that this long lifetime is the main cause for the low $H_{\frac{1}{2}}$ values observed in the various preparations of P. aestuarii. The lag phase of 10 Gauss found in each preparation, independent of the excitation or emission wavelength, may tentatively be accounted for by assuming an interaction between the electron spins on $P838^{+}$ and $BPheo^{-}$ [1, 20, 21].

II The MFE associated with the antenna complex

In oxidized isolated reaction centers (state $P^{+}I^{-}$) no MFE could be detected neither on carotenoid nor on bacteriochlorophyll excitation. However, in oxidized cells/chromatophores and in isolated antenna complexes of the purple bacteria studied, MFE is observed only upon direct carotenoid excitation but not upon selective BChl excitation. In the oxidized carotenoid lacking mutants no MFE was detected regardless the excitation wavelength

chosen. Therefore the processes described in this section most likely take place in the antenna and require the presence of a carotenoid molecule. The shape of the MFE as a function of the magnetic field strength strongly depends upon the species studied. The MFE associated with the antenna complex is absent in the green bacterium P. aestuarii and preparations therefrom.

a. R. rubrum S1

In R. rubrum S1 MFE is observed in oxidized cells/chromatophores and in the B880 complex upon excitation in the carotenoid region (Fig. 7B). The emission increase (Fig. 7A) applying a field of about 1200 Gauss was about 0.1 - 0.15% and is one order of magnitude smaller than reaction center associated MFE in the same species. This may explain why Rademaker et al. [7] detected no significant MFE in oxidized cells. Because $\Delta F_{max}/F$ is independent of the emission wavelength (not shown), we conclude that the emission predominantly arises from the B880 antenna. For all preparations $H_{\frac{1}{2}}$ exceeded 400 Gauss. These observations agree with earlier reports on MFE in reaction centerless mutants 54 and in cells and antenna complexes of Rps. capsulata([29],Frank, H.A., personal communication). The excitation spectra of $\Delta F_{max}$ in oxidized cells/chromatophores and in the B880 complex (Fig. 7B) are very similar and both closely follow the absorption spectrum in the carotenoid region (peaks at 480, 510 and 550 nm). In oxidized cells/chromatophores of the carotenoidless mutant R. rubrum FRVI no MFE is observed. We therefore conclude that in R. rubrum S1 MFE associated with the antenna exists and that it requires excitation of the only carotenoid present in the antenna, spirilloxanthin. To explain these phenomena either a radical pair mechanism involving a charge separation from the excited carotenoid or a singlet fission mechanism may be proposed. If a radical pair mechanism would be operative, the large $H_{\frac{1}{2}}$ value has to be ascribed to extremely high spin dipole-dipole interactions and/or exchange interactions or a short lifetime of the radical pair [20, 21, 43, 44]. However, Franck and McGaan [54] observed no spin polarized triplet in the ESR spectrum of reaction centerless mutants of Rps. capsulata B41424 and 4142 which indicates



that in this antenna at least the radical pair mechanism is not involved. Recently [55] it was reported that the antenna carotenoid triplet yield in chromatophores of R. rubrum, which partly is formed directly from the excited carotenoid, is formed within 100 ps, which again argues against the formation of the triplet via a radical pair mechanism. For these reasons we will assume that the process of singlet fission is responsible for both the magnetic field dependent antenna carotenoid triplet formation MFT([12], chapter V ; Kingma, H., van Grondelle, R. and Duysens, L.N.M., manuscript in preparation) and the observed MFE. The $H_{\frac{1}{2}}$ values for MFT and MFE are similar. The two members of the triplet pair must both be present in the B880 complex, which contains BChl and spirilloxanthin in a ratio 1 : 1 [56], the minimal unit is probably an octamer of B880 [56]. One of the members of the triplet pair will be spirilloxanthin, the other may be a second spirilloxanthin (homofission) or e.g. bacteriochlorophyll (heterofission).

The total BChl emission is not significantly quenched by products or intermediates of the fission process (Table 1) and the MFE thus arises either from the competition of the energy transfer of excited antenna carotenoid ($ACAR^*$) to BChl and fission or it may (partly) arise from fusion processes if BChl acts as the second partner of the triplet pair (Fig. 1) in the case of heterofission ( $^TACAR \cdot BChl^T$ ). First we will consider the possibility of heterofission, i.e. the triplet pair consists of a spirilloxanthin and a BChl molecule. Most likely aromatic aminoacids such as tryptophan or tyrosin present in the antenna protein complex have a triplet energy that is too high for triplet formation through the triplet pair. The triplet energies, however, of all molecules involved are poorly known and only rough estimates are possible (Moore, T., personal communication). Such an estimate results in an energy of the spirilloxanthin-BChl triplet pair of about 1.6 - 1.7 eV. The first excited singlet states of ACAR and BChl are about 2.2 and 1.4 - 1.55 eV, respectively [57, 58, 59].

However it might be that the triplet pair is not directly formed by fission of the state $CAR^*$. It has been shown [64] that the state $CAR^*$ might rapidly decay into a lower energetic state $CAR^{*'}$, which would have an energy of about 1.65 eV. If the

triplet pair is generated by fission of the state CAR*', which state can not be populated directly from the groundstate [64], fusion from $^{T}CAR \cdot BChl^{T}$ to CAR*' is probably possible (rate constant $K_2$,(Fig. 1). In this case a marked temperature dependence might occur [13], which was not observed. This might indicate that the pair is either generated by fission of the state CAR* directly or that the energy of the pair is less than 1.6 - 1.7 eV (e.g. homofission, see below).

In addition fission of BChl* into the triplet pair state can not be excluded, but the absence of MFE upon specific BChl excitation does not rule out the possibility of heterofission, considering the uncertainty of the energy difference between the triplet pair state and the excited BChl singlet state. However fission is a rather efficient process in organic crystals [13] which could result, in the case of heterofission, in an efficient fusion of the triplet pair state to BChl* (rate constant $k_7$) leading to a decrease of the bacteriochlorophyll emission in high magnetic field: both the rate constants of fission and fusion decrease with increasing magnetic field [13, 25, 27]. An increase of emission is clearly observed, which is also the case if the energy transfer from ACAR* directly to BChl (rate constant $k_d$) is more efficient than through the fission and fusion channel.

In the case of homofission the excitation spectrum (Fig. 7B) indicates that the two molecules involved are both spirilloxanthin. BChl excitation now obviously does not result in singlet fission whereas only the competition between the rate constants $k_1$ and $k_d$ accounts for the MFE increase. Due to the large energy difference between the triplet pair state $^{T}ACAR \cdot ACAR^{T}$ and the state ACAR* of about 2.2 - 1.3 = 0.9 eV [57] no temperature dependence is expected, which fully agrees with our results. The molecules present in the antenna complex are part of a more or less rigid structure and have a fixed orientation with respect to the external magnetic field vector. However, orientation of the sample and/or photoselection did not affect the magnetic field dependence if the direction of the magnetic field vector was altered. Therefore we did not find the low or high resonance as described by Svenberg and Geacintov [13] and Geacintov et al.



[28] for both homo- and heterofission. The simplest explanation is that even with perfect orientation of one chromophore with respect to the orientation axis, the orientation of the second chromophore will be circularly degenerate and destroys the characteristic changes in MFE (Geacintov, N.E., personal communication). In R. rubrum the yield of ACAR decreases with increasing magnetic field strength and a triplet is presumably formed in zero field by fission upon direct carotenoid excitation, considering the difference of the triplet yield of 0.2 upon BChl excitation (state $P880^{+}I\ Q_1$) and 0.3 upon carotenoid excitation [12].

Summarizing we conclude that the process of homofission involving two carotenoid molecules explains the pertinent experimental data, but the process of heterofission involving a carotenoid and a BChl molecule could, with some restrictions with respect to the energetics also account for the MFE observed. The presence of a single triplet formed by fission in zero field, however, seems to exclude the possibility of homofission with a very specific orientation of the molecules involved [13].

b. Rps. sphaeroides 2.4.1 and G1C

As in R. rubrum S1, in both Rps. sphaeroides 2.4.1 and G1C a magnetic field effect originating from a process associated with the antenna is found. MFE observed in cells/chromatophores in the state $P880^{+}I\ Q_1$, in isolated antenna complexes, is only found upon carotenoid excitation and is absent in oxidized reaction centers and the carotenoidless mutant R26. The MFE changes are larger than in R. rubrum which may be related to the differences in energy of the singlet excited states of the carotenoids involved ($E_{neurosporene}^{*} \approx 2.6$ eV, $E_{sphaeroidene}^{*} \approx 2.4$ eV, $E_{spirilloxanthin}^{*} \approx 2.2$ eV) and the triplet pair states ($E_{neurosporene}^{T} \approx 1.9$ eV, $E_{sphaeroidene}^{T} \approx 1.7$ eV, $E_{spirilloxanthin}^{T} \approx 1.65$ eV),([57-59],Frank, H.A., personal communication). It has recently been shown [64] that the first excited singlet state in carotenoids may rapidly decay into a lower energetic state (about 25% lower in energy than the first excited singlet state) which is not accessible by direct excitation. If fission of CAR* into the triplet pair state would occur via this lower

energetic state, fusion (rate constant $k_2$) would become possible.

The MFE in the antenna complexes does not depend upon the temperature (for the temperature dependencies in whole cells and chromatophores see section III). Again the excitation spectra (Figs. 8C, 9C) clearly indicate that at least one molecule of the triplet pair is a carotenoid, sphaeroidene in Rps. sphaeroides 2.4.1 and neurosporene in Rps. sphaeroides G1C. The absence of MFE in oxidized preparations of the carotenoidless mutant R26 confirms the conclusion that the carotenoids play a major role in these processes.

The shapes of the MFE saturation curves (Figs. 8B, 9B) markedly differ from the curves found in the reduced samples. A significant initial decrease of MFE is apparent at field strengths below 400 Gauss. This initial decrease in low field very nicely agrees with the MFE changes observed in organic crystals [13, 26]. The complex curve can be explained by a process of homofission, but if the molecules involved have similar D and E values, a process of heterofission may give a similar result. As has recently been shown([31], chapter V) the carotenoid triplet yield in the B880/850 complex of Rps. sphaeroides 2.4.1 and of Rps. sphaeroides G1C is similar upon BChl and upon carotenoid excitation (≃ 1.4 - 1.6%). Upon direct carotenoid excitation a magnetic field induced increase of the triplet yields in low field is found, whereas the triplet yields in zero field and high field are about the same. Upon BChl excitation no magnetic field effect clearly different from zero was found. These phenomena agree with a process of homofission involving two carotenoid molecules with a special mutual orientation, where no single triplet state can be formed in zero magnetic field by the fission process. In this special case, the substates of the pair have either pure triplet, pure quintet or mixed singlet-quintet character [13]. Because fission is a spin conserving process no single triplet (e.g. $CAR^T$) can be formed from an excited singlet state (CAR*) if no substate with a mixed singlet - triplet state is present. Similar as in R. rubrum the absence of a MFE change of a MFT upon BChl excitation and the fact that MFE is constant as a function of the temperature in the antenna complexes, is well explained by a process of homofission for which



no energetical considerations are required, as for the heterofission case. Assuming homofission, at low field the emission decreases and the triplet yield increases due to the mixing-in of singlet and triplet character in the substates of the pair. As the field strength increases the number of substates with singlet character decreases again and so does the rate constant of fission resulting in a decrease back to zero of the triplet yield formed by fission and an increase of the emission yield as compared to that in zero field.

The spectra of the ratio $\Delta F_{max}/F$ in several preparations of Rps. sphaeroides 2.4.1 and G1C together with the total emission spectra indicate that in intact cells/chromatophores the main contribution to the MFE is from the B880 complex. In chromatophores of Rps. sphaeroides WT which were prepared from cells that were specially grown to obtain a relatively large B880 complex as compared to the B850 complex (a generous gift from Dr. Niedermann), the ratio $\Delta F_{max}/F$ at 900 nm is about 5 times larger as compared to the ratio at 850 nm. This again indicates the important role of the B880 complex in the fission process. The B880 complex consists of a minimal unit of 6 BChl molecules[60] and 3 carotenoids, which on the basis of their CD spectra show relatively strong interactions[60]. The relatively low efficiency of energy transfer (60%) may be in agreement with the strongly competing fission process. In B800/850 MFE very similar to that found in cells/chromatophores is also observed, but its contribution is apparently smaller in the intact cells/chromatophores compared to the B880 contribution. The experiments suggest a major role for the carotenoid associated to B850. Homofission would require at least two strongly coupled carotenoid molecules in a unit of B800/850. This is not in contradiction with spectroscopic data, which suggests, that the minimal functioning unit of B800/850 contains at least 3 carotenoid molecules, 2 associated to the four B850-BChl molecules and one associated to the two B800-BChl molecules [60]. The higher efficiency of energy transfer from carotenoid to BChl (> 90%) also suggests a much weaker competing fission process in this antenna complex.

III The temperature dependence of the MFE

Although the integrated spectrum of the ratio $\Delta F_{max}/F$ in oxidized chromatophores/cells of Rps. sphaeroides G1C was independent of the temperature between 77 and 300 K, the shape of the spectrum drastically changed upon cooling (Table 2). However, based upon the results in oxidized chromatophores of R. rubrum and the isolated B880, B800/850 and B850 complexes we assume that the fission process in R. rubrum S1, Rps. sphaeroides 2.4.1 and G1C does not depend on the temperature. The temperature dependence of the MFE associated with the antenna process in cells and chromatophores of Rps. sphaeroides is then thought to be due to changes of the total emission spectrum. The absence of a temperature dependence of the MFE may be ascribed to a low rate constant $k_2$ of fusion (Fig. 1) and a low rate constant of fission $k_8$ (in the case of heterofission) resulting in only downhill reactions ($k_1$, $k_3$, $k_5$, $k_6$, $k_7$).

The MFE changes in the reduced samples upon BChl excitation (Figs. 2B, 4B, 5B, 6) which are selectively associated with the charge recombination of the radical pair, decrease upon cooling. Below 150 K no MFE can be detected upon carotenoid excitation; below 150 K we are left with the singlet fission process (Figs. 2B, 4B, 5). In agreement with others (Boxer, G., personal communication) we found that the $H_{\frac{1}{2}}$ values of the reaction center associated MFE in all preparations studied do not depend upon the temperature. In chromatophores of R. rubrum the decay time of the recombination luminescence (≃ 8 ns [47]) does not depend on the temperature between 77 and 300 K, whereas the amplitude decreases upon cooling. In contrast the reduction of the oxidized primary donor by charge recombination in reduced samples ($P880\ I\ Q_1^-$) increases from 10 ns at 300 K to about 25 ns at 77 K [47, 49]. These seemingly conflicting data can be explained by assuming at least two substates of $P^+I^-$ with slightly different energy (Van Bochove, A.C. et al., manuscript in preparation); this suggestion is analogous to the scheme used by Parson et al. [50] to explain the multiphasic decay of the luminescence in isolated reaction centers. The presence of several substates of $P^+I^-$ may eventually lead to an explanation of the discrepancies between the observed $H_{\frac{1}{2}}$ values for MFE and the measured $P880^+I^-$



lifetimes. It seems not impossible that $H_{\frac{1}{2}}$ is associated with the lifetime of the luminescence, both being constant as a function of the temperature.

The decrease of $\Delta F_{max}/F$ seems to be correlated with the decrease of the amplitude of the recombination luminescence upon cooling and should therefore reflect the energy difference between the states $P880^*I$ and $(P800^+I^-)^S$. If we assume that the MFE arises from recombination of the radical pair state, and that the magnetic field dependence can be roughly described by an apparent decrease, $\Delta k_T$ of the rate constant $k_T$ reflecting the decay of the state $(P800^+I^-)^S$ to a triplet state and if k represents the rate of energy transfer from $(P880^+I^-)^S$ to $B880^*$, the enthalpy difference ΔH can be calculated using the following equation:

$$\frac{\Delta F_{max}}{F} = \frac{\Delta k_T \; k \; e^{-\Delta H/kT}}{k_T(H)\{k_T(H = 0) + k \; . \; e^{-\Delta H/kT}\}}$$

If the energy trapped by the reaction center is rapidly transferred back to the surrounding antenna we find $k \simeq k_c$; if the energy in contrast is very efficiently trapped and is predominantly located in the reaction center, we find $k \approx k_h$ (Fig. 1). If we assume $100 \leq k/k_T \leq 10000$ the experimental results (Figs. 10A-G) can be fitted by $\Delta K_T/K_T = 0.02 \pm 0.01$ and $H = 0.12 \pm 0.03$ eV in the purple bacteria and $\Delta H = 0.25 \pm 0.05$ in P. aestuarii. The low ΔH values are obtained for $k/k_T \simeq 100$, i.e. if $k \approx k_c$. This result reasonably agrees with similar calculations involving the temperature dependence of the recombination luminescence $\Delta H = 0.11 - 0.15$ eV [19] in purple bacteria. This confirms that the amplitude of MFE is associated with the same state of $P800^+I^-$ that governs the total luminescence amplitude. The temperature dependence of the MFE in P. aestuarii (Fig. 10G) markedly differs from that found in the purple bacteria (Figs. 10A-F). For P. aestuarii an activation energy of 0.2 - 0.3 eV is calculated using $k/k_T > 100$. The relatively low energy level of the state

$(P^+I^-)^S$ compared to the energy level of the state P*I may also account for the long lifetime of the recombination luminescence [47] and the low $H_{\frac{1}{2}}$ values observed (Fig. 6).

## IV MFE in reduced samples upon carotenoid excitation

If in reduced cells/chromatophores of R. rubrum S1, Rps. sphaeroides 2.4.1 or G1C MFE is induced by direct carotenoid excitation, complex saturation curves are found (Fig. 4B, 5B). In R. rubrum $H_{\frac{1}{2}}$ shifts from 240 to 290 Gauss and $\Delta F_{max}/F$ slightly increases depending upon the excitation wavelength (420 - 570 nm). Under these circumstances both the singlet fission process in the antenna and the charge recombination in the reaction center contribute to ΔF/F. The relative contribution depends on the ratio of the quanta absorbed by the carotenoid and BChl. Because of the different shape of the saturation curves of the two processes in Rps. sphaeroides (Figs. 4B, 5B, 8B, 9B) these phenomena are more clearly observed in this bacterium. Several investigations [4, 7, 8] were done under these circumstances, which have to be interpreted not only in the light of the radical pair mechanism but also considering the fission process. First the absence of MFE in oxidized samples upon BChl excitation reported earlier in some preparations [7, 8] does not implicate, was concluded, that MFE is only present in reduced samples. We have shown in contrast that MFE can be induced upon carotenoid excitation in oxidized samples ([29, 30], this work). The initial decrease of MFE in low field observed in several bacteria under reducing conditions ([7, 8] Figs. 4B, 5B) are not associated with the reaction center as has been suggested by Elfimov et al. [64] or by interaction with the energy transfer ([62], Frank, H.A., personal communication), but arise exclusively from the fission process in the antenna. The temperature dependences of MFE and $H_{\frac{1}{2}}$ reported [3, 4] reflect both the reaction center and the antenna associated processes due to the direct carotenoid excitation. For instance, the increase of $H_{\frac{1}{2}}$ between 250 and 77 K reported by Rademaker et al. (Fig. 4b of ref. 3) was found to be due to the elimination of the reaction center contribution with a relatively low $H_{\frac{1}{2}}$ value upon cooling. The initial high value of 500



Gauss at 300 K (obtained from Fig. 3B of ref. 3) and the estimated decrease of $H_{\frac{1}{2}}$ between 320 K and 250 K are due to an incorrect interpretation of $H_{\frac{1}{2}}$ for the complex saturation curves upon carotenoid excitation. The temperature dependence of MFE reported by Rademaker et al. (Fig. 4A of ref. 3) is different from our results and reflects probably both categories of MFE. The remaining MFE at temperatures below 150 K has to be ascribed to the MFE associated with the antenna and/or orientational effects. In Chlorella vulgaris and spinach chloroplasts (Figs.5A and 5B of ref. 3)extremely high $H_{\frac{1}{2}}$ values of about 1000 Gauss were observed. Again, this may be ascribed to orientational effects in the stationary magnetic field applied or an antenna associated MFE could be present too. The MFE increase in PS I spinach particles measured by a 50 Hz modulated field indeed showed lower $H_{\frac{1}{2}}$ values of about 300 - 650 Gauss [63]. Recently Elfimov et al. [29] suggested that the singlet fission process in non-sulfur bacteria (e.g. Rps. capsulata) depends upon the temperature, but these results [61] were obtained under conditions where both the antenna and the reaction center associated processes were excited. In addition, as was discussed in section II, changes of the total emission spectrum could also account for the temperature dependence observed. The temperature curves shown in Figs. 10 - 15 clearly indicate the difference of the temperature dependence between BChl and carotenoid excitation. In the latter case both categories of MFE are observed.

## SOME CONCLUDING REMARKS

From our results we concluded that the fission process is operative in both the B850 and the B880 complex. It is remarkable that the shape of the saturation curves observed in Rps. sphaeroides in whole cells/chromatophores and the various antenna complexes, in Rps. capsulata [29, 62] and in organic crystals like anthracene or pentacene doped tetracene [13, 26] are very similar. The $H_o$ values are about 400 Gauss. Apparently these curves do not

strongly depend upon the type of molecules involved or the type of fission process (homo- or heterofission). However, in contrast the saturation curves observed in the B880 complex and oxidized cells/chromatophores of R. rubrum are clearly different from the curves found in the various species of Rhodopseudomonas and in organic crystals. In addition the yield of the carotenoid triplet formed by fission is high in R. rubrum (≈ 0.3), very low in Rps. sphaeroides 2.4.1 and G1C (< 0.01) (Kingma, H., van Grondelle, R. and Duysens, L.N.M.,

but again high in organic crystals [13]. Besides the structural differences of the antenna between the two families, the energy transfer efficiencies are very different too (30% in R. rubrum and about 90% in Rps. sphaeroides [12, 60]. So it is not at all clear what causes the observed differences of the saturation curves between R. rubrum and the various Rhodopseudomonaceae. The efficient triplet formation in R. rubrum by fission of carotenoid singlet energy does not quench the bacteriochlorophyll triplet formation and therefore does not prevent photodestruction of the antenna by excited oxygen. Spirilloxanthin protects the organism against photodestruction (by triplet energy transfer from $BChl^T$ to CAR) but the energy absorbed upon direct excitation is predominantly lost by internal conversion and triplet formation (singlet fission) while only 20-30% of the energy absorbed is used for photosynthesis,or in the case of heterofission, fusion of the triplet pair to BChl* might act as a route for energy transfer from the antenna carotenoids to BChl.
On the other hand one might speculate that the presence of a carotenoid in R. rubrum might have a function in preventing other carotenoid containing bacteria, in mixed cultures, from overgrowing R. rubrum by additional light absorption in the carotenoid region of the spectrum.

The temperature dependence of the relative MFE, $\Delta F_{max}/F$, can very well be described with the formula derived in section III. The simplified scheme of energy transfer in the reaction center used is similar to the scheme proposed in a previous paper [8] and although is has no specific physical meaning with respect to the underlying mechanism of the magnetic field dependence of the process of singlet-triplet mixing, it yields activation



energies which agree with earlier reports. In contrast, more elaborate models, incorporating the specific magnetic properties of the charge separation in the reaction center, could so far only partly explain the experimental results obtained earlier [1,7]. However, the discrepancies between the theoretically calculated values and the experimentally observed values may at least partly be caused by misinterpretation of the experimental data.

REFERENCES


1. Hoff, A.J. (1981) Quarterly Reviews of Biophysics 14, 4: 599-665
2. Voznyak, W.M., Elfimov, E.I. and Proskuryakov, I.I. (1978) Doklady Akad. Nauk. SSSR 242, 1200-1203
3. Rademaker, H.,Hoff, A.J. and Duysens, L.N.M. (1979), Biochim. Biophys. Acta 546, 248-255
4. Voznyak, W.M., Ganago, I.B., Moskalenko, A.A. and Elfimov, E.I. (1980) Biochim. Biophys. Acta 592, 364-368
5. Kingma, H., Duysens, L.N.M. and Peet, H. (1980) in Photosynthesis (Akoyunoglou, G., ed.), Vol. III, 981-988, Balaban Int. Science Services, Philadelphia, Pa.
6. Sonneveld, A., Duysens, L.N.M. and Moerdijk, A. (1980) Proc. Nat. Acad. Sci. USA 77, 5889-5893
7. Rademaker, H. (1980) Thesis, University of Leiden.
8. Kingma, H., Duysens, L.N.M. and van Grondelle, R. (1983), Biochim. Biophys. Acta. -in the press- chapter
9. Blankenship, R.E., Schaafsma, T.J. and Parson W.W. (1977) Biochim. Biophys. Acta 461, 297-305
10. Hoff, A.J.,Rademaker, H., van Grondelle, R., and Duysens, L.N.M. (1977) Biochim. Biophys. Acta 460, 547-554
11. Adrian, F.J. (1977) in Chemically Induced Magnetic Polarization, eds. Muus, L.T.,Atkins, P.W., McLaughlan., K.A. and Pederson, J.B. (Reidel, Dordrecht, The Netherlands), 77-105
12. Rademaker, H., Hoff, A.J., van Grondelle, R. and Duysens, L.N.M. (1980) Biochim. Biophys. Acta 592, 240-257
13. Svenberg, C.E. and Geacintov, N.E. (1973) in Organic Molecular Photophysics, Vol. 1 (J.B. Birks, ed.), 489-564
14. Dutton, P.L., Kaufman, K.H., Chance, B. and Rentzepis, P.M. (1975) FEBS Lett. 60, 275-280
15. Shuvalov, V.A. and Klimov, V. (1976) Biochim. Biophys. Acta 461, 297-305
16. Fajer, J., Brune D.C., Davis, M.S., Forman, A. and Spaulding L.D. (1975) Proc. Nat. Acad. Sci. USA 1972, 4956-5960
17. Van Grondelle, R. (1978) Thesis, University of Leiden





18. Van Grondelle, R., Kramer, H.J.M. and Rijgersberg, C.P. (1982) Biochim. Biophys. Acta 682, 208-215
19. Van Grondelle, R., Holmes, N.G., Rademaker, H., and Duysens, L.N.M. (1978) Biochim Biophys. Acta, 503, 10-25
20. Werner, H.J., Schulten, K. and Weller, A., (1978) Biochim. Biophys. Acta, 502, 255-268
21. Norris, J.R., Bowman, M.K., Budil, D.E., Tang, J., Wraight, C.A. and Closs, G.L. (1982) Proc. Natl. Acad. Sci. USA 79, 5532-5536
22. Parson, W.W. and Monger, T.G. (1976) Brookhaven Symp. Biol. 28.
23. Vredenberg, W.J. and Duysens, L.N.M. (1963) Nature 197, 355-357
24. Johnson, R.C., Merrifield, R.E., Aviakan, P. and Flippen, R.B. (1967) Phys. Rev. Lett. 19, 285-287
25. Merrifield, R.E. (1968) J. Chem. Phys. 48, 4318-4319
26. Geacintov, N.E., Burgos, J., Pope, M. and Strom, C. (1969) Chem. Phys. Letters 11 : 4, 504-508
27. Merrifield, R.E., Aviakan, P. and Groff, R.P. (1969) Chem. Phys. Lett. 3, 155-157
28. Geacintov, N.E., van Nostrand, F., Pope, M. and Tinkel, J.B. (1971) Biochim. Biophys. Acta 226, 486-491
29. Elfimov, E.I., Voznyak, V.M. and Prokhorenko, I.R. (1982) Doklady Akad. Nauk, 164, 248-255
30. Frank, H.A., McGann, W.J.,Macknicki, J. and Felber, M. (1982)Biochem.Biophys. Res. Commun. 106, 1310-1317
31. Kingma, H., van Grondelle, R., Duysens, L.N.M., van der Kooy, F.W. and Vos, M. (1983). Proc. VIth Int. Congr. Photosynth. Brussels, in the press
32. Cohen-Bazire, Sistrim, W.R. and Stanier, R.Y. (1957) J. Cell Comp. Physiol. 49, 25-60
33. Slooten, L. (1972) Biochim Biophys. Acta 256, 452-466
34. Matthews, B.W., Fenna, R.E., Bolognesi, M.C., Schmid, M.F. and Olson, J.M. (1979) J. Mol Biol. 131, 259-285
35. Holt. S.C., Conti, S.F. and Fuller, R.C. (1966) J. Bacteriol. 91, 311-323
36. Slooten, L. (1973) Thesis, University of Leiden.

37. Kendall-Tobias, M.W. and Seibert, M. (1982) Arch. Biochem. Biophys. 216 : 1, 255-258
38. Swarthoff, T.and Amesz, J. (1979) Biochim Biophys. Acta 548, 427-432
39. Clayton, R.K. and Clayton, B.J. (1972) Biochim. Biophys. Acta 283, 492-501
40. Cogdell, R. and Thornber, J.P. (1979) CIBA Symp. 61, 61-73
41. Abdourakhmanov, I.A., Ganago, A.O., Erokhin, Y.E., Solov'ev, A.A. and Shuganov, V.A. (1979) Biochim Biophys. Acta 546, 183-186
42. Kramer, H.J.M., Kingma, H.,Swarthoff, T. and Amesz, J. (1982) Biochim. Biophys. Acta 681, 359-364
43. Ogrodnik, A., Krueger, H.W., Orthuber, H., Haberkorn , R. and Michel-Beyerle, M. (1982) Biophys. J. 39, 91-99
44. Michel-Beyerle, M.E., Scheer, H., Seidlitz, H. and Tempus, D. (1980) FEBS Lett. 110, 129-132
45. Hoff, A.J. and Gast, P. (1979) J. Phys. Chem. 83: 3355-3358
46. Shuvalov, V.A., Klevanik, A.V., Sharkov, A.V., Matveetz, Yu.A. and Krukov, P.G. (1978) FEBS Lett. 91, 135-139
47. Van Bochove, A.C., Swarthoff, T., Kingma, H., Hof , R.M., van Grondelle, R., Duysens, L.N.M. and Amesz, J. (1983) Biochim. Biophys. Acta, in the press
48. Van der Wal, H.N., van Grondelle, R., Kingma, H. and van Bochove, A.C. (1982) FEBS Lett. 145, 155-159
49. Van Bochove, A.C., van Grondelle, R., Hof, R.M. and Duysens, L.N.M. (1983). Proc. VIth Int. Congr. Photosynth. Brussels, in the press
50. Parson W.W. (1983) VIth Int. Congr. Photosynth. Brussels
51. Mayhew, S.G. (1978) Eur. J. Biochem. 85, 535-547
52. Swarthoff, T. (1982) Thesis, University of Leiden
53. Olson, J.M. (1981) Biochim. Biophys. Acta 637, 185-188
54. Duysens, L.N.M. (1952) Thesis, University of Utrecht
55. Nuys, A.M., van Bochove, A.C., Joppe, H.L.P. and Duysens, L.N.M. (1983) Proc. VIth Int. Congr. Photosynth. Brussels
56. Kramer, H.J.M., van Grondelle, R., Hunter, C.N. and Amesz, J. (1983) Proc. VIth Int. Congr. Photosynth. Brussels, in the press
57. Bensasson, R., Land, E.J. and Maudinas, B. (1976) Photochem. Photobiol. 23, 189-193



58. Lebedev, N.N. and Krasnovskii,A.A. (1979) Biophysics 23, 1115-1117
59. Seely, G.R. (1978) Photochem. Photobiol. 27, 639-654
60. Lersch, W. and Michel-Beyerle, M.E. (1983) Chem Phys. Lett. 78, 115-126
61. Elfimov, E.I., Kazantsev , A.P. and Proskuryakov, I.I. (1980) Zh. Prikl. Spektrosk., 33 : 3, 439-443
62. Frank, H.A. and McGann, W.J. (1983) Proc. VIth Int. Congr. Photosynth. Brussels, in the press
63. Sonneveld, A., Duysens, L.N.M. and Moerdijk, A. (1981), Biochim, Biophys. Acta 636, 39-49
64. Trash, R.J., Fang,B.L. and Leroi, G.E. (1979) Photochem. Photobiol. 29, 1049-1050

# FORMATION OF TRIPLET STATES IN THE REACTION CENTER AND THE ANTENNA OF RHODOSPIRILLUM RUBRUM AND RHODOPSEUDOMONAS SPHAEROIDES. MAGNETIC FIELD EFFECTS.

H. Kingma, R. van Grondelle and L.N.M. Duysens, Department of Biophysics, Huygens Laboratory of the State University, P.O.Box 9504, 2300 RA Leiden, The Netherlands.

## SUMMARY

In cells, chromatophores, isolated reaction centers and isolated antenna complexes of various strains of Rhodospirillum rubrum and Rhodopseudomonas sphaeroides, we determined by absorbance difference spectroscopy the triplet yield, $\phi_t$, induced by a laser flash, as a function of the strength of a magnetic field, the redox state of the reaction center, the temperature and the excitation and detection wavelength. Three categories of triplet formation can be distinguished.

Category I is caused by the charge recombination of the triplet state of the radical pair in the reaction center. The triplet yield decreases in a magnetic field and increases upon cooling. The magnetic field dependence of $\phi_t$ is complementary to that of the magnetic field induced bacteriochlorophyll emission (MFE) change, associated with the reaction center (see Chapter IV) and is discussed in terms of the radical pair mechanism.

Category II is formed in the antenna complex of the carotenoid containing purple bacteria. The triplet yield depends on the strength of a magnetic field, but does not vary with the temperature in isolated antenna complexes between 100 and 300 K. The triplet is only formed upon direct antenna carotenoid excitation and is not observed in isolated reaction centers. The triplet formation is closely related to the antenna associated MFE (see Chapter IV) and is discussed in terms of the process of singlet-fission of the excited carotenoid singlet state into a triplet pair. Homofission, involving two carotenoid molecules explains all the pertinent data.

The triplet of the third category is formed upon both carotenoid and bacteriochlorophyll excitation in the antenna complex of all bacteria studied. The triplet yield in isolated antenna complexes does not depend on the temperature. No effect of a magnetic field upon the triplet yield is observed. The triplet formation is probably due to intersystem crossing of bacteriochlorophyll, followed by triplet energy transfer to an antenna carotenoid molecule, if present.

Upon carotenoid excitation of reduced cells/chromatophores all three categories are observed. The results of this study are summarized in table 1 (see discussion).



## INTRODUCTION

Several years ago Blankenschip et al [1]. showed that the yield of the triplet state that is formed in reduced isolated reaction centers (RC's) of Rhodopseudomonas sphaeroides R26 depends on the presence of a magnetic field. Qualitatively similar results were obtained in reduced isolated RC's, chromatophores and cells of Rps. sphaeroides 2.4.1 and Rhodospirillum rubrum S1 [2,3]. The process of triplet formation and the magnetic field dependent triplet (MFT) yield were discussed in terms of the so-called radical pair mechanism [4, 5, 6].

Within a few picoseconds after excitation of the RC-bacteriochlorophyll dimer $P_{880}$, a radical pair $P^+_{880}\ I^-$ is formed (I is bacteriophaeophytin;[7-12]), which starts initially in a singlet state 6 but may develop significant triplet character if the electron transport to the first quinone electron acceptor $Q_1$ is blocked (see Fig. 1). The singlet state $(P_{880}\ I)^S$ may recombine to the excited state of $P^*_{880}$ and give rise to delayed bacteriochlorophyll (BChl) emission. The triplet state $(P^+I^-)^T$ may recombine to a single triplet state $P^T_{880}$, which in carotenoid (CAR) containing purple bacteria is rapidly converted into a reaction center carotenoid triplet state ($RCAR^T$) [13-15]. Because the

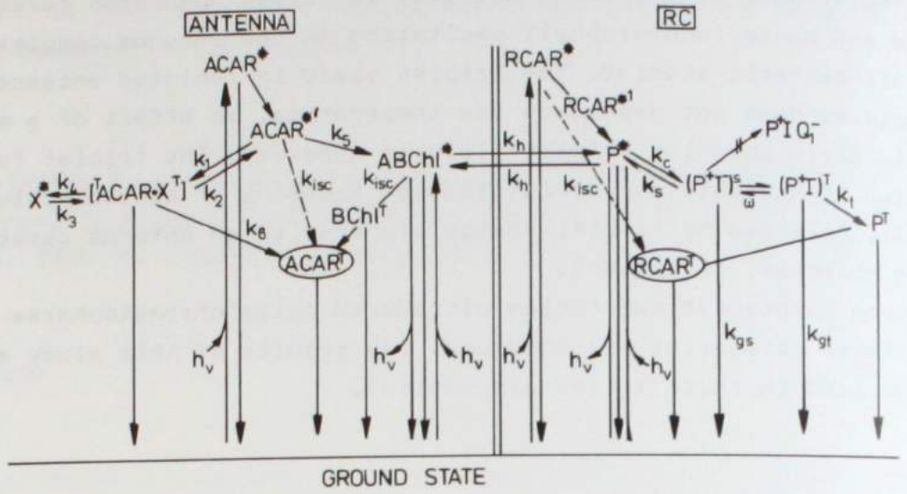


*Fig. 1. Scheme of energy transfer in a carotenoid containing purple bacterium with reduced quinone acceptor $Q_1$. The upper indices, *, 7, +, - indicate respectively the first excited singlet state, the triplet state, the oxidized and the reduced state of the molecules involved. ACAR*' represents the lowest excited state of a carotenoid molecule, transitions to this state from the ground state ACAR are not allowed. The energy of ACAR*' is for β-carotene approximately 25% lower than for the allowed transitions [34]. ABChl is antenna bacteriochlorophyll, ACAR is antennacarotenoid, RCAR is reaction center carotenoid, P is the primary donor a bacteriochlorophyll dimer and I bacteriopheophytin. The k's indicate the various rate constants involved. See text.*

mixing of the singlet and triplet states of the radical pair decreases in a magnetic field, the $RCAR^T$ yield decreases with increasing magnetic field (see also Chapter IV ).

In addition to a $RCAR^T$, in several purple bacteria an antenna carotenoid triplet state ($ACAR^T$) can be formed [3,16,17]. One of the possible mechanisms of $ACAR^T$ formation is by intersystem



crossing of an excited antenna bacteriochlorophyll, ABChl* to $ABChl^T$, followed by triplet energy transfer from $ABChl^T$ to $ACAR^T$.

A few years ago Rademaker et al.[3] discovered a magnetic field induced decrease of about 40% of the $ACAR^T$ yield upon excitation in whole cells of R. rubrum S1. In Chapter IV we showed that in oxidized cells/chromatophores and the B880 antenna complex of R. rubrum S1 a magnetic field induced emission change, MFE, exists upon ACAR excitation. In several photosynthetic strains of Rps. sphaeroides [17,18,19,chapter III]similar phenomena were observed. As a possible explanation for the antenna associated MFT and MFE the process of singlet fission has been proposed (for a discussion of this process see chapter IV and ref. 20). Rademaker et al. [3] suggested as an explanation of such phenomena that by fission of ACAR* a triplet pair $ACAR \cdot X^T$ is formed where X is an unspecified adjacent molecule (see Fig. 1). The rate constants of fission ($k_1$, $k_3$) and of fusion ($k_2$, $k_4$) increase with the number of substates of the triplet pair with an admixture of singlet character [38,39] . These processes yield either a single triplet ($ACAR^T$ and/or $X^T$) or an excited singlet state ACAR* of X*. Possible candidates for the acceptor X are either ABChl or a second ACAR molecule. If ABChl acts as the acceptor molecule X, it is possible that excitation of the ABChl has the triplet pair $^TACAR \cdot ABChl^T$ as an intermediate. An external magnetic field in that case may induce both MFT and MFE via the fission and fusion rate constants $k_3$ and $k_4$ in Fig. 1 and the observed magnetic field dependence would be analogous for MFT and MFE. If on the contrary excitation of ABChl would occur only via the excited state ACAR*, the fission process competes with the energy transfer to BChl and an opposite magnetic field effect is expected for MFE and MFT, independent on the nature of X.

In the previous chapter we have shown that the observed MFE has to be discussed in terms of an antenna associated and a RC associated process, which can be distinguished on the basis of the excitation wavelength, the redox state of the RC and the observed $H_{\frac{1}{2}}$ value. In this chapter we show that MFT associated with the light harvesting antenna exists in all purple bacteria examined and is well correlated with MFE observed under the same

conditions. RC and antenna associated MFT can be separated on a very similar basis as the respective MFE. There is a third path of triplet formation, i.e.intersystem crossing of bacteriochlorophyll of which the yield probably does not depend on the strength of a magnetic field.

## MATERIALS AND METHODS

Cells of Rhodospirillum rubrum S1 (wild type), Rhodospirillum rubrum FR1VI, Rhodopseudomonas sphaeroides 2.4.1 (wild type), Rhodopseudomonas sphaeroides G1C and Rhodopseudomonas sphaeroides R26 were grown as described in chapter II. The cells were harvested by centrifugation and resuspended in buffer containing 250 mM tricine, 5 mM $K_2HPO_4$ and 5 mM $MgCl_2$, PH = 8.0. After 15 minutes of flushing with nitrogen in the dark to obtain anaerobiosis, the cells were immediately used for sample preparation. Chromatophores were prepared by sonification for 20 minutes at 20,000 x g, the remaining supernatant was centrifuged for 2 hours at 110,000 x g. The pellet was resuspended in buffer containing 60% glycerol and stored in the dark at 240 K until use. RC's and light-harvesting complexes were isolated and purified as described in chapter IV and suspended in buffer containing 0.1% LDAO or 0.1% SDS. Reduced samples were prepared by adding 1 mg/ml $Na_2S_2O_4$ (5 mM) and oxidized samples were prepared by adding $K_3Fe(CN)_6$ up to a final concentration of 1-2 mM. For measurements at low temperatures glycerol (60% v/v) and o.5 M sucrose were present to prevent crystallization upon cooling. The absorbance changes were measured in a single beam spectrophotometer described in chapter II, designed to measure laser flash induced absorbance changes with a time resolution of $3 \times 10^{-8}$ sec. as a function of the strength of a magnetic field, which was sinusoidally modulated with a frequency of 50 Hz. Samples placed between the poles of the magnet, were excited by a frequency doubled JK Nd. YAG Laser System ( $\lambda$ = 532 nm, pulswidth 30 ns, maximum energy 0,2 Joule), by a home built tunable dye



laser using Rhodamine 6G or Rhodamine B ($\lambda$ = 560 - 620 nm, pulswidth 15 ns, maximum energy o.1 Joule) pumped by the JK Nd-YAG laser, or by a xenon flash pumped Phase-R dye laser system using Coumarin 503 ($\lambda$ = 490 - 510 nm, puls width 0.2 µs, maximum energy 10 mJoule). The laser beam passed through the middle of a transparent glass plate and the laser energy was determined by four silicon photodiodes placed at the four edges of the glass plate by measuring the scattered laser light. The photodiode currents were electronically summed and integrated, and via a 8-bits AD-converter stored in a LSI-II local computer system. The laser energy monitor was calibrated prior to each experiment using a calibrated energy monitor (JK).
The measuring light puls (3ms), the excitation pulse and the magnetic field were phase-locked. The chopped measuring light, provided by a 250 Watt tungsten-iodine lamp, reached the sample after passing through narrow-band interference filters (Schott AL or Balzers B40). The transmitted light was detected by a S20-type photomultiplier through a Bausch and Lomb monochromator (halfwidth 4.8 nm) and additional narrow band interference filters or absorbance filters, to prevent scattered laser light and fluorescence from reaching the photomultiplier. The photomultiplier was connected via a current-voltage converter and a differential amplifier to a Biomation 8100 transient recorder (sample rate 100 MHz), used in the pretrigger mode. If the laser-energy detected was found to be within the energy window selected (deviation from linearity less thans 2%), the memory of the transient recorder was stored in the LSI-buffer and averaged, if required. The LSI-buffer content was stored on magnetic tape or read out to the central PDP 11-44 computer system for further dataprocessing. The temperature was controlled using a special designed 1 mm cuvette (see chapter II) in which a heating element was mounted and cold nitrogen flowed through the cuvette walls. The temperature could be controlled by a feed back system, within 1 K. If not indicated otherwise the temperature was kept constant at 290 K.

## RESULTS AND INTERPRETATION

In cells/chromatophores of several strains of the photosynthetic bacteria R. rubrum and Rps. sphaeroides, triplet states are formed within the time resolution of the measurements (30 ns) upon excitation with a laser flash, under various redox conditions.

In the CAR-less mutants R. rubrum FR1VI and Rps sphaeroides R26 under reducing conditions, a state has been observed which at room temperature decays within 9 and 6 µs respectively and which can be ascribed to a $RBchl^T$ [16, 21, 37] . In the carotenoid containing strains R. rubrum S1, Rps. sphaeroides 2.4.1 and G1C a state is observed which decays within 1 - 10 µs and that has been attributed to a $RCAR^T$ [3, 13, 16, 21]. Triplet states are also observed in reduced isolated RC's and these most likely arise from charge recombination of the radical pair state $(P_{880}^+ I^-)^T$ followed by triplet energy transfer in CAR containing strains. At saturating flashes, the number of triplets formed is equal to the number of RC's in the state $P_{880} Q_1^-$ , the yield decreases in a magnetic field and increases upon cooling. These triplets will be described in section A which deals with the experiments performed on the isolated RC's.

A second mechanism of triplet formation occurs in isolated antenna complexes and, as will be discussed below, probably involves intersystem crossing, triplet energy transfer and fission/fusion processes in the antenna. The yield of these triplets does not significantly depend on the temperature between 293 K and 77 K and MFT is only found upon direct carotenoid excitation. These triplets will be described in section B which deals with the experiments performed on isolated antenna complexes and oxidized cells/chromatophores.

In section C the triplet formation in reduced chromatophores/cells is discussed, in which both RC-(section A ) and antenna-(section B ) triplets are formed simultaneously.



### A. Triplet formation in isolated RC's

The quantum yield of triplet formation in the RC's of R. rubrum S1, Rps. shpaeroides G1C and R26 was about 0.1 - 0.2 in the fresh preparations, stored for less than 60 hours after isolation and about 0.4 to 0.5 in RC-preparations stored for more than 6 days, in line with similar observations by M.R. Wasielewski (M.R.W., personal communication) and the wide range of quantum yields reported [3, 13, 21] . If not indicated otherwise, the experiments to be described below have been performed on fresh RC-preparation, stored for less than 60 hours at -40 C.

#### a. R. rubrum S1

Fig. 2A shows the absorbance difference spectrum of the 3.2 µs decaying component in reduced RC's of R. rubrum S1 upon 600 nm (●) and 532 nm (o) excitation and these spectra are identical to that reported earlier [13]. The absorbance increases at 585

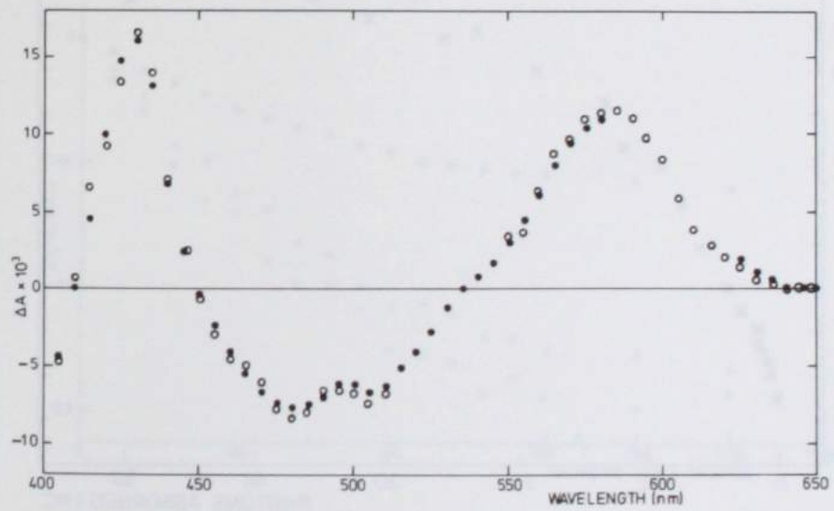


*Fig. 2A. Spectrum of the absorbance change (τ = 3.2 µs) in RC's of R. rubrum S1, induced by a non-saturating 600 nm laser flash, optical path length 1mm, absorbance at 865 - 960 nm was 0.29, 5 mM dithionite added (●) 600 nm excitation, (O) 532 nm excitation.*

nm and 430 nm can be attributed to the formation of spirilloxanthin-triplet bands. The absorbance decreases at 485 nm and 505 nm reflect the bleaching of the singlet absorption bands of spirilloxanthin [3, 13, 22] . The 430 nm absorbance increase is possibly only present if the spirilloxanthin is in 15-cis configuration [ 40,41 ]. The triplet state was formed within the time resolution of the measurements (30 ns).

Fig. 2B shows the $RCAR^T$ yield measured at 430 nm and at 585 nm as a function of the laser pulse energy, which saturated when about 50 photons were absorbed per RC. Using the fact that each RC contains one CAR molecule [23,24] , we calculate $\Delta\varepsilon_{430}$ = 63 $mM^{-1}cm^{-1}$ and $\Delta\varepsilon_{585}$ = 41 $mM^{-1}cm^{-1}$ from the plateau values in Fig. 2B and assuming that each RCAR can be converted into a triplet state. The maximum molar extinction coëfficient of spirilloxanthin-triplet minus singlet in cyclohexane (at 560 nm) is

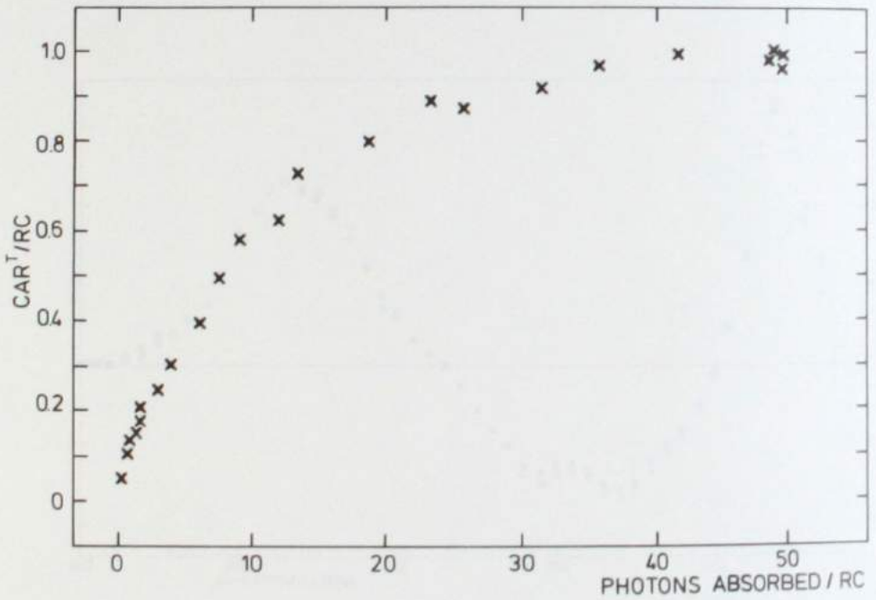


*Fig. 2B. Relative $CAR^T$ yield in RC's of R. rubrum S1, detected at 430 nm as a function of the laser energy. Conditions as in Fig. 2A.*



43 $mM^{-1}cm^{-1}$ [22], and this agrees with the value observed in RC's.

The quantum yield of $RCAR^T$ measured with a weak 600 nm laser flash (<0.1 $RCAR^T$/RC) was calculated to be 0.13. In 'old' RC's (stored for more than 6 days at -40 C) quantum yields varying between 0.31 and 0.43 were obtained. The quantum yield of $RCAR^T$ formation was about the same as upon direct Bchl excitation, which indicates, that if the $RCAR^T$ is formed via $(P^+_{880}\ I^-)^T$ recombination, the efficiency of transfer of singlet energy from $RCAR^*$ to $P^*_{880}$ is close to 1, in contrast with the singlet energy transfer efficiency of $ACAR^*$ to $ABchl^*$ in the antenna complex (30%;[3,25] ) of R. rubrum S1.

Fig.2C shows the relative MFT decrease, $\{\phi_T(H) - \phi_T(H = 0)\}/\phi_T\ (H = 0)$, as a function of the magnetic field strength in reduced RC's of R. rubrum S1, detected at 430 nm upon 600 nm excitation. Three saturation curves are shown, using excitation

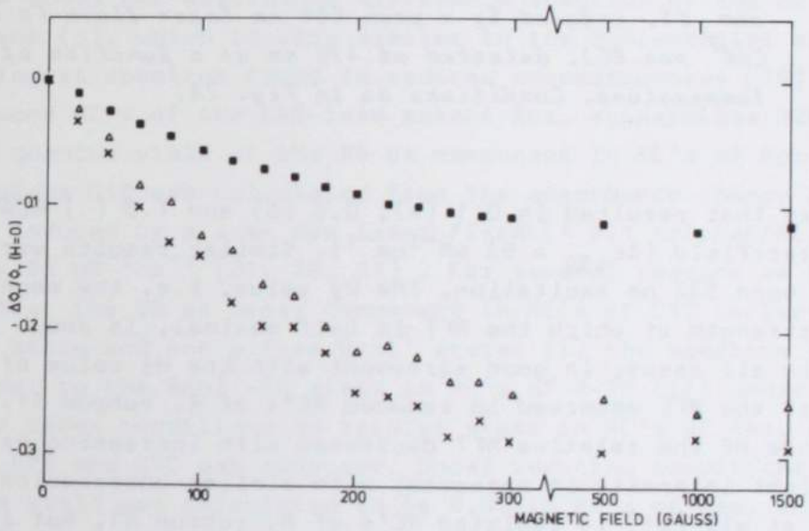


*Fig. 2C. Relative MFT in RC's of R. rubrum S1 detected at 430 nm as a function of the magnetic field strength, induced by a 600 nm laser flash resulting in 0.1 (X), 0.3 (Δ) and 1.0 (■) carotenoid triplet per RC in zerofield. Conditions as in Fig. 2A.*

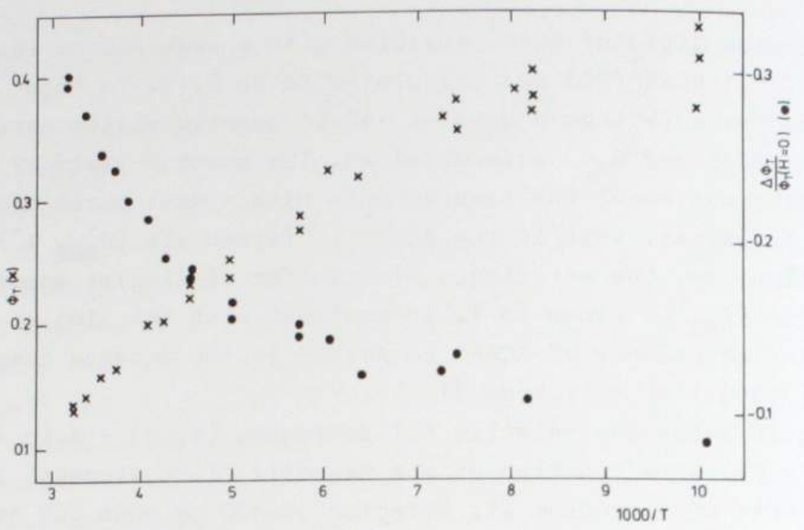


*Fig. 2D. $CAR^T$ yield $\phi_T$(×) and relative MFT (●) in RC's of R. rubrum S1, induced by a weak 600 nm laser flash (≈ 0.1 $CAR^T$ per RC), detected at 430 nm as a function of the temperature. Conditions as in Fig. 2A.*

energies that resulted in 0.1 (x), 0.3 (Δ) and 1.0 ( ) $RCAR^T$ per RC in zerofield ($\Delta\varepsilon_{430}$ = 63 $mM^{-1}cm^{-1}$). Similar results were obtained upon 532 nm excitation. The $H_{\frac{1}{2}}$ value, i.e. the magnetic field strength at which the MFT is half maximal, is about 90 Gauss in all cases, in good agreement with the $H_{\frac{1}{2}}$ value of 100 Gauss of the MFE observed in reduced RC's of R. rubrum S1. The amplitude of the relative MFT decreased with increasing excitation light intensity in agreement with similar observations by Schenk et al. [21] in isolated RC's of R. rubrum S1, but in contrast with the relative MFT in reduced chromatophores at various pulse intensities (see below). The magnetic field effect on the $RCAR^T$ yield is partly undone by using high laser pulse intensities, probably due to saturation effects.

Fig. 2D shows the $RCAR^T$ yield as a function of the temperature in reduced RC's of R. rubrum S1 (x). In old RC's the quantum yield increases from 0.4 to 0.8 upon cooling from 293 K to



100 K (not shown). The decay rate of the $RCAR^T$ did not depend on the temperature over the temperature range studied. A part of the increase of the $RCAR^T$ yield upon cooling may be due to bandsharpening. The closed circles (●) show the relative MFT, $\Delta\phi_T/\phi_T(H = 0)$ in RC's as a function of the temperature. The absolute MFT, $\Delta\phi_T$, did significantly vary with temperature. Therefore the temperature dependence of the relative MFT is the inverse of the temperature dependence of $\phi_T$. The $H_{\frac{1}{2}}$ value of the saturation curve of the MFT did not depend on the temperature again in agreement with the observation that the $H_{\frac{1}{2}}$ value of the MFE was independent of the temperature.

b. Rps. sphaeroides G1C and R26

In contrast with R. rubrum, the absorbance changes observed in reduced RC's of Rps. sphaeroides G1C induced by a 600 nm dye laser flash, showed a two exponential decay.
Fig. 3A shows the absorbance difference spectrum of the 80 μs component (o), which is very similar to the Bchl-triplet minus Bchl-singlet spectrum found in reduced chromatophores [16] and in reduced RC's of the CAR-less mutant Rps. shpaeroides R26 (●).

The quantum yield of the 80 μs component in RC's of Rps. sphaeroides G1C was calculated from the absorbance change at 430 nm induced by a weak dye laser flash (< 0.1 triplet/RC) using $\Delta\varepsilon_{430}$ = 65 $mM^{-1}cm^{-1}$ [21, 26, 27] . For several reasons we believe that the 80 μs decay component in RC's of G1C reflects a $RBchl^T$ state and not a free $Bchl^T$ state: (i) the spectrum is identical to the $Bchl^T$-RC state in RC's of R-26 (ii) under intermediate redox conditions no triplet state in RC's of Rps. sphaeroides R26 and G1C was observed. Under reducing conditions the quantum yield was calculated to be 0.03 in RC's of Rps. shpaeroides G1C and 0.14 in RC's of Rps. sphaeroides R26 (iii) the $Bchl^T$ yield decreased by about 22% ($H_{\frac{1}{2}}$ ≈ 50 Gauss) in RC's of Rps. sphaeroides R26 and by about 25% ($H_{\frac{1}{2}}$ = 65 Gauss) in RC's of Rps. sphaeroides G1C in a magnetic field of 1500 Gauss (iiii) the $RBchl^T$ yield showed a similar temperature dependence as the $RCAR^T$ yield (see below).An explanation may be that the $RBchl^T$ in G1C reflects a population of RC's that either have lost their RCAR or in which transfer of the triplet energy from $RBchl^T$ to

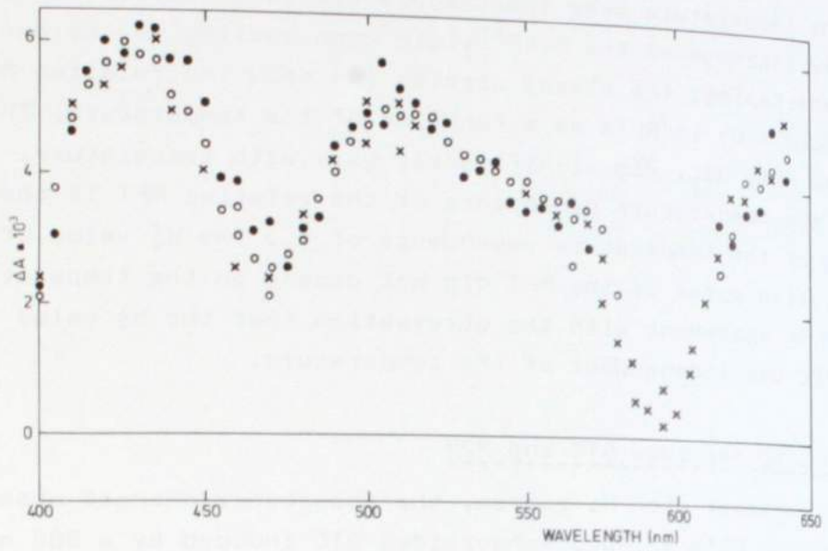


*Fig. 3A. Absorbance difference spectra induced by a non-saturating laser flash in reduced RC's. a.Spectrum of the 80 µs component in Rps. sphaeroides G1C upon 600 nm (o) and 532 nm (x) excitation; b.Spectrum of the 6 µs component in Rps. sphaeroides R26 upon 600 nm excitation (●). The spectra are normalized at 575 nm, 1 mg $Na_2S_2O_3$ was added per ml (5 mM).*

RCAR is not possible.

Fig. 3B shows the absorbance difference spectrum of the 9 µs component in reduced RC's of Rps. sphaeroides G1C upon 600 nm excitation. The maximum near 520 nm can be ascribed to $CAR^T$ absorption [22] and the minima at 430 nm and 460 nm to the peaks in the absorbance spectrum of neurosporene, the major CAR in G1C. The spectrum is very similar to the $CAR^T$ minus CAR-singlet difference spectrum observed in reduced RC's of Rps. sphaeroides G1C[13] although the main CAR associated with the RC in this bacterium is chloroxanthin and not neurosporene. These two carotenoids, however, are only slightly different, because neurosporene, a precursor of chloroxanthin in the CAR synthesis, is con-



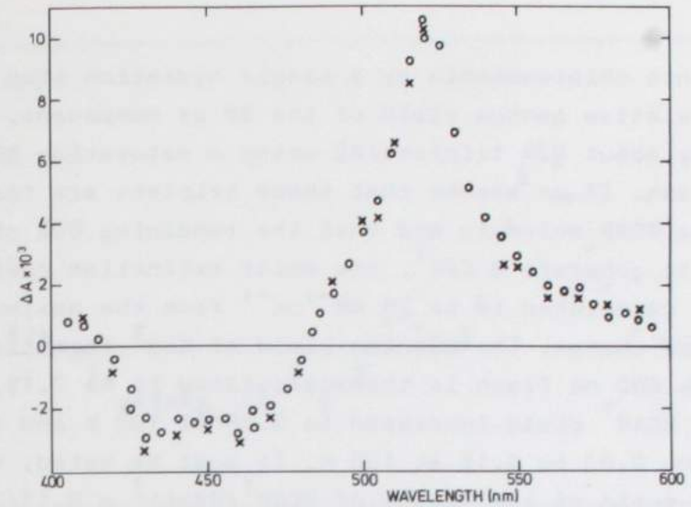


*Fig. 3B. Spectrum of the 9 µs component of the absorbance change in RC's of Rps. sphaeroides G1C induced by a weak laser flash. Optical path length 1 mm, absorbance at 865-960 nm was 0.56, 5 mM dithionite added. (o) 600 nm excitation; (x) 532 nm excitation, spectrum scaled to the 600 nm laser flash induced spectrum*

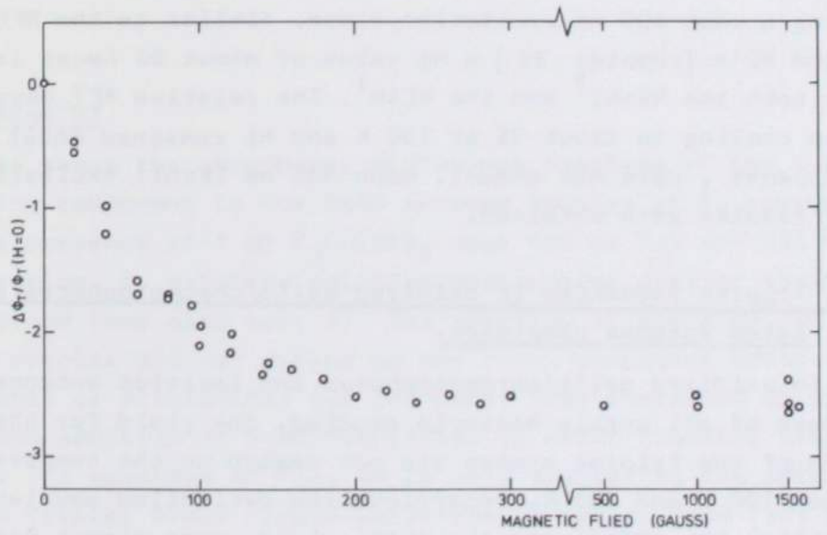


*Fig. 3C. The relative MFT in RC's of Rps. sphaeroides G1C detected at 520 nm as a function of the magnetic field strength, induced by a 600 nm laser flash resulting in 0.09 $CAR^T$ per RC in zerofield. Conditions as in Fig. 3B.*

verted into chloroxanthin by a single hydration step only [30].

The relative qantum yield of the 80 µs component, $P^T_{880}$, was maximally about 0.4 triplets/RC using a saturating 600 nm dye laser flash. If we assume that these triplets are formed in RC's lacking a RCAR molecule and that the remaining 60% of the RC's is able to generate a $CAR^T$, the molar extinction coëfficient $\Delta\varepsilon_{520}$ is calculated to be 26 $mM^{-1}cm^{-1}$ from the maximum 520 nm absorbance change. The quantum yield of $CAR^T$ formation measured in a weak 600 nm flash is then calculated to be 0.15. Upon cooling the $RCAR^T$ yield increased to 0.46 at 100 K and the $RBchl^T$ yield from 0.03 to 0.15 at 100 K. It must be noted, however, that the ratio of the yields of $RCAR^T/RBchl^T$ = 0.15/0.03 = 5 does not agree with the ratio of the fraction of RC's with a RCAR and those, which lack energy transfer to a RCAR ≈ 0.6/0.4 ≈ 1.5.

The $RBChl^T$ yield in Rps. sphaeroides R26 increased upon cooling from 14 at 293 K to .4 at 100 K.

Fig. 3C shows the relative MFT decrease as a function of the magnetic field strength in reduced G1C-RC's detected at 520 nm, using a weak 600 nm excitation flash. Similar to the MFE in reduced RC's [chapter IV ] a $H_{\frac{1}{2}}$ value of about 60 Gauss is observed for both the $RBchl^T$ and the $RCAR^T$. The relative MFT decreased upon cooling to about 5% at 100 K and $H_{\frac{1}{2}}$ remained about the same (55 Gauss , data not shown). Upon 530 nm (Bchl) excitation similar results were obtained.

B . Triplet formation in oxidized cells/chromatophores and isolated antenna complexes.

In oxidized cells/chromatophores and isolated antenna complexes of all purple bacteria studied, the yield for the formation of the triplet states did not depend on the temperature between 100 K and 293 K, regardless the excitation wavelength. In addition the $ABChl^T$ and the $ACAR^T$ yield, upon direct Bchl excitation, did not depend on the magnetic field strength within the accuracy of the measurements ( ca 2% of the triplet yield).



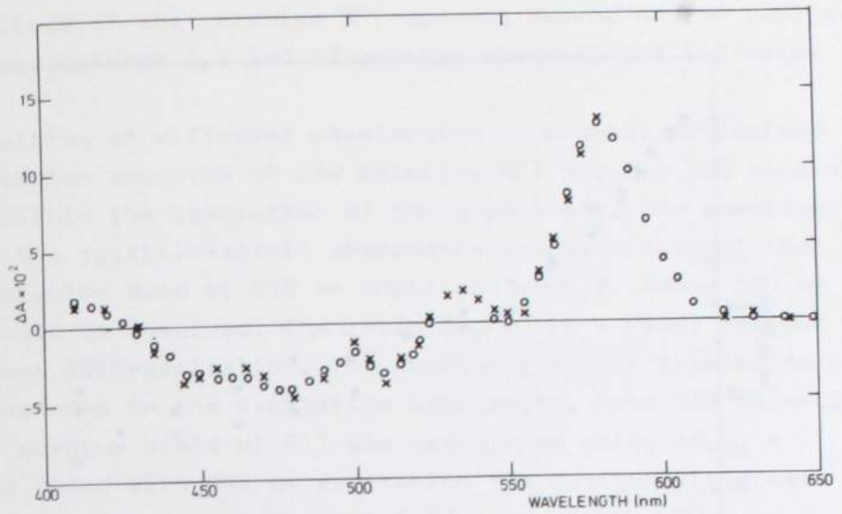


*Fig. 4A. Spectrum of the absorbance change (↑ = 1.8 µs) in the B880 complex of R. rubrum S1, induced by a laser flash, optical path length 1 mm, absorbance at 880-960 nm was 0.52, 1 mM $K_3Fe(CN)_6$ added. (x) 600 nm excitation, (o) 532 nm excitation spectrum scaled to the 600 nm laser flash induced spectrum.*

a. R. rubrum S1

Fig. 4A shows the absorbance difference spectrum of the 1.8 µs decaying component in the B880 antenna complex of R. rubrum S1 in the presence of 1 mM $K_3Fe(CN)_6$ upon 600 nm (x) and 532 nm (o) excitation. In oxidized cells/chromatophores similar results were obtained (see also ref. 3). The spectrum of the $ACAR^T$ in the B880 complex did not depend on the redox compounds added (ferricyanid or dithionite) but the decay time increased up to 3.6 µs upon addition of 5 mM dithionite or after flushing with nitrogen. The spectrum of Fig. 4A is very similar to the spirilloxanthin triplet minus singlet spectrum in cyclohexane [22] and apart from the absence of the absorbance increase at 430 nm resembles the spectrum of Fig. 3A measured in isolated RC's. It appears that the 430 nm absorbance increase is associated only with the $CAR^T$ formation in the RC (see section C )

Fig. 4B shows the magnetic field dependence of the relative

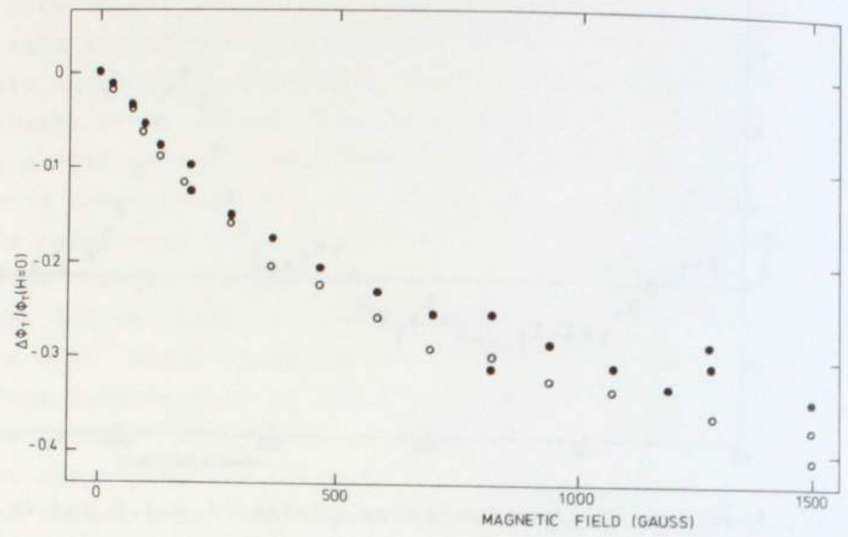


*Fig. 4B. The relative MFT in the B880 complex (o) and in oxidized chromatophores (●) of R. rubrum S1, detected at 580 nm as a function of the magnetic field strength, induced by a 532 nm non-saturating laser flash; absorbance at 880-960 nm was 0.57 (●) and 0.52 (o). Other conditions as in Fig. 4A.*

MFT in the oxidized B880 complex (o) of R. rubrum S1 upon CAR-excitation at 532 nm and detected at 580 nm. Similar results were obtained in oxidized chromatophores (●).

The $H_{\frac{1}{2}}$ values of more than 400 Gauss and the shape of the saturation curves of the MFT are very similar to those observed for the MFE in the same samples (see chapter IV). In contrast with Rademaker et al. [3] we did not observe an initial lag phase of 200 Gauss neither with the MFE (chapter IV) nor with the MFT. The use of large stationary magnetic fiels (by Rademaker et al.) might have introduced a shift of the abcissa due to remanent magnetism, which is absent in the experiments described here, because a 50 Hz modulated magnetic field was used to determine the MFT and MFE.



The amplitude of the relative MFT did not depend on the excitation energy between 0.1 and 13 photons absorbed per CAR-molecule.

By exciting at different wavelengths we roughly determined the excitation spectrum of the relative MFT between 560 nm and 620 nm. Within the resolution of the experiment, the spectrum followed the spirilloxanthin absorbance spectrum but <u>not</u> the Bchl-absorption band at 590 nm (data not shown). Above 580 nm no MFT could be observed. The ratio $\Delta\Phi_T/\Phi_T$ (H = 0)was maximum upon direct ACAR-excitation. The quantum yield of triplet formation depended on the excitation wavelength. Upon 532 nm excitation a quantum yield of 0.3 was calculated using $\Delta\varepsilon_{580}$ = 41 $mM^{-1}cm^{-1}$ and with 600 nm excitation the quantum yield was about 0.2 in good agreement with Rademaker et al. [3] .

In chromatophores of the CAR-less mutant R. rubrum FR1VI a $ABchl^T$ is formed under oxidizing conditions with a quantum yield of 0.17 upon 600 nm excitation . The absorbance difference spectrum was similar to the one shown in Fig. 3A and the absorbance change decayed with a single exponent with a time constant $\tau$ = 60 µs (data not shown). Regardless the wavelength of excitation no MFT clearly different from zero was observed. Similar results were obtained in oxidized chromatophores of Rps. sphaeroides R26 (see discussion table 1).
The presence of MFT upon ACAR-excitation and the absence of MFT upon Bchl-excitation in R. rubrum FR1VI are in agreement with the results presented in chapter IV concerning the antenna associated MFE. Upon 600 nm excitation the $ACAR^T$ is formed by intersystem crossing via $ABchl^T$, but upon 532 nm excitation the $ACAR^T$ is partly formed by a magnetic field dependent fission from $ACAR^*$. If we assume that about 30% of the energy absorbed at 532 nm is transferred to ABchl [25] , the quantum yield of $ACAR^T$ formation via fission is calculated to be 0.34.

b. Rps. sphaeroides

Fig. 5A shows the absorbance difference spectrum of the 6 µs component observed upon 495 nm (o) and 600 nm (●) excitation in the B800/B856 complex of Rps. sphaeroides 2.4.1.

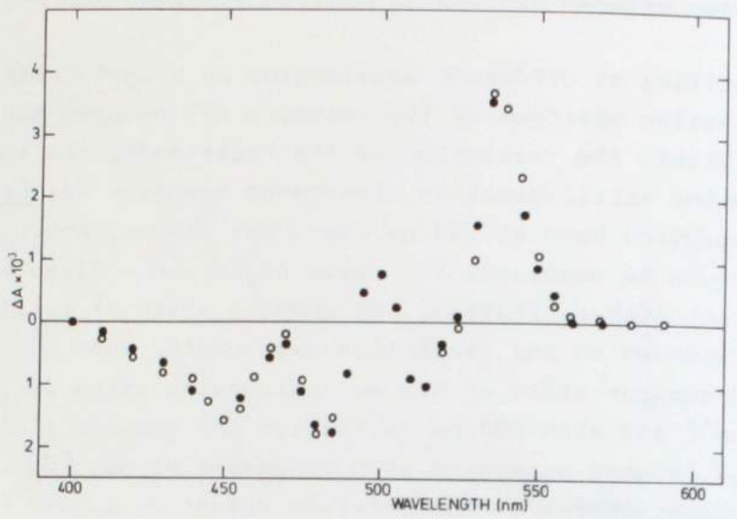


*Fig. 5A. Spectrum of the absorbance change (τ = 6 μs) in the B800/B850 complex of Rps. sphaeroides 2.4.1, induced by a laser flash, optical path length 1 mm, absorbance at 850 - 960 nm is 0.5, 1 mM $K_3Fe(CN)_6$ added. (•) 600 nm excitation, (o) 495 nm excitation.*

The spectrum shows a maximum absorbance increase at 540 nm, which can be ascribed to triplet-triplet absorption by sphaeroidene and two minima at 450 and 480 nm which are due to the bleaching of the singlet absorption bands of sphaeroidene [22, 30]. The quantum yield of triplet formation is calculated to be 1.8% upon 495 nm excitation and 1.9% upon 595 nm excitation ($\Delta\varepsilon_{540}$ = 29mM$^{-1}$cm$^{-1}$[22]), which is surprisingly low as compared to the values observed in R. rubrum.

Fig. 5B shows the relative MFT change (o) as a funtion of the magnetic field strength upon 495 nm excitation detected at 540 nm in the B800/B850 complex of Rphs sphaeroides 2.4.1. The maximum relative MFT change observed at H ≈ 250 Gauss is about 3%, which is very low as compared to the relative MFT change in the B880 complex of R. rubrum S1 (40%). At low magnetic field



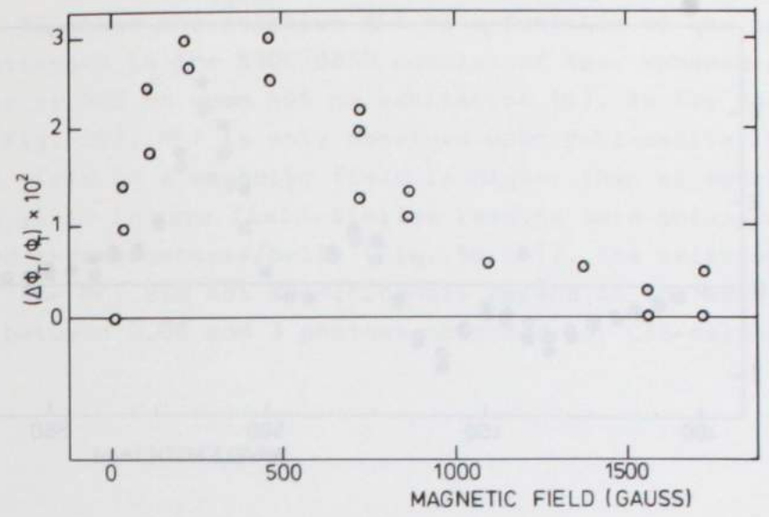


*Fig. 5B. The relative MFT in the B800/B850 complex of Rps. sphaeroides 2.4.1, detected at 535nm, as a function of the magnetic field strength. Conditions as in Fig. 5A. Excitation by a 495 nm laser flash.*

strengths an increase of MFT in a magnetic field is observed, in contrast with the large decrease observed in R. rubrum. Upon 600 nm excitation no MFT clearly different from zero could be found.

Fig. 6A shows the absorbance difference spectrum of the 6.4 μs decay-component observed upon 495 nm excitation (o) and 595 nm (•) excitation in the B800/B850 complex of Rps. sphaeroides G1C. The spectrum shows an absorbance increase at 515 nm, which is most likely due to the triplet band absorption of neurosporene. Further more bleaching of the peaks in the neurosporene absorption spectrum are observed at 430 nm, 460 nm and 495 nm. The spectrum is, however, clearly different from the neurosporene triplet-singlet spectrum observed in isolated RC's (Fig. 3B), where the bleaching at 495 nm is absent.
The quantum yield of $ACAR^T$ formation in this complex was calculated to be 1.4% upon 495 nm excitation and 1.5% upon 600 nm

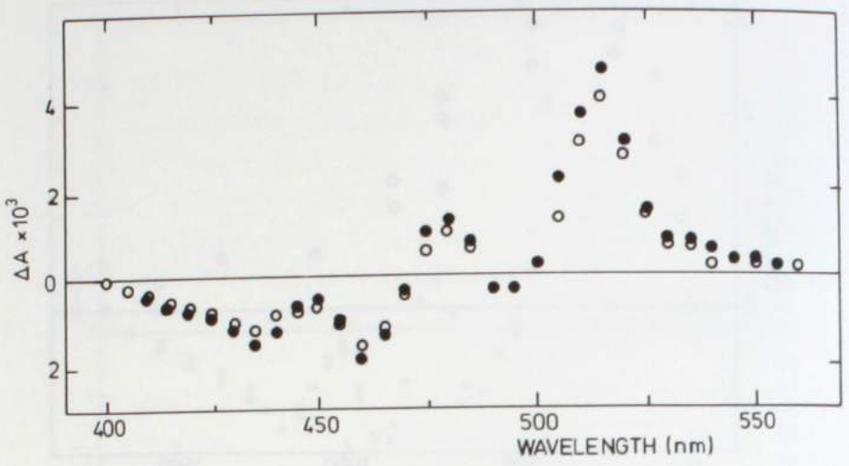


*Fig. 6A. Spectrum of the absorbance change (τ = 6.4 µs) in the B800/B850 complex of Rps. sphaeroides G1C, induced by a laser flash. Optical path length 1 mm, absorbance at 850-960 was 0.72, 1 mM $K_3Fe(CN)_6$ added. (●) 595 nm laser excitation. (o) 495 nm laser excitation.*

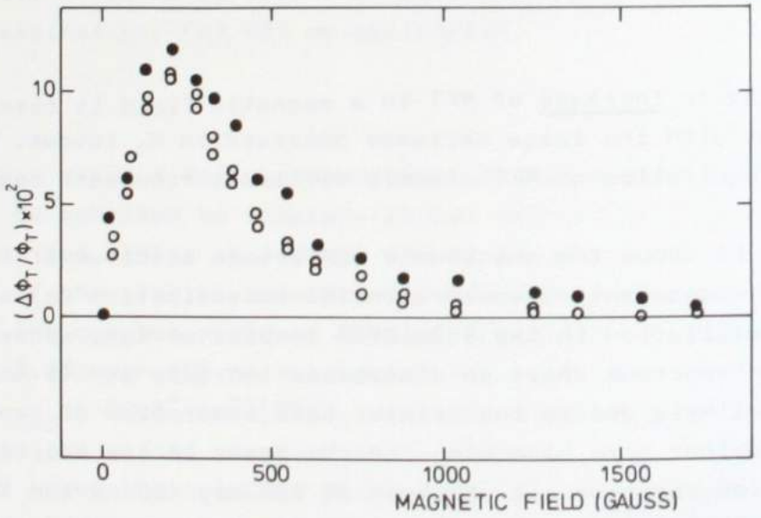


*Fig. 6B. The relative MFT in the B800/B850 complex(o) and in oxidized cells(●) of Rps.sphaeroides G1C, detected at 515 nm, as a function of the magnetic field strength. Excitation by a 495 nm laser flash. Conditions as in Fig. 6A.*



excitation, taking $\Delta\varepsilon_{515}$ = 26 $mM^{-1}cm^{-1}$.

Fig. 6B shows the relative MFT as a function of the magnetic field strength in the B800/B850 complex of Rps. sphaeroides G1C detected at 515 nm upon 495 nm excitation (o). As for the wild type (Fig. 5B), MFT is only observed upon Bchl-excitation. The triplet yield in a magnetic field is higher than or equal to the triplet yield in zero field. Similar results were obtained in oxidized chromatophores/cells (Fig. 6B (●)). The relative amplitude of the MFT did not significantly depend on the excitation energy between 0.06 and 3 photons absorbed per CAR-molecule.

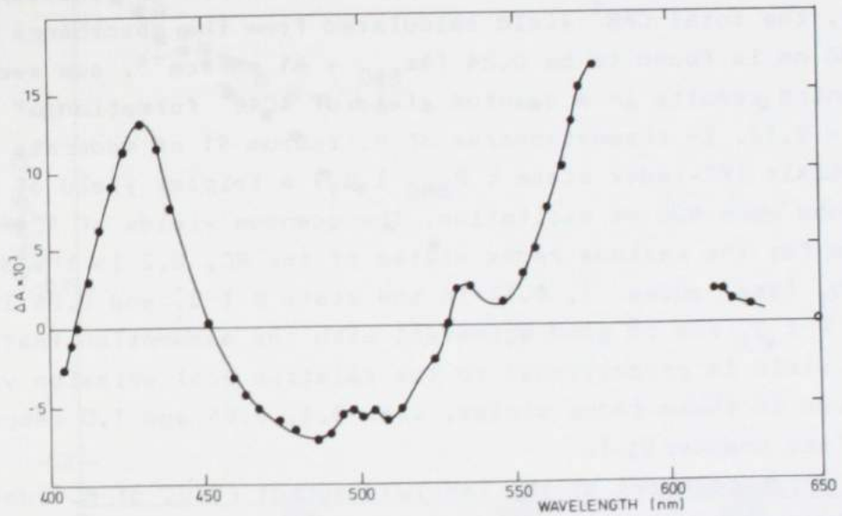


*Fig. 7A. Spectrum of the absorbance change (τ = 3.2 µs) in reduced chromatophores of R. rubrum S1, induced by a 600 nm laser flash, optical path length 1 mm, absorbance at 880 - 960 was 0.52, 5 mM dithionite added.*

C . Triplet formation in reduced cells/chromatophores.

a. R. rubrum

Fig. 7A shows the flash induced absorbance difference spectrum of the 3.2 µs component upon 600 nm excitation in reduced RC's. An absorbance increase at 430 nm is observed and the spectrum is very similar to a spirilloxanthin triplet minus singlet spectrum. Again the 430 nm absorbance increase reflects the $RCAR^T$ formation generated by charge recombination in the RC. The quantum yield of triplet formation in reduced chromatophores was calculated to be 0.12 from the 430 nm absorbance change ($\Delta\varepsilon_{430}$ = 63 $mM^{-1}cm^{-1}$), very similar to the quantum yield observed in isolated RC's. The 580 nm absorbance change reflects both the $RCAR^T$ and the $ACAR^T$ formation (see Figs. 2A and 5A). If we assume that the molar extinction coëfficient at 580 nm is the same for both the $RCAR^T$ and the $ACAR^T$ (both spirilloxanthin [30]), the total $CAR^T$ yield calculated from the absorbance change at 580 nm is found to be 0.24 ($\Delta\varepsilon_{580}$ = 41 $mM^{-1}cm^{-1}$, see section I), which results in a quantum yield of $ACAR^T$ formation of 0.24-0.12 = 0.12. In chromatophores of R. rubrum S1 of moderate redox potentials (RC-redox state : $P_{880}$ I $Q_1$) a triplet yield of 0.06 is found upon 600 nm excitation. The quantum yields of $ACAR^T$ obtained for the various redox states of the RC, 0.2 in the state $P^+$ I $Q_1$ (see above ), 0.12 in the state P I $Q_1^-$ and 0.06 in the state P I $Q_1$ are in good agreement with the assumption that the $ACAR^T$ yield is proportional to the relative Bchl emission yield observed in these redox states, i.e. 3.4, 2.05 and 1.0 respectively (see chapter VI ).

In chromatophores of the CAR-less mutant FR1VI of R. rubrum, we calculated a quantum yield of triplet formation upon Bchl excitation of 0.25 by comparison of the bleaching of the 880 nm absorbance band induced by oxidation of $P_{880}$ under intermediate redox-conditions and by triplet formation under reducing conditions, which is very similar to the triplet yield observed in the wild type. If we assume that the $RBChl^T$ yield in reduced chromatophores is similar to that in isolated RC's, i.e. 0.14, the $ABchl^T$ yield in reduced chromatophores is 0.25 - 0.14 = 0.11, very similar to the $ACAR^T$ yield in the wild type (.24). This is a clear indication that the molar extinction coëfficient used in



R. rubrum S1, i.e. $\Delta\varepsilon_{580}$ = 41 $mM^{-1}cm^{-1}$, is the same for the $ACAR^T$ and the $RCAR^T$. From the $BChl^T$ yield of 0.25 in R. rubrum FR1VI, we calculate a molar extinction coëfficient of about 16 $mM^{-1}cm^{-1}$ at 510 nm, in good agreement with earlier proposals [40].

Fig. 7B shows the relative MFT as a function of the magnetic field strength in reduced chromatophores of R. rubrum S1 detected at 430 nm upon 600 nm excitation (o) and detected at 580 nm upon 532 nm excitation (●). The saturation curves are markedly different and depend both on the wavelength of excitation and

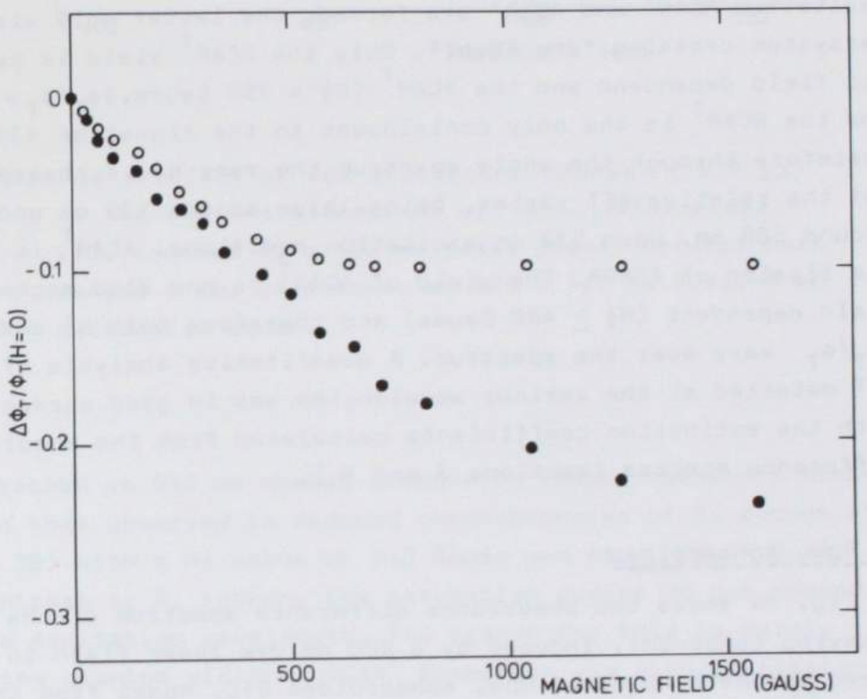


*Fig. 7B. The relative MFT in reduced chromatophores of R. rubrum S1, as a function of the magnetic field strength. (o): Excitation wavelength 600 nm (0.1 $CAR^T$ per RC), detection wavelength 430 nm. (●): Excitation wavelength 532 nm ( 0.08 $CAR^T$ per RC), detection wavelength 580 nm*

detection. Upon 600 nm excitation a $H_{\frac{1}{2}}$ value of about 250 Gauss is found regardless the wavelength of detection but the amplitude of the relative MFT is maximum at 430 nm. Upon 532 nm excitation (in the CAR-region of the absorbance spectrum), $H_{\frac{1}{2}}$ shifts to longer values depending on the detection wavelength: around 430 nm $H_{\frac{1}{2}}$ = 250 Gauss and at 580 nm $H_{\frac{1}{2}}$ exceeds 400 Gauss. The $H_{\frac{1}{2}}$ values of 250 and 400 Gauss corresponds reasonably well with the $H_{\frac{1}{2}}$ values observed for the RC-associated MFE (240 Gauss) and of the antenna associated MFE ($\geq$ 400 Gauss) (see the previous chapter).

These experiments can be explained as follows. Upon 600 nm excitation $RCAR^T$ and $ACAR^T$ are formed, the latter only via intersystem crossing from ABchl*. Only the $RCAR^T$ yield is magnetic field dependend and the $RCAR^T$ ($H_{\frac{1}{2}}$ = 250 Gauss, $\Delta\phi_T/\phi_T \approx 0.10$) and the $RCAR^T$ is the only contribuant to the signal at 430 nm. Therefore through the whole spectrum the same $H_{\frac{1}{2}}$ is observed, but the relative MFT varies, being large around 430 nm and small around 580 nm. Upon 532 nm excitation additional $ACAR^T$ is formed via fission of ACAR*. The yield of $ACAR^T$ is now also magnetic field dependent ($H_{\frac{1}{2}} \geq$ 400 Gauss) and therefore both $H_{\frac{1}{2}}$ and $\Delta\phi_T/\phi_T$ vary over the spectrum. A quantitative analysis of the MFT detected at the various wavelengths was in good agreement with the extinction coëfficients calculated from the absorbance difference spectra (sections A and B ).

b. Rps. sphaeroides

Fig. 8A shows the absorbance difference spectrum of the 9 µs decaying component, induced by a 600 nm dye laser flash in reduced chromatophores of Rps. sphaeroides G1C. Apart from the absorbance increase at 550 nm, the spectrum is very similar to the absorbance difference spectrum observed in the B800/B850 complex (see Fig. 6A). Note that the increase at 550 nm is also absent in the spectrum obtained in G1C-RC's (Fig. 3B). It may be speculated that the 550 nm absorbance increase arises from a $ACAR^T$ state generated in the B880 complex. Both the 515 nm and the 550 nm absorbance change depend on a magnetic field in the reduced chromatophores.



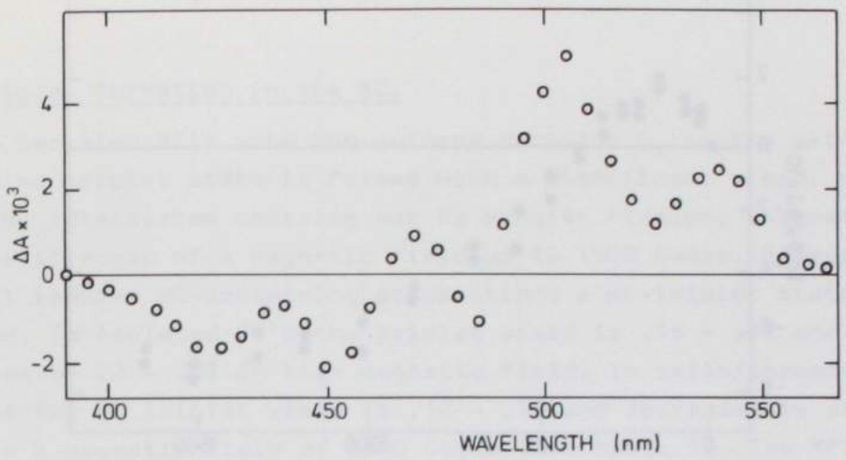


*Fig. 8A. The spectrum of the absorbance change (τ = 9 µs) in reduced chromatophores of Rps. sphaeroides G1C, induced by a 600 nm laser flash, optical path length 1 mm, absorbance at 870 - 960 is 0.92, 5 mM dithionite added.*

$\phi_T$ detected at 515 nm showed a magnetic field dependence similar to that observed in reduced chromatophores of R. rubrum S1 (Fig. 7B) with a $H_{\frac{1}{2}}$ value of 230 Gauss and $\Delta\phi_{Tmax}/\phi_T$ = 0.12. In contrast to R. rubrum, the saturation curves do not depend on the excitation wavelength. The reason for this is mainly that the quantum yield of $ACAR^T$ formation via singlet-fission is essentially zero in zero field and maximally $1.4 \times 10^{-3}$ at H ≈ 250 Gauss. In addition the quantum yield of $ACAR^T$ formation via intersystem crossing is only about 1.8%. Therefore, at all wavelengths of excitation, the $RCAR^T$ is the dominating species being formed and $H_{\frac{1}{2}}$ and $\Delta\phi_T/\phi_T$ are more or less constant.

On the contrary the shapes of the relative MFT saturation curves detected at 550 nm did depend on the excitation wavelengths (Fig. 8). Upon Bchl excitation a curve typical for the RC-associated MFT is observed, but upon CAR-excitation (λ = 495

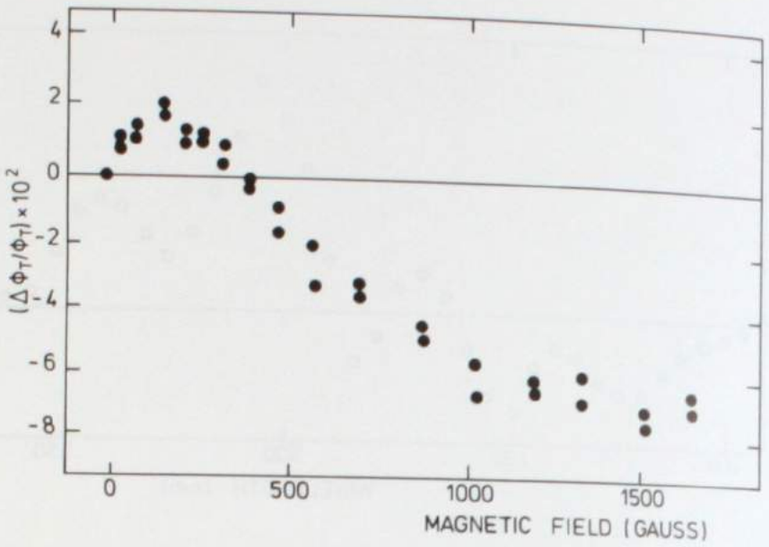


*Fig. 8B. The relative MFT in reduced chromatophores of Rps. sphaeroides G1C as a function of the magnetic field strength. Excitation wavelength 430 nm, detection wavelength 540 nm. Conditions as in Fig. 8A.*

nm) the shape of the saturation curve (Fig. 8B) reflects contributions of both the RC-associated and the antenna associated MFT. Either the 550 nm absorbance change is predominantly arising from the antenna triplet formation sited in e.g. the B880 complex, or the MFT associated with this ACAR is relatively large (see also chapter IV). The difference of the maximum absorbance changes, at 515 nm and 550 nm is remarkable and hard to explain. As assumed [29], only one type of ACAR, i.e. neurosporene is supposed to be present in this bacterium. The presence of a small amount of sphaeroidene or oxidized neurosporene can explain the data.



DISCUSSION

a. Triplet formation in the RC.

In isolated RC's with the quinone acceptor $Q_1$ in the oxidized state no triplet state is formed with a significant yield, neither by intersystem crossing nor by singlet fission, independent of the strength of a magnetic field up to 1500 Gauss. However, in all reduced RC-containing preparations a RC-triplet state is formed. In isolated RC's the triplet yield is .15 - .18 and decreases by 22 - 30% in high magnetic field. In cells/chromatophores the RC triplet yield is .12 - .15 and decreases by about 10% in a magnetic field of 1500 Gauss (see table 1). The MFT shows a magnetic field dependence complementary to that of the RC-associated MFE (see chapter IV, Figs. 2B and 3C). Therefore, in agreement with earlier reports [1,2,3,14,16,21,24] , we conclude that the RC-triplet state is formed by charge recombination of a radical pair triplet state. In the CAR containing bacteria the $RBChl^T$ , probably shared between $P_{800}$ and $P_{880}$ [10,12, 21], is rapidly transferred into the $RCAR^T$. The decay time of the RC-triplet state is 3 - 9 µs except for the $RBChl^T$ in RC's of Rps. sphaeroides G1C, which shows a remarkable long decay time of 80 µs. Such a long lifetime has been observed too in the CAR-less mutants R. rubrum G9 (≈ 50 µs[16]) and in P. aestuarii (≈ 80 µs, [41]). That we are dealing with a RC-triplet state is shown by the following observations:
(i) the magnetic field dependence of the $BChl^T$ is very similar to that of the $RCAR^T$ in G1C-RC's, (ii) the spectrum of the 80 µs component is identical to that of the 6 µs component of R26-RC's, which has been attributed to the formation of a $RBChl^T$ state, (iii) in oxidized RC's no such state is observed.

The large range of quantum yields of the RC triplets [1,2,3, 14,15,16,21,24] ranging from 0.1 to 0.6 may at least partly be explained by our observation that in RC's the triplet yield increase by a factor of 2 - 4 upon aging. In reduced cells/chromatophores of R. rubrum the quantum yield of RC-triplet formation may have been overestimated because also antenna triplet states are formed. In cells/chromatophores of Rps. sphaeroides the

TABLE 1. RC-ASSOCIATED TRIPLET STATES
BChl-excitation, reducing conditions

| | Isolated RC | | | | cells/chromatophores | | | |
|---|---|---|---|---|---|---|---|---|
| | $\tau$ | $\Phi_T$ | $\frac{\Delta\Phi_T}{\Phi_T}$ | $H_{\frac{1}{2}}$ | $\tau$ | $\Phi_T$ | $\frac{\Delta\Phi_T}{\Phi_T}$ | $H_{\frac{1}{2}}$ |
| R. rubrum S1 | 3.2 | .13 | -.3 | 90 | 3.2 | .12 | -.1 | 250 |
| Rps. sphaer. G1C | 9 | .15 | -.27 | 60 | 9 | .15 | -.1 | 230 |
| | 80 | .03 | -.25 | 65 | | | | |
| R. rubrum FR1VI | | | | | 9 | .13 [4] | -.1 | 240 |
| Rps. sphaer. R26 | 6.0 | .14 | -.22 | 50 | | | | |

TABLE 1 (CONTINUED) ANTENNA-ASSOCIATED TRIPLET STATES

| | Car-excitation | | | | BChl-excitation | |
|---|---|---|---|---|---|---|
| | magnetic field dependent | | | | magnetic field independent | |
| | $\tau$ | $\Phi_T$max | $\frac{\Delta\Phi_T}{\Phi_T}$ | $H_{max}$ | $\tau$ | $\Phi_T$ |
| R. rubrum S1 | 1.8 [3] | .3 [3] | -.4 [3] | >400 [3] | 1.5-3.6 | .06 [1] .12 [2] .20 [3] |
| Rps.sphaer.2.4.1 | 6.0 [5] | $6\times10^{-4}$ [5] | +1.0 [5] | 300 [5] | 6.0 [5] | .018 - 0.19 [5] |
| Rps.sphaer. G1C | 6.4 [6] | $1.4\times10^{-3}$ [6] | +1.0 [6] | 250 [6] | 6.4 [6] | .014 - 0.15 [6] |
| | 9 [7] | ? | ? | | 9 [7] | = .07 [7] |
| R. rubrum FR1VI | NOT OBSERVED | | | | 90 [3] | 0.17 [3] |
| Rps. sphaer. R26 | NOT OBSERVED | | | | 70 [3] | 0.19 [3] |

H in Gauss and $\tau$ in µs

1. RC in state $P\,Q_1$
2. RC in state $P\,Q_1^-$
3. RC in state $P^+Q_1$
4. Assuming that the total triplet yield measured (0.25) reflects both the antenna (.12) and RC triplet state (0.13)
5. B800-B850 complex
6. B800-B850 complex detected at 515 nm
7. reduced chromatophores detected at 540 nm

latter effect can be neglected, because the antenna triplet yield is found te be one order of magnitude smaller than the RC-triplet yield (table 1). However in R. rubrum S1 the RC-triplet state (Fig.s 2A, 4A, 7A) could be estimated from the 430 nm absorbance increase to have a quantum yield of 0.12 while the 580 nm absorbance change, reflecting both the antenna and the RC triplet, results in a quantum yield of 0.25 to 0.38 depending on the excitation wavelength.

The amplitude of the relative MFT is about the same for all species, about 10% in cells/chromatophores and about 25% in RC's, which agrees with the observation that the RC-associated MFE is about 1 - 2% in cells/chromatophores and about 1 - 3% in RC's [chapter IV]. In addition, the $H_{\frac{1}{2}}$ values of the RC-associated MFT and MFE are about the same. In isolated RC's the $H_{\frac{1}{2}}$ values are 50 - 100 Gauss but in cells/chromatophores 230 - 250 Gauss. The absence of fast energy transfer from the RC back to a surrounding antenna in isolated RC's might increase the effective lifetime of the radical pair state and to some extent account for the low $H_{\frac{1}{2}}$ observed in RC's (see chapter IV and VI). However the observed difference between RC's and cells/chromatophores seems to be far too large and sofar we have only an adhoc explanation (see chapter IV for a detailed discussion).

The nature of the decrease of the relative MFT with increasing excitation energy observed in RC's is probably a complex phenomenon.At high pulse intensities multiple hits will occur, leading to a saturation of the triplet yield. The decreased probability of triplet formation in a magnetic field will be partly compensated by these saturation effects, leading to a smaller MFT. In addition, at these high pulse intensities (50 photons/RC) multiple excitation processes will occur, which may even give rise to additional magnetic field effects [20]. In reduced cells/chromatophores the variation of the MFT with the strength of the magnetic field appeared to be more or less independent of the excitation energy. It should be noted, however, that the observed MFT was relatively small ($\leq$ 10%) as compared to that in RC's ($\simeq$ 30%) and that the relative MFT in RC's even at high pulse intensities is maximally reduced about 10%.



The increase of the RC triplet yield in reduced RC's of R. rubrum S1 upon cooling is about the same as the corresponding increase observed in reduced cells/chromatophores ([14], H. Kingma-unpublished results) and can partly be ascribed to a decrease of the recombination rate-constant $K_s$ (Fig. 1, chapter IV,[14]). Below 150 K no recombination luminescence [14] or RC-associated MFE (chapter IV) is observed, which has been explained by assuming that at these temperatures significant recombination of $(P^+I^-)^S$ to $P^*_{880}$ occurs. Therefore the decrease of the MFT and the increase of $\phi_T$ may be related to an increase in $K_c$, $K_t$, the singlet-triplet mixing, or by a decrease in $K_{gs}$ and or $K_{gt}$. A decrease in $K_{gt}$ as a function of the temperature was recently suggested by Schenck et al.[21] to explain the temperature dependence of $\phi_T$ in RC's of Rps. sphaeroides and R.rubrum. However, we recall that the absolute MFT was independent of the temperature, which seems to exclude large changes in $K_c$, $K_t$ or $K_{gt}$ [5]. Moreover temperature dependent S-T mixing would probably also affect the $H_{\frac{1}{2}}$ [5,6] which is contrary to our observations. According to the work of Werner and Schulten [5], a decrease in $K_{gs}$ by a factor of 4 - 5 could result in the decrease of $\Delta\phi_T/\phi_T$ and increase of $\phi_T$, while the $H_{\frac{1}{2}}$ value will remain more or less constant, in agreement with our observations. At 100 K the RC-triplet yield is about 50%,indicating approximately equal probabilities for $P^+I^-$ to finally recombine via $K_{gs}$ directly to the ground state P I or via $K_t$ to $RBChl^T$. At room temperature we have estimated the former probability to be about 7 times larger than the latter (chapter VI) and these numbers support the proposed substantial decrease in $K_{gs}$ upon lowering the temperature. However this is in disagreement with the earlier proposals [14] that a major fraction of the $P^+_{880}I^-$ decay occurs via the excited states $P^*_{880}$ and $B^*_{880}$. This fitted for instance the observed $\phi_E$ as a function of the temperature very well. In addition the energy scheme proposed in chapter IV could not be used to explain the observed variation of $\phi_T$ and $\Delta\phi_T/\phi_T$ with temperature. We will return to this question later (see chapter VII).

b. antenna triplet formation

The magnetic field dependent triplet formation, MFT, in the antenna is only found upon ACAR excitation in antennacomplexes and oxidized cells/chromatophores and is not observed in the CAR-less mutants R. rubrum FR1VI and Rps. sphaeroides R26. Thus, as for the antenna associated MFE (chapter IV), the presence of an ACAR appears to be required. The absence of a spin polarized triplet state in the antenna of Rps. capsulata [31] seems to exclude the formation of a radical pair state, which could possibly account for the magnetic field dependent processes observed in the antenna [15]. However, the antenna associated MFE and MFT can be explained by singlet fission of an excited ACAR into a triplet pair. The absence of a temperature dependence of the triplets formed by fission favour the idea that fusion (rateconstants $K_2$,$K_4$) is not important.

R. rubrum S1

The MFT in R. rubrum S1 shows a magnetic field dependence compared complementary to that of the antenna associated MFE (chapter IV). The shapes of the curves do not permit to distuingish between homofission, involving the triplet pair $^{T}ACAR.ACAR^{T}$ and heterofission (e.g. $^{T}ACAR{\cdot}ABchl^{T}$ ,[20],N.E. Geacintov (personal communication) ). Let us first consider the case of heterofission. As was argued in the previous chapter, ABChl seems to be the only pigment present in the antenna of R. rubrum, which apart from spirilloxanthin has a sufficiently low triplet energy (about 1.0 eV [ 32,33]) to be generated via singlet fission from the spirilloxanthin excited state (≃ 2.2 eV [22]). Moreover, the energy available in the excited carotenoid may only be 1.65 eV [22,34]. The energy of the triplet pair state $^{T}ACAR.ABchl^{T}$ (about 1.65 eV) can only roughly be estimated [20, 22],N.E. Geacintov and T.A. Moore (personal communication) . As these energies are so close, fusion to ACAR* seems not impossible. This would however result [20] in a temperature dependent triplet yield, contrary to our observations. For this case of heterofission, it might be expected that also ABchl excitation (ABchl*



≃ 1.4 - 1.55 eV) could lead to formation of the triplet pair, again contrary to the observation that no MFT is observed upon ABChl excitation. The only reason for this may be the energy difference of at least 0.1 eV. Finally the triplet pair [$^{T}ACAR.ABChl^{T}$] could be expected to fuse at least partly into $ABChl^{*}$. The triplet yield of 0.3 for $ACAR^{T}$ is similar to the energy transfer efficiency of 0.3 [25] of $ACAR^{*}$ to $ABChl^{*}$ and this seems to disagree with the large relative MFT of 40% and the extremely low MFE of 0.1%. In conclusion, heterofission can not be excluded, but of all the possible fates of the [$^{T}ACAR{\cdot}ABchl^{T}$] state, only the decay to $ACAR^{T}$ or [ACAR·ABChl] seem to be significant.

In the case of homofission where the triplet pair consists of [$^{T}ACAR.ACAR^{T}$] no restrictions with respect to the energetics are required to explain that CAR excitation is necessary in order to observe MFT. The large energy difference between ACAR* and [$^{T}ACAR.ACAR^{T}$] is now directly responsible for the absence of a temperature dependence. It seems not unlikely that the carotenoids associated to B850 occur in pairs, which may have a relatively strong interaction as manifested by a strong conservative CAR-CD spectrum (Kramer, H., van Grondelle, R., Hunter, N. and Amesz, J., manuscript in preparation). However the large amplitude difference between the MFE and MFT remains puzzling and suggests that it is not only the rate constant $K_1$, which depends on a magnetic field but also the ratio $K_6/K_7$.

Rps. sphaeroides

In contrast to R. rubrum both in Rps. sphaeroides G1C and 2.4.1, a MFT increase is observed in antenna complexes. The relative MFT is small, 3 - 10% and is only observed upon ACAR excitation. No MFT is found in the CAR-less mutant R26. If we assume that the efficiency of energy transfer from $ACAR^{*}$ to ABChl exceeds 90%, the similarity of the difference spectra (Fig. 6A), the equality of the quantum yields and the absence of the magnetic field dependence upon BChl excitation, can be explained by the hypothesis that the antenna CAR triplet in zerofield is formed predominantly via intersystem of $BChl^{*}$ ($CAR^{*} \rightarrow BChl^{*}$ $\xrightarrow{isc}$ $BChl^{T} \rightarrow CAR^{T}$). Apparently no single triplet state is formed by singlet fission in zero field. Together with the initial increase

of the triplet yield with increasing magnetic field and the need for specific carotenoid excitation, this can be understood by assuming that the triplet pair consists of two identical carotenoid molecules (sphaeriodene in Rps. sphaeroides 2.4.1 and neurosporene in Rps. sphaeroides G1C) with a special mutual orientation [15]. The shape of the curves shown in the Figs. 5B and 6B can then be explained as follows: In zerofield a triplet can not be formed by homofission, because fission is a spin-conserving process and the nine possible substates of the triplet pair are now pure quintet, triplet and mixed singlet-quintet states. As the magnetic field increases, the substates will be mixed and there will be substates with a mixed singlet-triplet character, resulting in triplet formation. At high fields the rate constants of fission decreases due to a lower number of substates with some singlet character. The triplet yield in zerofield will therefore be equal to or lower than that in the presence of a magnetic field.
Heterofission can not account for the observed magnetic field dependence of the MFT observed, because then the triplet pair state may have triplet character, even in zerofield, and a single triplet state would be formed [15].

## SOME CONCLUDING REMARKS

Carotenoids in photosynthetic bacteria appear to have the following functions:

1. Increasing the absorption of light energy in the blue region of the spectrum and transfer of this energy, in the form of singlet excitation, to bacteriochlorophyll.
2. Accepting the harmfull triplet energy from bacteriochlorophyll triplets formed from an excess of excited singlet bacteriochlorophylls.

In both R. rubrum and Rps. sphaeroides, homofission can very well explain the observed antenna associated MFE and MFT. The observation that the antenna carotenoids in Rps. sphaeroides generate



a strong conservative CD signal [8], indicates that a strong interaction is present between the carotenoids involved as might be expected in the case of homofission. In R. rubrum magnetic field dependences of the MFT and the MFE are complementary which indicates that the triplet pair does not act as an intermediate state of the energy transfer from ACAR* to ABChl, but forms an additional decay route for the excitation energy. It may well be that about 60 to 70% of the excitation energy decays via the triplet pair state, of which 30% results in a single triplet state and the remaining 30 to 40% decays to the ground state.

REFERENCES


1. Blankenship, R.E., Schaafsma, T.J. and Parson, W.J. (1977) Biochim. Biophys. Acta 461, 297-305
2. Hoff, A.J., Rademaker, H., van Grondelle, R. and Duysens, L.N.M. (1977) Biochim. Biophys. Acta 460, 547-554
3. Rademaker, H., Hoff, A.J., van Grondelle, R. and Duysens, L.N.M. (1980) Biochim. Biophys. Acta 592, 240-257
4. Adrian, F.J. (1977) in Chemically Induced Magnetic Polarization eds. Muus, L.T., Atkins, P.W., McLaughan, K.A. and Pedersen, J.B. (Reidel, Dordrecht, The Netherlands), 77-105
5. Werner, H.J., Schulten, K. and Weller, A. (1978) Biochim. Biophys. Acta 502, 255-268
6. Norris, J.R., Bouwman, M.K., Budil, D.E., Tang, J., Wraight, C.A. and Closs, G.L. (1982) Proc. Natl. Acad. Sci. USA 79, 5532-5536
7. Zankel, K.L., Reed, D.W. and Clayton, R.K. (1968) Proc. Natl. Acad. Sci. USA 61, 1243-1249
8. Rockley, M.G., Windsor, M.W., Cogdell, R.J. and Parson, W.W. (1975) Proc. Natl. Acad. Sci. USA 72, 2251-2255
9. Holten, D., Hoganson, C., Windsor, M.W., Schenck, C.C., Parson, W.W., Migus, A., Fork, R.L. and Shank, C.V. (1980) Biochim. Biophys. Acta 592, 461-477
10. Shuvalov, V.A., Klevanik, A.V., Sharkov, A.V., Matveetz, Yu.A. and Krukov, P.G. (1978) FEBS Lett. 91, 135-139
11. Dutton, P.L., Prince, R.C., Tiede, D.M., Petty, K.M., Kaufmann, K.J., Netzel, T.L. and Rentzepis, P.M. (1977) Brookhaven, Symp. Biol. 28, 213-232
12. Shuvalov, V.A. and Parson, W.W. (1981) Proc. Natl. Acad. Sci. USA
13. Cogdell, R.J., Monger, T.G. and Parson, W.W. (1976) Biochim. Biophys. Acta 408, 189-199
14. Van Grondelle, R., Holmes, N.G., Rademaker, H. and Duysens, L.N.M. (1978) Biochim. Biophys. Acta 503, 10-25
15. Rademaker, H. (1980), Thesis, University of Leiden





16. Monger, T.G., Cogdell, R.J. and Parson, W.W. (1976) Biochim. Biophys. Acta 1149, 136-153
17. Kingma, H., van Grondelle, R., Duysens, L.N.M., van der Kooy, F.W. and Vos, M. (1983) Proc. VIth Int. Congr. Photosynth. Brussels, in the press
18. Elfimov, E.I., Voznyak, V.M. and Prokhorenko, I.R. (1982) Doklady Akademii Nauk 164, 248-255
19. Frank, H.A. and Macgann, W.J. (1983) Proc. VIth Int. Congr. Photosynth., Brussels, in the press
20. Svenberg, C.E. and Geacintov, N.E. (1973) in Organic Molecular Photophysics, Vol. 1 (J.B. Birks, ed), 489-564
21. Schenk, C.C., Blankenship, R.E. and Parson, W.W. (1982) Biochim. Biophys. Acta 680, 44-59
22. Bensasson, R., Land, E.J. and Maudinas, B. (1976) Photochem. Photobiol. 23, 289-193
23. Van der Rest, M. and Gingras, G. (1974) J. Biol. Chem. 249, 6446-6449
24. Cogdell, R.J., Parson, W.W. and Kerr, M.A. (1976) Biochim. Biophys. Acta
25. Duysens, L.N.M. (1952) Thesis, University of Utrecht
26. Slooten, L. (1973) Thesis, University of Leiden
27. Van Grondelle, R., Duysens, L.N.M. and van der Wal, H.N. (1976) Biochim. Biophys. Acta 449, 169-187
28. Feher, G. and Okamura, M.V. (1978) In Photosynthetic Bact. Plenum Press. New York, 349-386 (R.K. Clayton and W.R. Sistrom, Eds)
29. Hipkins, M.F., Cogdell, R.J., MacDonald, W. and Truscott, T.G. (1981) In Photosynthesis I (Edited by G. Akoyknoglou) 143-153 Balaban Int. Science Services, Philadelphia, Pa.
30. Schmidt, K. (1978) In Photosynth. Bact., Plenus Press, New York, 729-750 (R.K. Clayton and W.R. Sistrom, Eds.)
31. Frank, H.A. MacGann, W.J. Macknicki, J. and Felber, M. (1983)
32. Lebedev, N.N. and Krasnovskii, A.A. (1979) Biophysics 23, 1115-1117
33. Seely, G.R. (1978) Photochem. Photobiol. 27, 639-654
34. Trash, R.J., Fang, L.B. and Leroi, G.E. (1979) Photochem. Photobiol. 29, 1049-1050

35. Van Grondelle, R., Kramer, H.J.M. and Rijgersberg, C.P. (1982) Biochim. Biophys. Acta 682, 208-215
36. Kramer, H.J.M., van Grondelle, R., Hunter, C.N. and Amesz, J. (1983) Proc. VIth Int. Congr. Photosynth. Brussels, in the press
37. Holmes, N.G., van Grondelle, R, Hoff, A.J. and Duysens, N.L.M. (1976) FEBS Lett. 70, 185-190
38. Merrifield, R.E. (1968) J. Chem. Phys. 48, 4318-4319
39. Merrifield, R.E., Aviakan, P. and Groff, R.P. (1969) Chem. Phys. Lett. 3, 155-159
39. Lutz, M., Kléo, J. and Reiss-Husson, F. (1976) Biochim.Biophys. Res. Commun. 69, 711-717
40. phys. Res. Commun. 69, 711-717
41. Koyama, Y.M., Takii,T., Saiki, K. and Tsukida, K. (1983)



# MAGNETIC FIELD-STIMULATED LUMINESCENCE AND A MATRIX MODEL FOR ENERGY TRANSFER. A NEW METHOD FOR DETERMINING THE REDOX STATE OF THE FIRST QUINONE ACCEPTOR IN THE REACTION CENTER OF WHOLE CELLS OF RHODOSPIRILLUM RUBRUM

H. KINGMA, L.N.M. DUYSENS and R. van GRONDELLE
Department of Biophysics, Huygens Laboratory of the State University, P.O. Box 9504, 2300 RA Leiden (The Netherlands).
Department of Biophysics, Physics Laboratory of the Free University, De Boelelaan 1081, 1081 HV Amsterdam, The Netherlands.

## SUMMARY

In whole cells of Rhodospirillum rubrum the light-induced absorbance difference spectrum of the reduction of the first quinone electron acceptor $Q_1$ was determined in order to relate the emission yield $\phi$ and the magnetic field-induced emission increase $\Delta\phi$ to the redox state of $Q_1$. It was found that $\Delta\phi/\phi^2$ is a linear function of the number of reaction centers in which $Q_1$ is reduced, independent of the fraction of reaction centers in the oxidized state. The emission yield is a hyperbolic function of the fraction of closed reaction centers, either by reduction of the acceptor $Q_1$ or by oxidation of the primary electron donor P. Apparently in whole cells of Rhodospirillum rubrum a matrix model for energy transfer between various photosynthetic units can be applied. A model is presented, which is a generalization of theoretical considerations reported before (Duysens, L.N.M. (1978) in Chlorophyll Orga-

---

Abbreviations: TMPD, N,N,N',N'-tetramethyl-1,4-Phenylene diamine dihydrochloride; DAD, 2,3,5,6 tetra-methyl-p-phenylene diamine; Tricine, N-tris hydroxymethyl methyl glycine.

nization and Energy Transfer in Photosynthesis, Ciba Foundation Symposium 61 (new series), pp. 323-340, Elsevier/North-Holland, Amsterdam) and which is in excellent agreement with the experiments. From simultaneous measurements of $\Delta\phi$ and $\phi$ the redox state of the reaction center can relatively easily be determined. So far this is the only method for simultaneously measuring the fractions $P^+$ and $Q_1^-$ in intact cells under steady state conditions.

## INTRODUCTION

If the quinone acceptor $Q_1$ of the reaction center complex of purple bacteria is in the oxidized state before illumination, electron transport mainly proceeds towards $Q_1$ and the second quinone acceptor $Q_2$ [1,2,3,4,5] (see Fig. 1). Upon reduction of $Q_1$ both the light-induced bacteriochlorophyll emission and the reaction center triplet yield increase 6 . The increase in emission (by a factor of about two [7,8,9]) can be ascribed to luminescence caused by charge recombination of the singlet state of the radical pair $(P^+I^-)^S$ (P is the primary donor, a bacteriochlorophyll dimer and I is bacteriopheophytin [6,10,11,29].

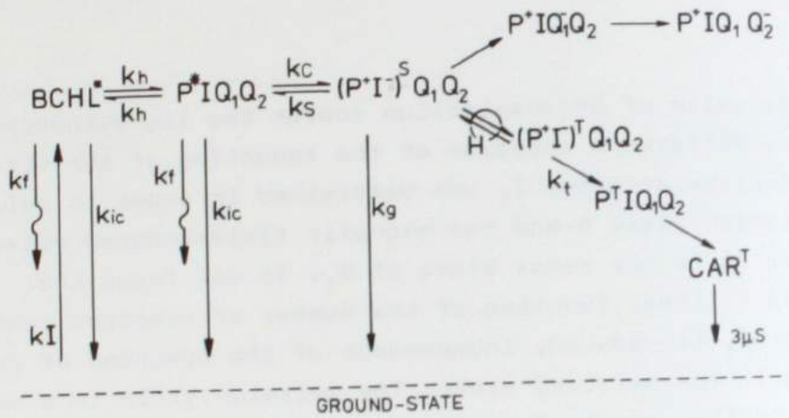


*Fig. 1 Scheme of energy and early electron transfer in R. rubrum S1. BChl is antenna bacteriochlorophyll; P is the reaction center bacteriochlorophyll; I is bacteriopheophytin ; $Q_1$ and $Q_2$ are ubiquinones; CAR is a reaction center carotenoid; $k_f$, $k_{ic}$, $k_c$ are the rate constants for fluorescence, internal conversion and charge separation; $k_s$, $k_g$ and $k_t$ are the rate constants for charge recombination of the radical pair to $P^*$, P and $P^T$, respectively. See text.*

A weak magnetic field (H) increases the luminescence yield and decreases the reaction center triplet yield [12,13,14,15]. In a previous paper [16] this is discussed in terms of a magnetic field dependent steady-state distribution between singlet and triplet states of the radical pair $P^+I^-$. It was shown that upon excitation of bacteriochlorophyll, this magnetic field-induced emission increase ($\Delta F$) only occured when the acceptor $Q_1$ was prereduced.

Here we show that the magnetic field-induced emission increase can be used as a monitor specific for the concentration of $PIQ_1^-$. This was done by correlating the emission yield increases with the light-induced absorbance changes due to the reduction of $Q_1$ in whole cells of Rhodospirillum rubrum. In many cases the magnetic field-induced emission increase will provide a more simple and reliable probe for determining the redox state of the reaction center than the small absorbance changes in the near-ultraviolet region of the spectrum due to the reduction of $Q_1$.

The yield of bacteriochlorophyll emission not only depends on the concentration of $Q_1^-$ and the intensity of a magnetic field, but also on the type of energy transfer in the antenna pigment system (lake or matrix model vs. separated units). Fig. 2 pictures a model based upon energy transfer in a matrix of pigment molecules with ten or more reaction centers, which very well describes the results presented here.

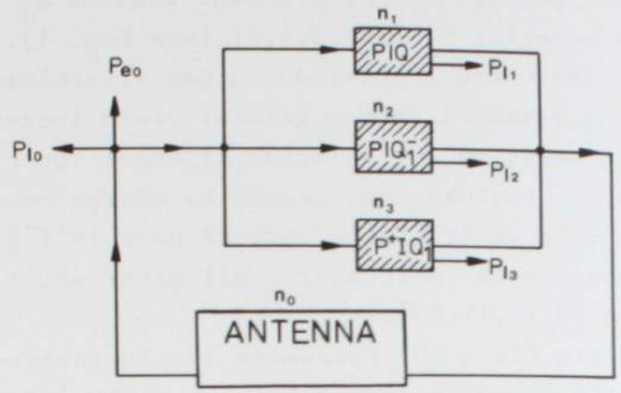


*Fig. 2 Schematic representation of the model used for computer simulation based upon the matrix model. A light quantum absorbed by the antenna molecules ($n_o$ is the number of antenna molecules per reaction center) has a probability $P_{eo}$ of emission, $P_{lo}$ of losses and $(1-P_{eo}-P_{lo})$ of transfer to the reaction center in the various states. $n_1$, $n_2$ and $n_3$ indicate the fraction of traps in the state $P\,I\,Q_1$, $P\,I\,Q_1^-$, respectively. After trapping, excitation energy is either lost with a probability $P_{lk}$ (k = 1, 2, 3) due to photochemistry, triplet formation, and other losses or energy is transferred back to the antenna*

## THEORETICAL

In this section we will derive a set of equations which describe the relation between the emission yield and the fractions of reaction centers in various states for a matrix of antenna molecules and reaction centers. Let $n_k$ be the average number of molecules of the type of the state k per reaction center. By $n_o$ (k = 0) the number of antenna molecules per reaction center is designated, by $n_1$ the fraction of reaction centers in the photoactive state $P\,I\,Q_1$ and by $n_2$ and $n_3$ the fractions of reaction centers in the states $P\,I\,Q_1^-$ and $P^+I\,Q_1$, respectively, with:



$$n_1 + n_2 + n_3 = 1 \qquad (1)$$

$P_{ik}$ is the probability that a process (e.g. emission) occurs on a molecule of type k before energy transfer to any other molecule takes place. $P_{lk}$ is the probability that energy is lost or converted and not transferred after arriving on a molecule of type k. If the probability of loss of energy for each excited molecule is low compared to the probability for transfer, and if the transfer probabilities are equal for all antenna molecules , then the excitation will visit a representative part of the molecules of the matrix with equal probability. The quantum yield for the process i is then given by:

$$\Phi_i = \sum_{k=o}^{3} n_k P_{ik} \Big/ \sum_{k=o}^{3} n_k P_{lk} \qquad (2)$$

All terms in the numerator of eq. (2) are small compared to $n_o P_{eo}$ for the process of emission (i = e), because $n_o \approx 50$ and $n_1 + n_2 + n_3 = 1$, and $P_{ek} \ll P_{eo}$ for k = 1, 2 of 3. $P_{ek}$ is defined as the probability of emission of an excited molecule of type k. By taking the inverse of both sides of eq. (2) we find:

$$\frac{1}{\Phi_e} = \frac{n_o P_{lo} + n_1 P_{l1} + n_2 P_{l2} + n_3 P_{l3}}{n_o P_{eo}} \qquad (3)$$

Only the states $P\,I\,Q_1$, $P\,I\,Q_1^-$ and $P^+I\,Q_1$ may be expected to be present because of the relatively high rate of the back reaction $P^+I\,Q_1^- \rightarrow P\,I\,Q_1$ in moderate continuous light [8]. This proved to be consistent with the experiments (see below). A saturating magnetic field causes a decrease $\Delta P_{12}$ in the probability $P_{12}$ of loss processes occurring in reaction centers in the state $P\,I\,Q_1^-$ and thus results in an increase of $\Delta\Phi_e$ in emission. By taking the differential of eq. (3) we obtain in first approximation ($\Delta\Phi \ll \Phi$):

$$\frac{\Delta\phi_e}{\phi_e^2} = - \frac{\Delta P_{12}}{n_o P_{eo}} \cdot n_2 \qquad (4)$$

In a similar way as was done for eq. (3), an expression for the reaction center triplet yield is found :

$$\frac{1}{\phi_t} = \frac{n_o P_{1o} + n_1 P_{11} + n_2 P_{12} + n_3 P_{13}}{n_2 P_{t2}} \qquad (5)$$

where $P_{t2}$ represents the probability of triplet formation in the reaction center in the state P I $Q_1$ ($P_{to} = P_{t1} = P_{t3} = 0$; $\Delta P_{t2} \simeq \Delta P_{12}$). The form of the equations 2 and 3, giving the emission yield as a function of the concentrations of the various states of the reaction centers does not depend on the type of emission whether it is fluorescence or luminescence. The equations 3, 4 and 5 have been derived using the condition that the rate constant of transfer of excitation energy $k_h$ is so large that the excitation energy visits a representative part of the matrix of $P_{11}$ < 0.3. Probably the linear relation between the fractions $n_k$ and the increase of $\phi_e$ remains approximately valid if the condition of very rapid transfer is relaxed, provided that the excitation can visit ten or more units and the ratio $P_{11}/P_{13}$ is not too high (Den Hollander et al., manuscript in preparation).

## MATERIALS AND METHODS

Whole cells of R. rubrum strain $S_1$ were grown in a continuous culture at a light intensity of about 5 mW/cm² (incandescent light). The absorbance (880 nm - 960 nm) of the suspension was kept constant at 0.5 by a feed back system. After centrifugation cells were washed twice in buffer containing 50 mM Tricine, 5mM $K_2HPO_4$, 5mM $MgCl_2$ (pH = 8.0) and resuspended in the same buffer. Samples were then immediately prepared as follows. The cells ($OD_{880-960}$ = 0.5) were aerated and put in the dark for 5 min to prevent accumulation of reduced



acceptors. Then orthophenanthrolin was added up to a final concentration of 2.0 mM to block the electron transport between $Q_1$ and the next quinone acceptor $Q_2$ [17,18]. After 5 min of flushing with nitrogen in the dark to obtain anaerobiosis, ascorbate and DAD were added to final concentrations of 0.20 mM and 10.0 mM, respectively, as an efficient donor system to prevent accumulation of the state $P^+I\,Q_1$ or $P^+I\,Q_1^-$ upon illumination. Gramicidin (200 - 250 µM) was added to prevent the formation of a membrane potential. The relatively high concentration of gramicidin as compared to that usually applied to chromatophores (∿ 1 µM) was found to be necessary to completely eliminate electrochromic absorbance changes upon illumination as judged from the absorbance difference spectrum of $P^+$ - P at high light intensities (see results). Samples in which $Q_1$ was completely reduced were prepared by adding sodium dithionite (final concentration 5.0 mM) after 5 min of dark adaption and flushing with nitrogen. During all experiments the temperature was controlled at 288 ± 1 K.

The magnetic field-induced emission and the absorbance change associated with the increase in $Q_1^-$ were measured simultaneously by means of the apparatus described previously [16]. To improve the resolution at low measuring light intensity, this apparatus was altered slightly. A beam splitter was placed in the measuring light beam so that small changes in intensity could be detected using a photodiode. By means of a differential amplifier a correction was made for instabilities of the measuring light. By applying a sinusoidal 50 Hz-modulated magnetic field with an amplitude of maximally 130 mT, it was possible to compute the stimulated emission saturation curve from half a period, averaged at low light intensities up to 270 000 times to increase the signal-to-noise ratio. Excitation occurred through appropriate interference filters with light of 603 nm, that excited the bacteriochlorophyll but not the carotenoids. The emission was detected at 905 nm by means of an S1-type photomultiplier with a Kodak Wratten 87C absorbance filter and an interference filter Schott AL 905. Simultaneously, absorbance changes were detected by means of a

S20-type photomultiplier with a Balzers interference and a Corning CS 7-59 filter. The wavelengths of the beams for the absorption measurements were selected by a monochromator (bandwidth 3.2 nm). During these experiments, no actinic effect of these beams, which were only admitted during a short period, was detected. The absorbance difference spectrum of the acceptor $Q_1$ was determined in a chopped single beam spectrophotometer described elsewhere [19]. The absorbance change due to the decay of the reaction center carotenoid triplet (see scheme of Fig. 1) and the magnetic field-induced decrease of the reaction center carotenoid triplet yield were measured at 432 nm upon excitation with a 602 nm dye laser flash (halftime 10 ns). The light-induced absorbance difference spectrum of the reaction center carotenoid triplet shows a maximum at 432 nm where no absorbance change due to the formation of an antenna carotenoid triplet is observed [20]. The 432 nm absorbance increase also reflects the oxidation/reduction of P, but can be distinguished from the 3.2 µs carotenoid triplet decay kinetically. The oxidation of P occurs within ca. 10 ps [21,22] the reduction of $P^+$ by recombination of the radical pair in ca. 3 ns [24] and the reduction by DAD or cytochrome in several milliseconds.

RESULTS

I. Light-induced absorbance difference spectrum.

Fig. 3A shows the kinetics of the light-induced absorbance changes at 330, 350 and 450 nm upon illumination of whole cells of R. rubrum. Three traces are depicted, measured at an excitation light intensity of 3 mW/cm² at 603 nm, which saturated the changes at the wavelengths shown. At light intensities below 5 mW/cm² the absorbance changes showed similar simple kinetics with decay times, which were independent of the light intensity.



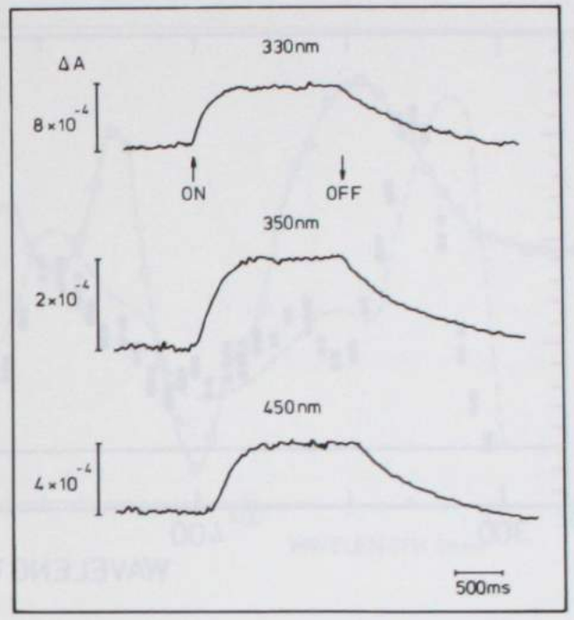


*Fig. 3 A. Kinetics of the absorbance changes at 330, 350 and 450 nm in whole cells of R. Rubrum upon 603 nm excitation ( 3 mW/cm² ) in the presence of 10.0 mM DAD, 2.0 mM orthophenonthroline, 0.20 µM Na-ascorbate and 250 µM gramicidine.*

For the Spectrum shown in Fig. 3B a saturating excitation light intensity of 3 mW/cm² was used. Although the kinetics showed some variation, the same difference spectrum was obtained with different samples. To obtain reproducible kinetics the sequence of additions and the dark adaptation times had to be rigorously standardized. The same spectrum was found with TMPD as electron donor instead of DAD. This indicates that the spectrum was not affected by absorbance changes due to oxidation of the electron donor. In the experiments

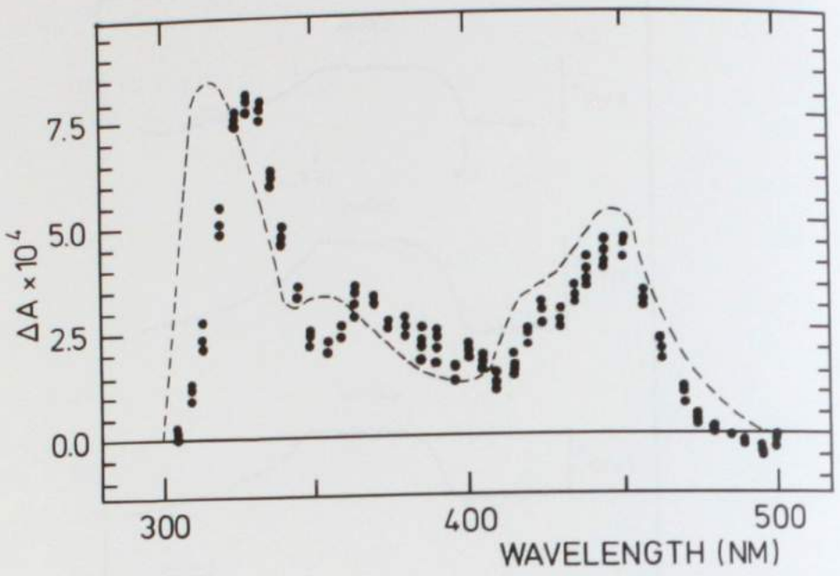


*Fig. 3 B. Light-induced absorbance difference spectrum in whole cells of R. rubrum (●). Absorbance at 880 nm, after correction for the absorbance at 960 nm, 0.5. Samples were excited at 603 nm ( 3 mW/cm²). The dotted line represents the absorbance difference spectrum of ubisemiquinone - 10 minus ubiquinone - 10 in methanol (---).*

discussed below, the 450 nm absorbance change was measured in order to relate the magnitude of the magnetic field-induced emission change to the fraction of the acceptor $Q_1^-$.

At excitation light intensities above 25 mW/cm² the kinetics of the absorbance changes became more complex and the difference spectrum indicated the accumulation of $P^+$.



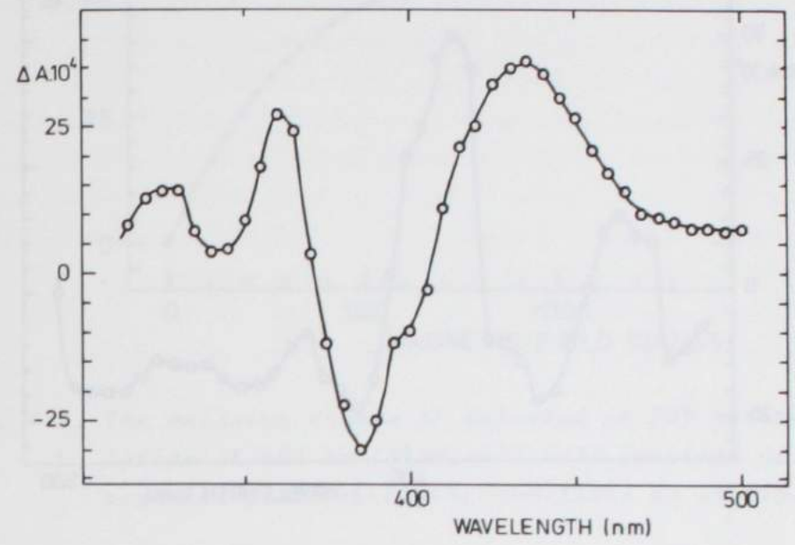


*Fig. 3 C. Light-induced absorbance difference spectrum in whole cells of R. rubrum. Samples were excited at 603 nm (45 mW/cm²). Conditions as in Fig. 3A and 3B.*

The spectrum shown in Fig. 3C was found if the excitation light intensity exceeded 40 mW/cm². At light intensities between 25 - 45 mW/cm² a spectrum was found that appeared to be a linear combination of the spectra shown in Fig. 3B and 3C.

If no gramicidin was added, the absorbance difference spectrum was markedly affected by electrochromic changes. Fig. 3D shows the absorbance difference spectrum without gramicidin minus the absorbance difference spectrum in presence of gramicidin at an excitation light intensity of 45 mW/cm². Similar results were obtained in chromatophores of R. rubrum S1.

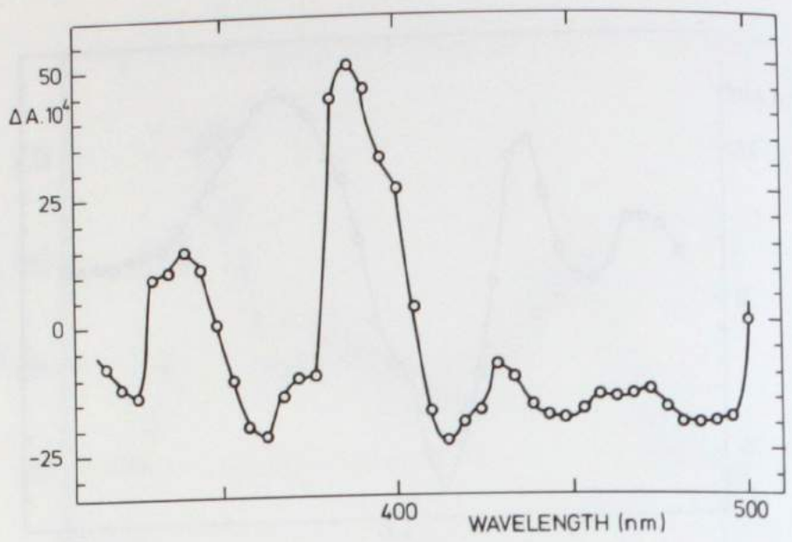


*Fig. 3 D. The light-induced absorbance spectrum without gramicidin minus the light-induced absorbance spectrum in the presence of 200 µM gramicidin. Excitation light intensity (603 nm) 45 mW/cm². Conditions as in Fig. 3A and 3B.*

II. Magnetic field-induced emission change ΔF

Fig. 4A shows the increase in emission at 905 nm in whole cells of R. rubrum induced by a magnetic field. The addition of gramicidin dit not affect the shape or amplitude and similar curves were obtained at various light intensities and after chemical reduction by dithionite. The absorbance change at 450 nm during conitnuous 603 nm excitation was simultaneously detected. By varying the light intensity I of the actinic light more than thousand times from 35 µW/cm² to 45 mW/cm², different steady-state concentration of reduced acceptor $Q_1$ were established. For a number of intensities I we determined the relation between emission yield increase and magnetic field strength resulting in curves similar to the one shown



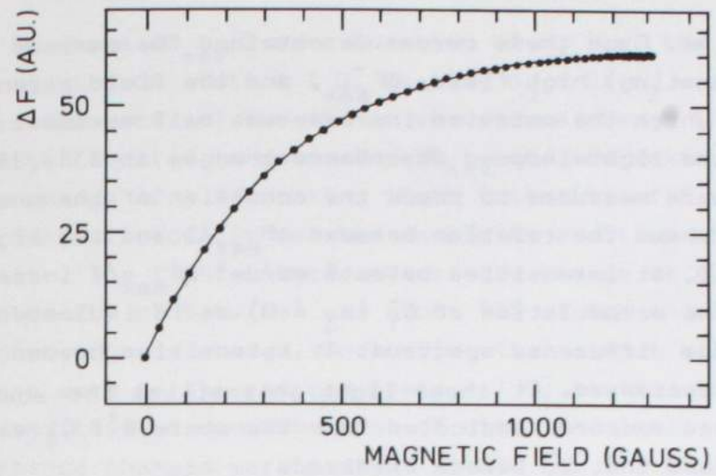


*Fig. 4 A. The emission change ΔF detected at 905 nm upon excitation at 603 nm (4 mW/cm²) as a function of the magnetic field strength. Conditions as in Fig. 3A.*

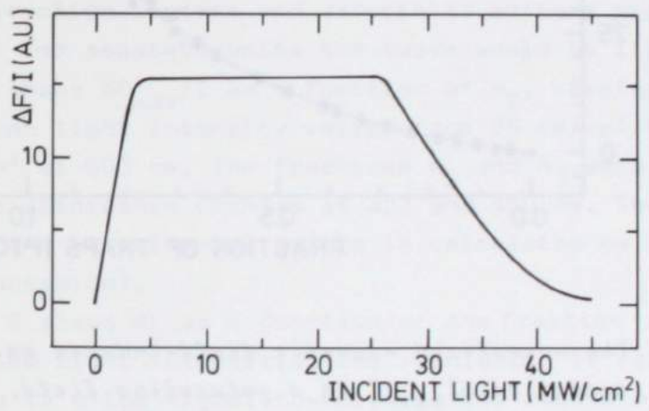


*Fig. 4 B. The magnetic field-induced emission increase $\Delta F_{max}$ detected at 905 nm in a saturating field normalized for the excitation light intensity, as a function of the 603 nm excitation light intensity I. Conditions as in Fig. 3A.*

in Fig. 4A. From these curves we obtained the maximum change in (saturating) high field, $\Delta F_{max}$, and the field strength $H_{1/2}$ at which the emission increase was half maximum. In each sample the light-induced absorbance changes at 330, 380 and 450 nm were measured to check the condition of the sample. Fig. 4B shows the relation between $\Delta F_{max}/I$ and the light intensity I. At intensities below 5 mW/cm² $\Delta F_{max}/I$ increases due to the accumulation of $Q_1^-$ ($n_3 = 0$) as is indicated by the absorbance difference spectrum. At intensities beyond 25 mW/cm² $\Delta F_{max}/I$ decreased. At these light intensities the absorbance difference spectrum indicated that the state $P^+I\,Q_1$ was accumulated and that $Q_1^-$ became oxidized.

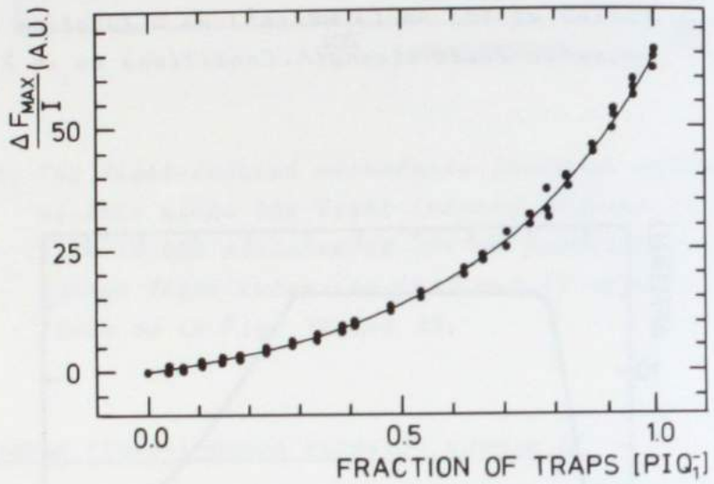


*Fig. 5 A. The normalized magnetic field-induced emission increase of $\Delta F_{max}/I$ in a saturating field, monitored at 905 nm, as a function of the fraction $n_2$ of traps $P\,I\,Q_1^-$ ($n_3 = 0$). Excitation at 603 nm (35 μW/cm² - 5 mW/cm²). $n_2$ is calculated from the 450 nm absorbance change due to the reduction of $Q_1$. Conditions as in Fig. 3A. The curve through the experimental points is calculated using eq. (3) (see Discussion).*



Fig. 5A shows $\Delta F_{max}/I$ as a function of $n_2$ i.e. the fraction of traps in the state $P\,I\,Q_1^-$ keeping $n_3 = 0$; $n_2$ was calculated as the ratio of the 450 nm absorbance change induced by the light applied to determine $\Delta F_{max}$ and the maximum absorbance change of a saturating light intensity of 5 mW/cm² after chemical reduction of the sample by addition of 5 mM dithionite. The light-induced absorbance change at 450 nm at an intensity of 5 mW/cm² was about 95% of the chemically induced absorbance change, indicating that almost all reaction centers were in the reduced state $P\,I\,Q_1^-$ at this light intensity and that no contributions of other chemically induced absorbance changes were present at 450 nm. The maximum relative magnetic field-induced emission change $\Delta F_{max}/F$ measured 1.5%. The curve through the experimentally obtained points was calculated by using equation 3, assuming that the magnetic field induced emission increase can be ascribed to a decrease of $P_{12}$ (see discussion).
The curve in Fig. 5A is markedly non-linear which can be explained by energy transfer in a matrix consisting of a number of reaction centers and associated antenna pigments (units); for separate units the curve would be linear [28]. Fig. 5B shows $\Delta F_{max}/I$ as a function of $n_2$, keeping $n_1 = 0$. Excitation light intensity varied from 25 mW/cm² to 45 mW/cm² at 603 nm. The fractions $n_2$ and $n_3$ were calculated from the absorbance changes at 432 and 450 nm. The curve through the experimental points is calculated by using eq. 3 (see discussion).

Fig. 6 shows $H_{\frac{1}{2}}$ as a function of the fraction of traps $n_2$. At low light intensities the resolution is relatively poor due to a low signal-to-noise ratio, caused by small signals.

Fig. 7 shows the reaction center carotenoid triplet yield (fraction of carotenoid triplets per reaction center) induced by a non-saturating 10 ns dye laser flash (602 nm) as a function of the fraction of traps $n_2$ varied by different intensities of the continuous background illumination (603 nm).

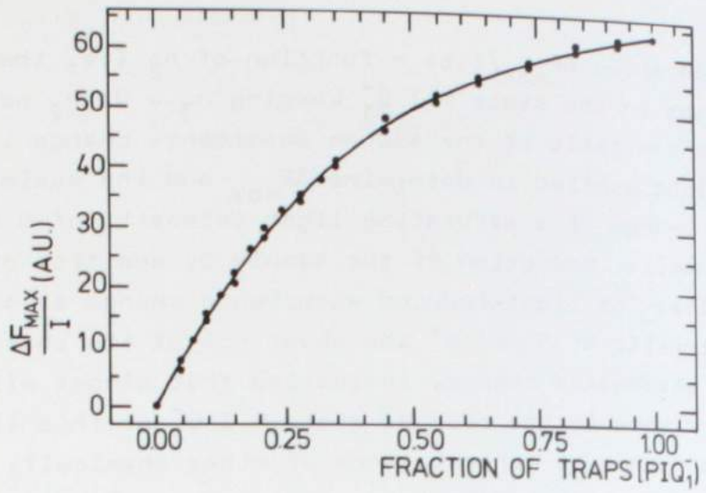


*Fig. 5 B. The normalized magnetic field-induced emission increase $\Delta F_{max}/I$ in a saturating field at high excitation light intensity (25 mW/cm² - 45 mW/cm²) as a function of $n_2$ ($n_1$ = 0). Conditions as in Fig. 3A. The curve through the experimental points is calulated using eq. (3) (see Discussion), for which $n_2$ and $n_3$ are calculated from the absorbance change at 432 and 450 nm.*

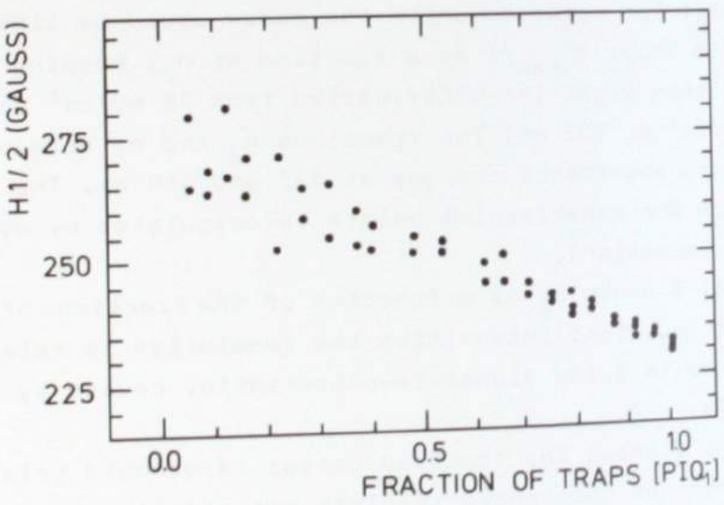


*Fig. 6. The magnetic field strength $H_{½}$ at which the emission increase is half maximum (see Fig. 4A) as a function of $n_2$. Conditions as in Fig. 3A. $n_2$ is calculated from the absorbance change at 450 nm.*



The absorbance increase at 432 nm due to the formation of the carotenoid triplet decays with a single exponent of 3.2 µs. At 432 nm no absorbance change due to antenna carotenoid triplet formation is observed. The oxidized primary donor is completely reduced by the artificial donor system within 3 ms [16]. The curve drawn through the experimental points is calculated by using eq. 5 (see discussion). The carotenoid triplet yield decreased by about 10% in high magnetic field (1300 Gauss).

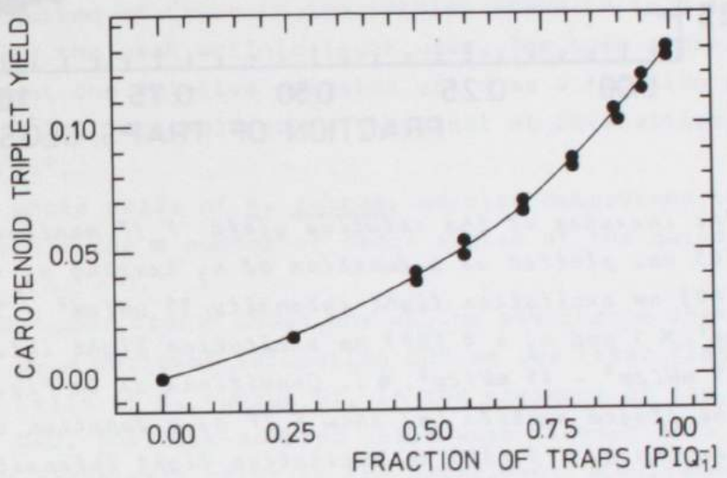


*Fig. 7. The reaction center carotenoid triplet yield $\Phi_t$ in a non-saturating 10 ns dye laser flash (602 nm) as a function of $n_2$ ($n_3$ = 0). The triplet yield is monitored at 432 nm ($\Delta\varepsilon$ = 60 $mM^{-1}$ $cm^{-1}$). $n_2$ is varied by using different intensities (35 µW/cm² - 5 mW/cm²) of the continuous excitation light and calculated from the 450 nm absorbance change. Conditions as in Fig. 3A. The curve through the experimental points is calculated by using eq. 5 (see text).*

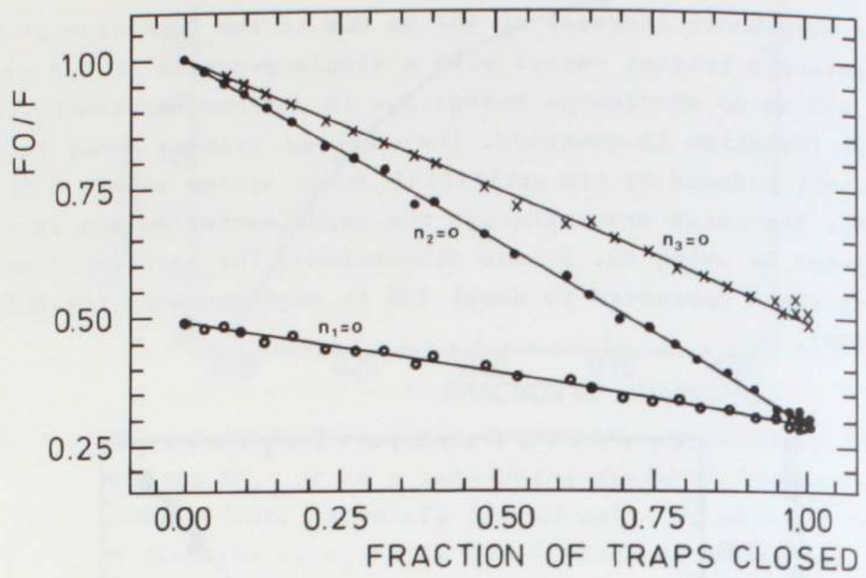


*Fig. 8. The increase of the relative yield $F_o/F$, monitored at 905 nm, plotted as a function of $n_2$ keeping $n_3$ = 0 (603 nm excitation light intensity 35 µW/cm² - 5 mW/cm², × ) and $n_1$ = 0 (603 nm excitation light intensity 25 mW/cm² - 45 mW/cm², o ). Conditions as in Fig. 3A. The closed symbols (•) show $F_o/F$ as a function of $n_3$ keeping $n_2$ = 0 (603 nm excitation light intensity 35 µW/cm² - 45 mW/cm²). Samples prepared in the presence of 250 µM gramicidin only. $n_2$ and $n_3$ were calculated from the absorbance changes at 450 and 432 nm, respectively (see text).*

III. Relative emission yield of the state P I $Q_1$, P I $Q_1^-$ and $P^+$I $Q_1$

For the interpretation of the curves shown in Figs. 5 and 7 we also determined the relative emission yield of suspensions with reaction centers in the states P I $Q_1$, P I $Q_1^-$ and $P^+$I $Q_1$. In Fig. 8 the inverse of the relative emission yield is plotted as a function of the fraction of traps, either by



accumulation of the reduced acceptor $Q_1^-$ (x) keeping $n_3$ = 0, or by accumulation of $P^+$ (•), keeping $n_2$ = 0. The fraction of reaction centers in the oxidized state $P^+$I $Q_1$, $n_3$ was determined for $n_2$ = 0, by measuring the absorbance increase at 432 nm due to the oxidation of the primary donor. As predicted by the trapping-limited matrix model (see introduction), the inverse of the emission yield is a linear fuction of the fraction of closed traps. The slope of the straight line is a measure for the relative trapping rate of a trap in the state $P^+$I $Q_1$ or P I $Q_1^-$. Because of the short lifetime of the reaction center bacteriochlorophyll triplet ($\tau_t$ ≈ 10 ns), the fraction of traps in the triplet state ($P^T$I$Q_1^-$) is negligible in the weak actinic light used. The open symbols (o) represent the relative emission yield as a function of the traps $P^+$I $Q_1$ accumulated in the light at intensities above 25 mW/cm².

In whole cells of R. rubrum, we also determined the emission yield for a number of redox states of the quinone acceptor $Q_2$, $n_3$ = 0.
Fig. 9 (upper trace) shows the 450 nm absorbance change induced by a series of saturating 602 nm dye laser flashes in whole cells of R. rubrum S1, in the presence of the electron donor DAD. The dark-adapted cells were flushed with air to obtain aerobiosis prior to the experiment. simultaneuously both the total bacteriochlorophyll emission F (lower trace) and ΔF/F were detected by using weak 603 nm continuous light. No significant magnetic field-induced emission change was found independent the number of flashes (see discussion).

## DISCUSSION

The absorbance difference spectrum induced by 603 nm continuous light (Fig. 3B) is, apart from a red shift of the 320 and 365 nm bands, very similar to the absorbance difference spectrum of ubisemiquinone-10 minus ubiquinone-10 in methanol as reported by Bensasson and Land [25] and confirms

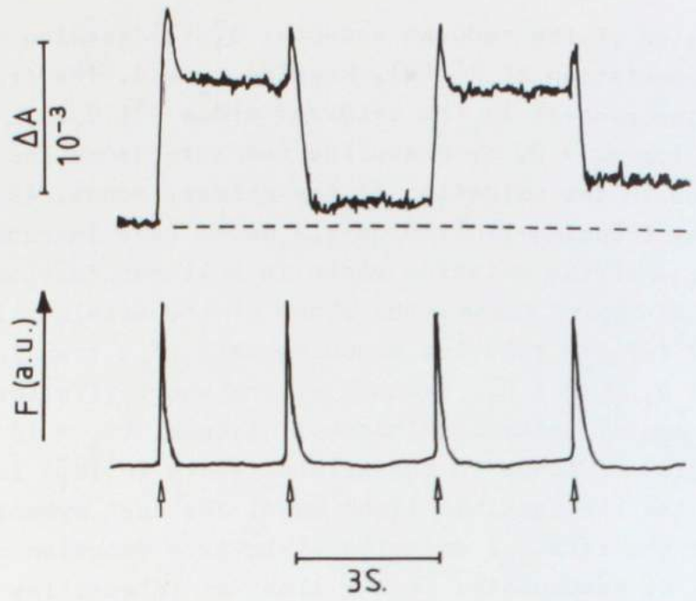


*Fig. 9. Upper trace: kinetics of the 450 nm absorbance changes induced by a 602 nm dye laser flash in whole cells of R. rubrum in the presence of 10 mM DAD, 0.20 mM Na-ascorbate and 200 µs gramicidin under aerobic conditions. Sample was darkadapted during 10 minutes prior to illumination. Lower trace: total bacteriochlorophyll emission detected at 905 nm with weak continuous 603 nm measuring light.*

the conclusion in an earlier report concerning the identity of the first quinone acceptor in isolated reaction centers of Rps. sphaeroides by Slooten [3]. The spectrum of Fig. 3B presumably contains no contributions from the redox changes of other quinones than $Q_1$, because the secondary electron transport from $Q_1$ to $Q_2$ was blocked by orthophenanthrolin. In a previous paper we concluded that presumably the magnetic field-induced emission only occurred if the acceptor $Q_1$ was reduced [16]. Indeed a magnetic field-induced emission change was detected only if the absorbance changes shown in the spectrum of Fig. 3B were observed, which shows that



both the absorbance changes at 450 nm and the emission change ΔF can be used to establish the redox state of $Q_1$. At excitation light intensities beyond 25 mW/cm² (see Fig. 3C) the absorbance difference spectrum indicates the accumulation of the oxidized primary donor while the reduced quinone acceptor $Q_1$ becomes oxidized.

The absorbance difference spectrum found at an excitation light intensity of about 45 mW/cm² is very similar to that found in whole cells of R. rubrum S1 (without additions) 50 µs after a saturating xenon flash [30] which has been ascribed to the oxidation of the primary donor $P_{890}$. In contrast to the experiments performed at intensities below 25 mW/cm², the reduction of $P^+$ seems to become the limiting reaction at these light intensities. The explanation for this phenomenon in which accumulation of $P^+$ and of $Q_1^-$ depends upon the excitation light intensity is not trivial and may be due to a secondary light-induced reaction which does not depend upon the concentration of $Q_1^-$.

Fig. 3D shows the gramicidin sensitive part of the light induced absorbance difference spectrum at a saturating light intensity of 45 mW-cm². The spectrum can be ascribed to electrochromic shifts of the bacteriochlorophyll and carotenoid absorbance bands. In whole cells the shifts only disappeared completely after addition of 200-250 µM gramicidin. In chromatophores 1-5µM gramicidin sufficed to eliminate the electrochromic changes. Due to the preparation technique of chromatophores (French Press) the Cytochrome c (the natural electron donor of the primary donor P [30]) concentration is low as compared to that in intact cells. In addition a relatively high concentration of the electron donor DAD was present in the samples studied and the cyclic electron transport via $Q_2$ and cytochrome b is probably blocked by orthophenanthroline. Therefore it seems unlikely that absorbance changes due to the reduction or oxidation of cytochromes are part of the spectrum shown in Fig. 3D.

In chromatophores of R. rubrum in the presence of dithionite a membrane potential is induced upon addition of ATP while $\Delta F_{max}/F$ decreases and $H_{\frac{1}{2}}$ increases [24]. Addition of gramicidin restored the initial shape and amplitude of the saturation curve of the magnetic field-induced emission change. The absorbance difference spectrum of the reduction of $Q_1$ (Fig. 3B) was affected by electrochromic shifts if no gramicidin was added. However, upon addition of gramicidin no change of $\Delta F_{max}/F$ or $H_{\frac{1}{2}}$ is detected, neither in samples chemically reduced by 5 mM dithionite nor in the samples with blocked secondary electron transport by orthophenanthroline. Apparently the electrochromic shift present in our samples without gramicidin (Fig. 3D) is not correlated with a large membrane potential which affects both $\Delta F_{max}/F$ and $H_{\frac{1}{2}}$ as was observed in the presence of ATP [24].

If the pigment system would consist of identical 'separate' units, i.e. units each containing a single reaction center and its associated antenna molecules without the possibility of energy transfer between the units, then a linear relationship would attain between the emission change and the number of reaction centers in the state P I $Q_1^-$. The non-linear curves shown in Fig. 5A and 5B thus show that energy transfer between units occurs. This can be explained by means of the model of Fig. 2, where no barriers exist between the various photosynthetic units.

The $H_{\frac{1}{2}}$ values of the saturation curves of the stimulated emission decrease as the number of traps P I $Q_1^-$ increases (Fig. 6). In an experiment under similar conditions in which the emission decay after a weak 30 ps flash was measured in the nanosecond range, it was found that the lifetime of the recombination luminescence increases as a function of the fraction $n_2$ of traps P I $Q_1^-$ (Van Bochove, A.C., Kingma, H. and Van Grondelle, R., unpublished results). Both these effects thus indicate an increase of the lifetime of the radical pair [23]. A decrease of the rate constant $k_s$ (Fig. 1) by the formation of a light-induced membrane potential will induce such an increase of the lifetime of $(P^+I^-)$ [24].



However, all experiments were done in the presence of gramicidin preventing the built-up of a significant membrane potential.

A second possibility occurs if an important fraction of the radical pair $(P^+I^-)^S$ decays via the singlet excited states (P* and BChl*) (see Fig. 1). The decay rate of the radical pair will then be significantly smaller and the lifetime longer if most of the traps are in the state P I $Q_1^-$ when compared with most of the traps in the state P I $Q_1$. A calculation of the increase in lifetime, as a function of $k_s$ and other parameters, will be given elsewhere (Van Bochove, A.C., Kingma, H. and Van Grondelle, R., in preparation).

The linear relation between the inverse relative emission yield and the fraction of traps in the state P I $Q_1^-$ of $P^+I\ Q_1$, respectively (Fig. 8), supports the hypothesis that the antenna system in reduced whole cells of R. rubrum is organized as a matrix [28]. In the state P I $Q_1^-$ the emission is for an appreciable part delayed fluorescence (luminescence), and its yield appears to be lower than the prompt fluorescence in the state $P^+I\ Q_1$, because apparently the losses (probably mainly caused by triplet formation) are higher than those caused by fluorescence quenching by $P^+$. For an estimation of the ratios of the probabilities $P_{ek}$ in Fig. 2 the value of the emission yield of the state $P^+I\ Q_1$ ($n_3 = 1$) suffices. The emission yield in R. rubrum is about 40 - 50% (data not given) of the yield of Rps. sphaeroides, which is about 0.25/18 = 0.014 (the lifetime of fluorescence in the state $P^+I\ Q_1$ *in vivo* is 0.25 ns [26] and the natural lifetime is about 18 ns [27]). From eq. (3) we find for $n_3 = 1$:

$$\frac{1}{\Phi_e} = (n_o P_{1o} + P_{13})/n_o P_{eo} = \frac{1}{0.007} = 143$$

Furthermore we can write:

$$P_{eo} = \frac{k_f}{k_f + k_1 + k_h}$$

where, $k_f$, $k_h$ and $k_1$ are the rate constants of emission, energy transfer and loss processes of an excited antenna bacteriochlorophyll molecule. Further assuming that $k_1 = 5\ k_f$, $k_h >> k_1$, $n_o = 50$ and $k_f = 1/18\ ns^{-1}$ we find:

$$P_{13} = 138\ n_o k_f/k_h = 138 \times 50 \times 5.6 \times 10^7/k_h = 3.9 \times 10^{11}/k_h$$

So, if the reaction center in the state $P^+I\ Q_1$ is an irreversible trap, the rate constant of trapping would be about $3.9 \times 10^{11} s^{-1}$. Since $\phi_e\ (n_3 = 1) \simeq 3.4\ \phi_e\ (n_1 = 1)$, we find $P_{11} \simeq 3.4\ P_{13} = 1.3 \times 10^{12}/k_h$ ($k_h > 10^{12}\ s^{-1}$; Van Grondelle et al., in preparation). In a similar way we find $P_{12} = 8.0 \times 10^{11}/k_h$. Assuming that $P_{1o} = 5\ k_f/k_h = 2.8 \times 10^8/k_h$ and using the experimental result of Fig. 7 that $\phi_t\ (n_2 = 1) = 0.13$ we find using eq. (5) $P_{t2} = 0.13 \times (n_o P_{1o} + P_{12}) = 1.1 \times 10^{11}/k_h$. The relative magnetic field-induced emission change $\Delta\phi_e/\phi_e$ measures $1.5 \times 10^{-2}$ which, in our model, is ascribed to a decrease $\Delta P_{12}$ of $P_{12}$ and with eq. (3) results in

$$\Delta P_{t2} = \Delta P_{12} \simeq 0.015 \times (P_{12} + n_o P_{1o}) \simeq 1.3 \times 10^{10}/k_h$$

Similarly we find that $\Delta\phi_t/\phi_t \simeq \Delta P_{t2}/P_{t2} \simeq 0.12$ which reasonably agrees with the experimental result of 0.10. We are now able to calculate the emission and triplet yield as a function of the redox state of the reaction center in the curves in Figs. 5, 7, 8 and 9. Apparently, application of the matrix model used yieldsa good agreement with the experimental findings. The fluorescence yield of the state P I $Q_1$ ($n_1 = 1$) is $1/3.4 \times 0.017 \simeq 0.25\%$. The total loss in the antenna will then be $5 \times 0.25\% + 0.25\% = 1.5\%$ ($k_1 = 5\ k_f$). So 98.5% of the excitation energy may be trapped in the reaction center.



A calculation of the efficiency of $Q_1$ reduction, based upon the initial slope of the light-induced change at 330 nm results in an efficiency of 92% ± 6%. Because carotenoid excitation induces a secondary magnetic field emission change in the antenna, the model presented can only be applied if excitation of bacteriochlorophyll is established (see chapter IV).

In whole cells and chromatophores of R. rubrum it was shown that after darkadaptation a special molecule of ubiquinone UQ, closely bound to the reaction center was reduced by ubisemiquinone by flashes of an odd number [32, 33, 34, 35]. In R. rubrum such changes only occurred under aerobic conditions. The oscillations of the 450 nm absorbance changes can be explained by means of the following scheme [5, 17, 30].

$$Q_1Q_2UQ \xrightarrow[200\ ps]{h\nu_1} Q_1^-Q_2UQ \xrightarrow[1\ ms]{} Q_1Q_2^-UQ \xrightarrow[200\ ps]{h\nu_2} Q_1^-Q_2^-UQ \xrightarrow[1\ ms]{} Q_1Q_2^=UQ$$

$$Q_1Q_2^=UQ \xrightarrow[0.5\ \mu s]{2H^+} Q_1Q_2UQH_2$$

The light-induced absorbance changes due to oxidation or reduction of the quinones involved are very similar [5,25]. The absorbance increase after the first flash (Fig. 9) can be ascribed to the reduction of $Q_1$ within 200 ps followed by the reduction of $Q_2$ within about 1 msec. Upon the second flash a second electron is transported via $Q_1$ to $Q_2^-$ followed by a two-electron reduction of UQ and subsequent protonation. The netto reaction after the second flash, $Q_1Q_2^-UQ \xrightarrow{h\nu 2} Q_1Q_2UQH_2$ results in an absorbance decrease at 450 nm. Therefore the oscillations seen at 450 nm reflect the subsequent reduction and oxidation of $Q_2$. The lower trace of Fig. 9 shows that the emission yield does not depend upon the redox state of $Q_2$. In addition no magnetic field induced emission change could be detected within 1 °/oo of the emission, neither after the first nor after the second flash.

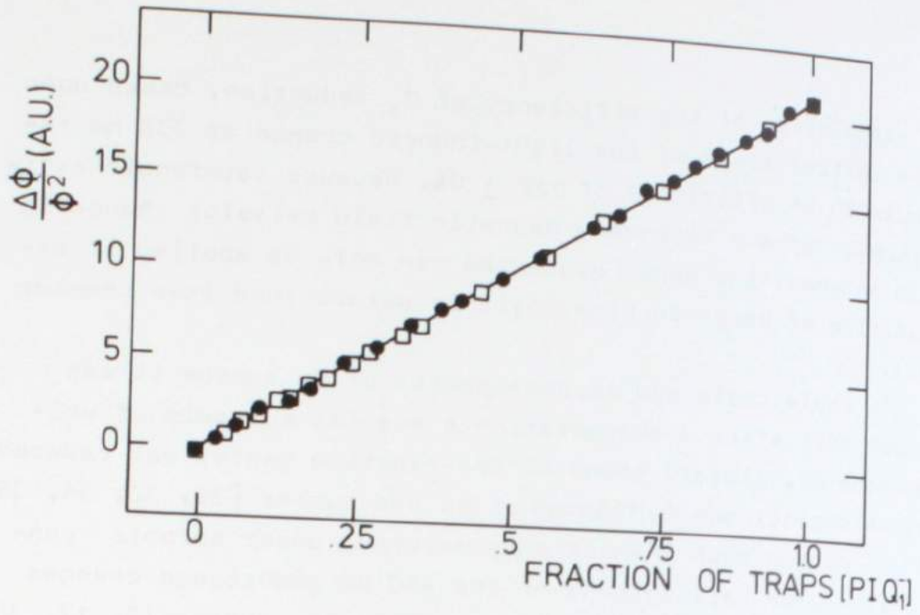


*Fig. 10. The magnetic field induced emission increase $\Delta\phi$ in a saturating field divided by the square of the relative emission yield $\phi^2$ as a function of $n_2$ at low 603 nm excitation light intensities (●. $n_3 = 0$) and at high light intensities (□ , $n_1 = 0$). Conditions as in Fig. 3A (see text).*

Fig. 10 shows $\Delta\phi/\phi^2$ as a function of $n_2$ under reducing conditions ($n_3 = 0$) and under oxidizing conditions ($n_1 = 0$). For both conditions identical linear relationships are found, as predicted by eq. (4).

From relative measurements of $\Delta\phi$ and $\phi$ for a certain suspension, $n_1$, $n_2$ and $n_3$ are determined as follows. First four calibration measurements are performed. All reaction centers are forced into the state $n_2 = 1$ by one of the methods described [16], and $\phi$ and $\Delta\phi$ are determined. Similarly $\phi$ is determined for the states $n_1 = 1$ and $n_3 = 1$. For the suspension in an unknown state, $n_2$ is directly found from the following equation, obtained from eq. (4):



$$n_2 = \frac{\Delta\phi/\phi^2}{(\Delta\phi/\phi^2)_{n_2=1}} \qquad (6)$$

In order to obtain the unknown $n_1$, $n_3$ is eliminated from eqs. (1) and (3):

$$1/\phi = a + bn_1 + cn_2 \qquad (7)$$

in which a, b and c are constants. The three calibration measurements of $\phi$ for $n_1 = 1$, $n_2 = 1$ and $n_3 = 1$ result in three equations, from which the three unknowns a, b and c are easily obtained . Eq. (7) now is solved for the only remaining $n_1$, and $n_3$ is then obtained from eq. (1).

## CONCLUSION

Within the relatively high precision of the experiments our results indicate that in whole cells of R. rubrum a matrix type of energy transfer between various photosynthetic units occurs. The model presented here , which is a generalization of several theoretical considerations reported earlier [28], is in excellent agreement with the experimental findings. In a suspension of cells or chromatophores, $n_2$ can be found from eq. (4) by simultaneous measurements of $\Delta\phi$ and $\phi$. Subsequently $n_1$ and $n_2$ can be determined from eqs (1) and (3). The method is especially suited to determine the concentration of $Q_1^-$ under steady state conditions in continuous light. Moreover, the emission yield is less sensitive to scattering changes than are measurements of absorbance changes. In addition we found that the emission yield $\phi$ and $\Delta\phi$ do not depend on the redox state of the second quinone acceptor $Q_2$.

REFERENCES


1 Clayton, R.K. and Straley, S.C. (1970) Biochem. Biophys. Res. Comm. 38, 1114-1119

2 Clayton, R.K. (1972) Proc. Natl. Acad . Sci. USA 69, 44-49

3 Slooten, L. (1972) Biochim. Biophys. Acta 275, 208-218

4 Kakuno, T., Hosoi, K., Higuti, T. and Horio, T. (1973) J. Biochem. 74, 1193-1203

5 Parson, W.W. (1978) in The Photosynthetic Bacteria (Clayton, R.K. and Sistrom, W.R., eds.), pp. 455-469, Plenum Press, New York

6 Fajer, J. Brune, D.C., Davis, M.S., Forman, A. and Spaulding, L.D. (1975) Proc. Natl. Acad. Sci. USA 72, 4956-4960

7 Vredenberg, W.J. and Duysens, L.N.M. (1963) Nature 197, 355-357

8 Holmes, N.G., Van Grondelle, R., Hoff, A.J. and Duysens, L.N.M. (1976) FEBS Lett. 70, 185-190

9 Van Grondelle, R., Holmes, N.G., Rademaker, H. and Duysens L.N.M. (1978) Biochim. Biophys. Acta 503, 10-25

10 Dutton, P.L., Kaufman, K.J., Chance B. and Rentzepis, P.M. (1975) FEBS Lett. 60, 275-280

11 Shuvalov, V.A. and Klimov, V.V. (1976) Biochem. Biophys. Acta 440 ,587-599

12 Blankenship, R.E., Schaafsma, T.J. and Parson, W.W. (1977) Biochim. Biophys. Acta 461, 297-305

13 Hoff, A.J., Rademaker, H., Van Grondelle, R. and Duysens, L.N.M. (1977) Biochim. Biophys. Acta 460, 547-554

14 Voznyak, W.M., Elfimov, E.I. and Proskuryakov, I.I. (1978) Doklady Akad. Nauk. SSSR. 242, 1200-1203

15 Rademaker, H., Hoff, A.J. and Duysens, L.N.M. (1979) Biochim. Biophys. Acta 546, 248-255

16 Kingma, H., Duysens, L.N.M. and Peet, H. (1981) in Photosynthesis (Akoyunoglou, G., ed.), Vol. III, pp.981-988, Balaban Int. Science Services, Philadelphia, Pa.
This work chapter III





17 Parson, W.W. and Case, G.D. (1970) Biochim. Biophys. Acta 205, 232 -245

18 Vermeglio, A. and Clayton, R.K. (1977) Biochim. Biophys. Acta 461, 159-165

19 Visser, J.W.M. (1975), Thesis, University of Leiden

20 Rademaker, H., Hoff, A.J., Van Grondelle, R. and Duysens, L.N.M. (1980) Biochim. Biophys. Acta 592, 240-257

21 Rockley, M.G., Windsor, M.W., Cogdell, R.J. and Parson, W.W. (1975) Proc. Natl. Acad. Sci. USA 72,2251-2255

22 Kaufman, K.J., Dutton, P.L., Netzel, T.L., Leigh, J.S. and Rentzepis, P.M. (1975), Science 188, 1301-1304

23 Werner, H.J., Schulten, K. and Weller, A. (1978) Biochim. Biophys. Acta 502,255-268

24 Van der Wal, H.N., Van Grondelle, R., Kingma, H. and Van Bochove, A.C. (1982) FEBS Lett. 145, 155-159

25 Bensasson, R. and Land, E.J. (1973) Biochim. Biophys. Acta 325, 175-184

26 Sebban, P. and Moya, I (1983) Biochim. Biophys. Acta 722, 436-442

27 Connoly, J.S., Samuel, E.B., Janzen, A.F. (1982) Photochem. Photobiol. 36, 565-574

28 Duysens, L.N.M. (1978) in Chlorophyll Organization and Energy Transfer in Photosynthesis, Ciba Foundation Symposium 61 (new series), pp. 323-340 Elsevier/North-Holland, Amsterdam

29 Van Grondelle, R., Romijn, J.C. and Holmes, N.G. (1976) FEBS Lett. 72, 187-192

30 Van Grondelle, R., Duysens, L.N.M. and Van der Wal, H.N. (1976) Biochim. Biophys. Acta 449, 169-187

31 De Grooth, B.G. and Amesz, J. (1977) Biochim.Biophys. Acta 462, 237-246

32 Wraight, C.A. (1977) Biochim.Biophys. Acta. 459, 525-531

33 Vermeglio, A. (1977) Biochim.Biophys. Acta. 459, 516-524

34 Barouchy, Y and Clayton, R.K. (1977) Biochim. Biophys. Acta 462, 785-788

35 De Grooth, B.G., Van Grondelle, R., Romijn, J.C. and Pulles, M.P.J. (1978) Biochim. Biophys. Acta 503, 480-490

CONCLUDING REMARKS

In this chapter I will discuss the temperature dependencies of the emission yield, the triplet yield, the relative MFT and the relative MFE; in the preceeding chapters these phenomena have been discussed more or less separately. In addition, I will discuss the losses of excitation energy, that occur in the antenna complex as well in the reaction center. A model will be presented, which describes the various processes occurring in purple bacteria and which shows that under reducing conditions, the major losses occur in the reaction center.

a. The temperature dependence

In chapter IV it was shown that the temperature dependence of the MFE can be explained by a simple model (see Fig. 1), assuming that the decay of $(P^+I^-)^S$ partly occurs via the thermally activated recombination rate constant $K_s$. In order to fit the experimental data, it was found that:

$$\frac{\Delta k_t}{k_T} = \frac{(k_t(H=0)-k_t(H_{max}))}{k_t(H=0)+k_g} = .02 \pm .01$$

$$\text{with } k_T = k_t(H=0)+k_g$$

which, together with MFT = .10 leads to $k_g \approx 5k_t$.

In chapter VI it was shown that, at room temperature, the relation between MFE, MFT, $\Phi_e$ and $\Phi_t$ and the redox state of the RC can be explained by energy transfer in a matrix of antenna molecules, in which most losses occur in the RC. It was calculated that the probability of losses in the RC of reduced cells of R. rubrum S1, $P_{L2}$ is about 6 to 7 times larger than the probability of triplet formation, $P_T$. If we assume that, upon BChl excitation, the major losses in the antenna occur by triplet formation via intersystem crossing of $BChl^*$ with a yield of .12 (see chapter V), then the efficiency of trapping of the exci-



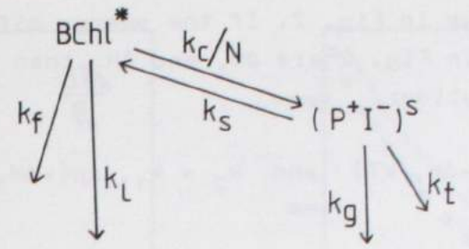


*Fig. 1. Scheme of energy and electron transfer in R. rubrum S1 under reducing conditions. $BChl^*$ is the first excited singlet state of bacteriochlorophyll. $(P^+I^-)^S$ is the singlet state of the radical pair, P is the reaction center bacteriochlorophyll dimer and I is an electron acceptor, N is the number of antennabacteriochlorophyll molecules per reaction center. (See text).*

tation energy by the RC is 0.8 - 0.87. This disagrees with the trapping efficiency calculated in chapter VI of more then 0.98, based on the fluorescence lifetime of 250 ps, reported by Sebban et al. [1]. In the following I assume that the trapping efficiency of the reduced RC is about 0.85.

In chapter IV it is observed, that the relative MFE is about the same in reduced RC's and reduced cells/chromatophores, which again indicates that a major part of the losses occur in the RC and not in the antenna complex.

However the temperature dependence of the relative MFT and $\Phi_t$ can not be explained by the model described in the chapters IV and VI (see also chapter V), which results in a maximum RC-triplet yield of 0.15 at low temperature, in contrast to our observations $\Phi_t$ = .4 at 100 K (chapter V). I therefore propose a refinement of the model of energy transfer, which incorporates the simple model depicted in Fig. 1, but also accounts for the temperature behaviour of the MFT and $\Phi_t$ and might explain the different temperature dependencies of the recombination luminescence and the radical pair state $(P^+I^-)^S$[2]. The energy trans-

fer scheme is shown in Fig. 2. If the energy difference between the states shown in Fig. 2 are $\Delta H_1$ and $\Delta H_2$, then according to the Boltzmann distribution:

$$k_s = k_c.\exp(-\Delta H_1/kT) \quad \text{and} \quad k_2 = k_1.\exp(-\Delta H_2/kT)$$

It is assumed that at room temperature the losses will occur via $k_{gl}$, but that the losses upon cooling due to a decrease of $k_2$, will predominantly occur via $k_t$, resulting in an increase of $\phi_t$. Then because of the effective decrease of charge recombination of $(P^+I^-)^{S1}$ to the ground state P I, a decrease of the relative MFT occurs (3).

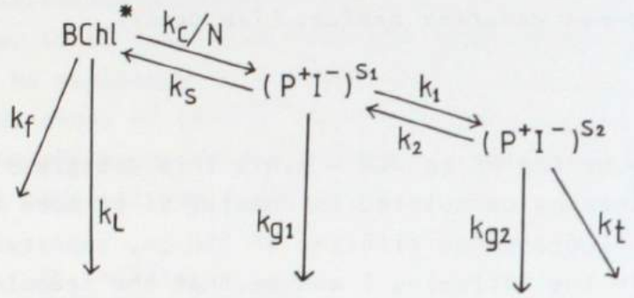


*Fig. 2. Expanded scheme of energy transfer in R. rubrum S1, under reducing conditions. $(P^+I^-)^{S1}$ is a singlet state of the radical pair, which rapidly decays into a singlet state $(P^+I^-)^{S2}$ of lower energy. The states may differ in conformation, e.g. have a different $\Delta H$. Further symbols as in Fig. 1 (see text).*

The relative MFT, MFE, $\Phi_t$ and $\Phi_e$ can now be calculated as a function of the temperature by solving the first order differential equations, that describe the electron and energy transfer scheme depicted in Fig. 2. The results are shown in Fig. 3.



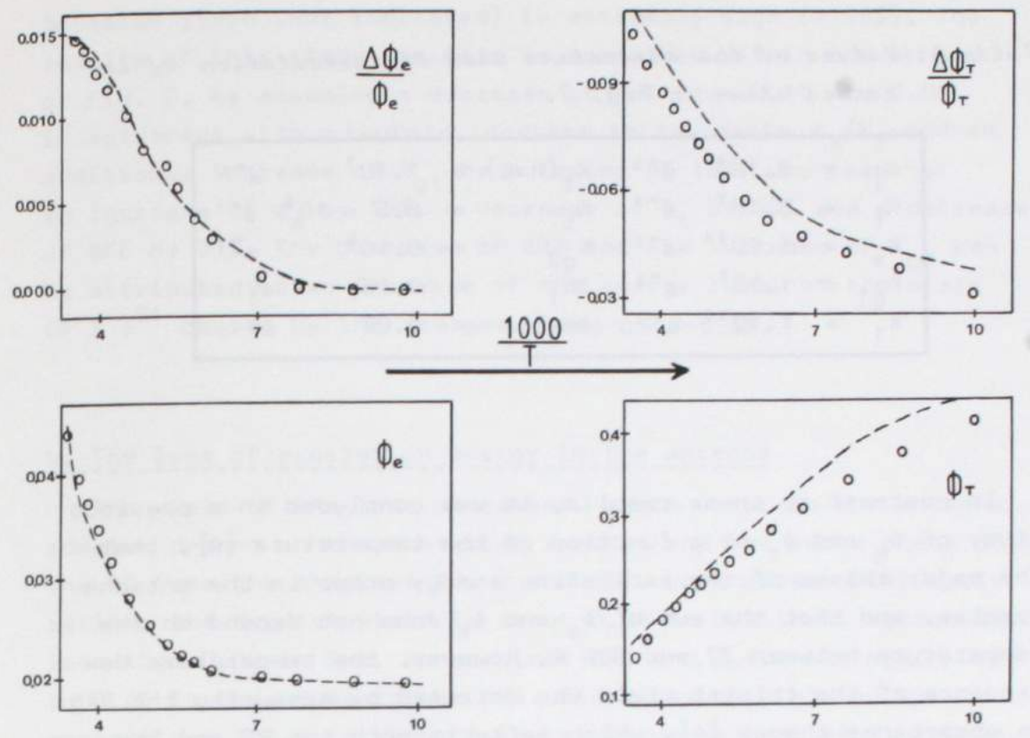


*Fig. 3. The maximum MFE, $(\Delta\Phi_e/\Phi_e)$, the maximum relative MFT $(\Delta\Phi_7/\Phi_7)$, the emission yield $\Phi_e$ and the triplet yield $\Phi_7$ as a function of the inverse of the temperature 7. The open symbols represent the experimental data, obtained in cells of R. rubrum S1 in the presence of 5 mM dithionite. $\Phi_e$ was detected at 905 nm, $\Phi_7$ was detected at 430 nm. Excitation wavelength 603 nm, magnetic field strength 1400 Gauss. The curves are calculated from the differential equations of Fig. 2, using the parameters of Table 1.*

Within about 20% all data can be fitted, using the parameters shown in Table 1.

*Table 1. Values of the parameters used for calculation of the curves shown in Fig. 3.*

| | | | | | | | |
|---|---|---|---|---|---|---|---|
| $K_1$ | = | $2.10^8$ | $s^{-1}$ | $K_t(H=0)$ | = | $1.10^7$ | $s^{-1}$ |
| $K_f$ | = | $5.10^7$ | $s^{-1}$ | $K_t$ | = | $8.5 \times 10^6$ | $s^{-1}$ |
| $K_e$ | = | $1.10^{11}$ | $s^{-1}$ | $K_{g2}$ | = | $5.10^6$ | $s^{-1}$ |
| $K_{g1}$ | = | $1.10^9$ | $s^{-1}$ | $\Delta H_1$ | = | 0.10 | eV |
| $K_1$ | = | $1.10^{10}$ | $s^{-1}$ | $\Delta H_2$ | = | 0.07 | eV |

In contrast to these results, it was concluded in a previous study of $\phi_e$ and $\phi_t$ as a function of the temperature [4], that the major losses of the excitation energy occur in the antenna complex, and that the sum of $\phi_e$ and $\phi_t$ does not depend on the temperature between 77 and 300 K. However, the temperature dependence of the triplet yield was detected by measuring the 545 nm absorbance change [4], which reflects both the RC and the antenna triplet yield (see chapter V). In addition, it was assumed that the RC-triplet yield at 77 K was 1.0, in contrast to our observations (chapter V) and those of Schenk et al. [5], that lead to a RC-triplet yield of 0.4 to 0.5 at 77 K. Therefore it seems no longer justified to neglect the recombination rate constant $K_{g1}$ to the ground state. An analysis of our results shows that the sum of $\Delta\phi_e$ and $\Delta\phi_t$ increases significantly upon cooling.

In another study [6], we showed that in reduced chromatophores of R. rubrum S1, a transmembrane potential can be induced by adding ATP to the sample. This results in an increase of $\phi_e$ by about 17%, a decrease of the RC-triplet yield by about 37% and a decrease of the RC-associated MFE by about 33%. Again neglecting a significant contribution of $K_g$, these phenomena were explained by an increase of $K_s$ by a factor of two, which agrees reasonably well with the observed decrease of the recombination luminescence lifetime [6]. However, the calculated



emission yield (not indicated) is extremely high (> 15%). The results of this study can also be explained within the scheme of Fig. 2, by assuming a decrease of ΔH1 from 0.10 to 0.08 in agreement with a twofold increase in the ratio $K_s/K_c$ and an additional increase of $K_{g1}$ by a factor of two, who lead to an increase of $\phi_e$ by 19%, a decrease of $\phi_t$ by 35% and a decrease of MFE by 31%. The decrease of ΔH1 and the increase of $K_{g1}$ can be attributed to an increase of the energy level of the state $(p^+I^-)^{S1}$ caused by the transmembrane potential.

b. The loss of excitation energy in the antenna

The yield of the loss processes, which occur in the antenna complex depend on the bacterial species and the redox state of the RC (see the chapters IV, V and VI). Upon direct BChl excitation, the triplet yield is about 0.06 to 0.2 in R. rubrum S1, less than 0.02 in Rps. sphaeroides G1C and 2.4.1 but again 0.13 to 0.25 in Rps. sphaeroides R26. The emission yield of Rps. sphaeroides 2.4.1 is about twice as large as that of R. rubrum. So it appears that the ratio of losses by triplet formation and the losses by emission is not constant. It could be that, in contrast to what is generally assumed, the ratio of the various decay routes in a BChl molecule is varying from species to species.

Alternatively it may be that due to a process not taken into account, 90% of the triplets formed are not observed by us, particularly so because in Rhodopseudomonas sphaeroides R26 again a high antenna triplet yield was obtained.

Upon carotenoid excitation in R. rubrum 60 - 70% of the excitations are lost, half of which by $CAR^T$ formation via the fission process, the remaining 30% is transfered to bachteriochlorophyll. In Rps. sphaeroides G1C and 2.4.1 more than 90% of the excitations are transferred to bacteriochlorophyll and no significant amount of $CAR^T$ is formed via fission of $CAR^*$. The most plausible explanation is that energy transfer from $CAR^*$ to BChl in R. rubrum is much slower than in Rps. sphaeroides G1C and 2.4.1. Alternatively it may be that only 30% of the carotenoid

molecules in R. rubrum are in a configuration that allows singlet excitation transfer although all the carotenoid molecules seem available for singlet excitation quenching once they are in a triplet state [7] . Sofar the decisive conclusion can be drawn concerning these and possible other alternatives.

In R. rubrum about 30% of the excitation energy absorbed by carotenoid molecules remains unaccounted for. Tentatively we suggest that this 30% is either lost by direct internal conversion of $CAR^{*}$ to the ground state or by a direct recombination of the triplet pair to the ground state. The latter case would imply that the formation of a single triplet state from the triplet pair state, which is always formed in a singlet state, requires time to dephase the spins of the pair. This process would be magnetic field dependent and might explain the large change of the triplet yield in a magnetic field as opposed to the small change of the emission yield.

In Rps. sphaeroides only less than 10% of the excitation energy absorbed by carotenoid molecules can not be retraced. Again internal conversion from $CAR^{*}$ may occur, a triplet pair may be formed, which now does not result in a single triplet state, may be due to a shorter lifetime of the radical pair. A magnetic field allows some triplet to be formed via a fission of $CAR^{*}$.

REFERENCES


1. Sebban, P. and Moya, I (1983) Biochim. Biophys. Acta 722, 436-442
2. Van Bochove, A.C., van Grondelle, R., Hof, R.M. and Duysens, L.N.M. (1983) Proc. VIth Int. Congr. Photosynth. Brussels, in the press
3. Werner, H.J., Schulten, K. and Weller, A. (1978) Biochim. Biophys. Acta 502, 255-268
4. Holmes, N.G., van Grondelle, R., Hoff, A.J. and Duysens, L.N.M. (1976) FEBS Lett. 70, 185-190
5. Schenck, C.C., Blankenship, R.E. and Parson, W.W. (1982) Biochim. Biophys. Acta 680, 44-59
6. Van der Wal, H.M., van Grondelle, R., Kingma, H. and van Bochove, A.C. (1982) FEBS Lett. 145, 155-159
7. Rademaker, H. (1980) Thesis, University of Leiden.




SUMMARY


Immediately after the absorption of light energy in the photosynthetic apparatus, energy losses occur by emission and radiationless decay processes like triplet formation. Previous studies have shown that some of the energy transfer and loss processes depend on the strength of a magnetic field and the redox state of the reaction center. In this thesis, a study of the magnetic field dependence of the bacteriochlorophyll emission and triplet formation is described, which was performed in order to gain more insight in the primary processes of photosynthesis. In addition, a new method is described to determine the redox state of the reaction center in intact cells in continuous light.

Chapter I is a concise introduction of the bacterial photosynthesis and gives a description of the general issue of this thesis.

Chapter II gives a description of the apparatus designed for this study, i.e. two high resolution spectrophotometers for measuring the absorption and emission changes in a sinusoidally magnetic field.

In chapter III the relation is described between the redox state of the reaction center and the magnetic field induced emission (MFE) in several purple bacteria. It is concluded that the magnetic field dependence and the amplitude of the MFE strongly depend upon (i) the redox state of the first quinone electron acceptor, (ii) the bacterial strain and (iii) the type and integrity of the sample used, i.e. cells, chromatophores or isolated reaction centers. In order to improve the reproducibility of the measurements, the growth conditions of the bacteria were standardized by using a continuous culture, described in chapter II.

Chapter IV gives a description of the MFE as a function of

the temperature, the excitation and emission wavelength and the magnetic field strength in cells, chromatophores and isolated antenna and reaction center preparations. Two mutual independent, magnetic field dependent processes are distuinguished. One process is associated with the charge recombination of the radical pair in the reaction center and is only observed, if the first quinone electron acceptor has been reduced. The second process occurs in the antenna complex and is only observed upon direct carotenoid excitation.

In chapter V these two processes are further characterized by measuring the effect of a magnetic field upon the triplet formation in the antenna and the reaction center as a function of the temperature, the excitation and detection wavelength. The magnetic field dependence of the antenna associated process can be ascribed to homofission of the first excited singlet state of an antenna carotenoid molecule, resulting in a intermediate triplet pair state,which decays into a single carotenoid triplet state or to the ground state. This process appears to be independent of the temperature. By competition between the singlet energy transfer from the carotenoid to bacteriochlorophyll and the magnetic field dependent decay into the triplet pair state, the prompt fluorescence yield is indirectly affected by a magnetic field. The reaction center associated process depends upon the temperature and is discussed in terms of the radical pair mechanism.

In chapter VI the reaction center associated MFE and the triplet yield are measured as a function of the fractions of reaction centers in the various states. First the light-induced absorbance difference spectrum of the reduction of the first quinone acceptor $Q_1$ was determined in cells of R. rubrum S1.
Based on simultanuous measurements of the MFE, the emission and the triplet yield and, by absorbance spectroscopy, the fractions of reaction centers in the various redox states, a quantitative method could be developed to determine the redox state of $Q_1$ from the MFE and the emission yield under steady state conditions



in continuous light. In addition, it was shown that, regardless of the redox state of the reaction center, the energy transfer can be described by a matrix model.

In chapter VII a quantitative analysis was made of the temperature dependence of the emission yield, the reaction center triplet yield and the reaction center associated magnetic field dependencies. From the results obtained together with those obtained in the chapters IV, V and VI, it was concluded that also under reducing conditions, the major losses of the excitation energy occurs in the reaction center.
In R. rubrum S1, upon carotenoid excitation, about 60 to 70 percent of the energy absorbed is not transfered to the reaction center; about half of this energy is lost by fission via the triplet pair state into carotenoid triplet formation.

SAMENVATTING

In het fotosynthetisch apparaat treden direkt na de lichtabsorptie energieverliezen op door emissie en stralingloos verval zoals bijvoorbeeld de vorming van tripletten. Eerdere studies hebben laten zien, dat sommige verlies- en electronoverdrachtsprocessen afhankelijk zijn van een magneetveld en van de redox toestand van het reactiecentrum. In dit proefschrift is een studie beschreven van de magneetveldafhankelijkheid van de bacteriochlorophyllemissie en de tripletvorming, teneinde meer inzicht te krijgen in de primaire processen van de fotosynthese. Tevens is een methode beschreven om de redox-toestand van het reactiecentrum in intacte cellen in continu licht te bepalen.

Hoofdstuk I bevat een beknopte introduktie tot de bacteriële fotosynthese en de probleemstelling, die tot dit onderzoek geleid heeft.

Hoofdstuk II geeft een beschrijving van de apparatuur, ontwikkeld ten behoeve van het hier beschreven onderzoek, waaronder een tweetal spectrofotometers voor het meten van de absorptie- en emissieveranderingen in een sinusoidaal gemoduleerd magneetveld.

Hoofdstuk III bevat een beschrijving van een studie naar de relatie tussen de redox-toestand van het reactiecentrum en van de magneetveld gestimuleerde emissie (MFE) in verscheidene purper bacteria. Uit dit onderzoek blijkt, dat de magneetveldafhankelijkheid en de amplitude van de MFE sterk afhankelijk zijn van (i) de redox-toestand van de eerste quinone electron acceptor $Q_1$, (ii) de bacteriestam, (iii) het preparaat, i.e. cellen, chromatoforen of geïsoleerde reactiecentra.

Teneinde de reproduceerbaarheid van de metingen te verbeteren, werden de groeicondities van de bacteriën gestandaardiseerd met behulp van een continue cultuur, beschreven in hoofdstuk II.



Hoofdstuk IV beschrijft het vervolg van de studie van de MFE, nu in afhankelijkheid van de temperatuur, de excitatie- en emissiegolflengte, zowel in cells, chromatoforen, geïsoleerde antenna- als reactiecentrum-preparaten. Het blijkt, dat er twee onderling onafhankelijke, magneetveld-afhankelijke processen te onderscheiden zijn. Eén proces is geassocieerd met de ladingsrecombinatie van het radicaal paar in het reactiecentrum en wordt alleen waargenomen als de eerste quinone acceptor $Q_1$ gereduceerd is. Een tweede magneetveld afhankelijk proces vindt plaats in het antennacomplex alleen bij caroteenexcitatie.

In hoofdstuk V zijn de twee processen verder getypeerd door de invloed van het magneetveld na te gaan op de tripletformatie in de antenna en in het reactiecentrum als funktie van de temperatuur, de excitatie- en detectiegolflengte. Het met de antenna geassocieerde proces kan toegeschreven worden aan homofissie van de eerste aangeslagen toestand van een antenne caroteenmolecuul, waarbij een triplet paar wordt gevormd, dat hetzij naar de grondtoestand vervalt of een caroteentriplet vormt. Dit proces blijkt onafhankelijk van de temperatuur te zijn. Door de competitie tussen de energie-overdracht van caroteen naar bachteriochlorophyll en de magneetveld-afhankelijke decay naar het triplet pair, wordt de prompte fluorescentie indirekt door een magneetveld beïnvloed. De met het reactiecentrum geassocieerde magneetveldafhankelijke processen zijn afhankelijk van de temperatuur. Deze worden bediscussieerd in het kader van de radicaal paar theorie.

In hoofdstuk VI zijn de met het reactiecentrum geassocieerde emissie, MFE, en de triplet yield gemeten als funktie van het aantal reactiecentra met geblokkeerd elektrontransport ($PQ_1^-$). Allereerst werd het licht geïnduceerde absorptie verschil spectrum ($Q_1^- - Q_1$) bepaald in cellen van R. rubrum S1. Door gelijktijdig de MFE, de emissie yield en, met behulp van absorptieverschilmeting, het aantal reactiecentra in verschillende redoxtoestanden te meten, kon een kwantitatieve methode ontwikkeld worden om de redox-toestan van $Q_1$ te bepane met behulp de MFE en de emissie yield. Voorts werd aangetoond dat, onafhankelijk van de redox-toestand van de reactiecentrum, de energie-over-

dracht plaatsvindt volgens het matrix model.

In hoofdstuk VII is een kwantitatieve analyse uitgevoerd van de temperatuursafhankelijkheid van de emissieyield, de reactiecentrumtripletyield en de daarmee geassocieerde magneetveldafhankelijkheden. Mede op grond van de resultaten beschreven in de hoofdstukken IV, V en VI, wordt geconcludeerd, dat bij BChl excitatie, het verlies aan excitatie energie onder gereduceerde omstandigheden voornamelijk in het reactiecentrum optreedt. In R. rubrum gaat bij caroteenexcitatie circa 60 - 70% van de excitatie energie niet naar het reactiecentrum. Minstens de helft van deze energie gaat hierbij verloren door fissionprocessen via het triplet paar en caroteen-tripletvorming.



CURRICULUM VITAE

Ik werd geboren op 3 oktober 1950 te Rotterdam, alwaar ik van 1963 tot 1968 het Charloise Lyceum bezocht. Na het behalen van het einddiploma HBS-B begon ik in 1971 met de studie Biologie aan de Universiteit van Amsterdam, waamee de basis voor mijn verdere studie van de Biofysica gelegd werd. In april 1975 heb ik het Candidaatsexamen Biofysica afgelegd, met als hoofdvakken Biologie en Natuurkunde.

Van augustus 1975 tot september 1976 heb ik in het kader van mijn doktoraal studie het bijvak Electronica gedaan bij het Natuurkundig Laboratorium van de Universiteit van Amsterdam. Vervolgens verichtte ik tot januari 1979 electrofysiologisch onderzoek naar spatiële eigenschappen van de retina van de goudvis bij de Vakgroep Medische Fysika onder leiding van Dr. N.A.M. Schellart en Prof. Dr. Ir. H.Spekreijse. In januari 1979 heb ik het doctoraal examen Biologie met als hoofdvak Biofysica afgelegd. Van 1 februari 1979 tot 1 februari 1983 was ik aangesteld als wetenschappelijk assistent bij de Vakgroep Biofysica van de Rijksuniversiteit Leiden, alwaar ik onder leiding van Prof. Dr. L.N.M. Duysens het in dit proefschrift beschreven onderzoek verrichtte. Per 1 december 1983 ben ik aangesteld als wetenschappelijk medewerker in vaste dienst bij de Capaciteitsgroep Keel-, Neus- en Oorheelkunde van de Rijksuniversiteit Limburg te Maastricht.

NAWOORD

Graag wil ik alle leden van de Vakgroep Biofysica, de mensen van de Algemene Dienst en vele anderen in het Huygens Laboratorium en niet te vergeten mijn o zo geduldige typiste heel erg bedanken voor de hulp en vriendschap, die zo nodig waren voor het tot stand komen van dit proefschrift.

ERRATA

| page | linenumber | wrong text | correct text |
|---|---|---|---|
| 38 | 28 | descrepancies | discrepancies |
| 40 | 6 | difference | differences |
| 41 | 10 | 21 | 21,45 |
| 41 | 25 | $p^F$ | $p^T$ |
| 42 | 6 | trytophan | tryptophan |
| 43 | 15 | $Mgcl_2$ | $MgCl_2$ |
| 45 | 31 | dit | did |
| 47 | 12 | (■) | (□) |
| 49 | 14 | 515 | 510 |
| 50 | legend 48 | ΔFmax | ΔF |
| 51 | legend 58 | 660 | 600 |
| 53 | 2 | 32 | 42 |
| 57 | 2 | ( ) | (●) |
| 72 | 34 | Franck and McGaan | Frank and McGann |
| 82 | 9 | — | add: (Chapter V) |
| 84 | ref.8 | chapter | chapter VI |
| 91 | 15 | $ACAR.X^T$ | $^TACAR.X^T$ |
| 102 | 17 | 14 | .14 |
| 122 | 6 | 15 | 20 |
| 122 | 21 | 15 | 20 |
| 123 | 1 | 8 | 36 |
| 124 | ref.12 | — | add: V78 p957-961 |
| 125 | ref.24 | — | add: 430, 83-93 |
| 125 | ref.31 | (1983) | (1982) Biochim.Biophys. |
| | | — | Res.Com. 106, 1310-1317 |
| 126 | 10 | 39. Phys. | Phys. |
| 126 | 11 | Lutz, | 40. Lutz, |
| 126 | ref.41 | — | add: Photobiochem.Photobiph. |
| | | — | 5, 139-150 |
| 127 | 5 | van Grondelle | van Grondelle* |
| 127 | 8 | Department | *Department |
| 151 | 11 | by | to |
| 167 | 3 | cells | cellen |
| 167 | 20 | bachteriochloro- | bacteriochloro- |
| 167 | 34 | toestan | toestand |
| 167 | 34 | bepane | bepalen |
| 167 | 34 | de MFE | van de MFE |

STELLINGEN

I

In de caroteen houdende stammen van de purperbacteriën Rhodospirillum rubrum en Rhodopseudomonas sphaeroides, kunnen twee onderling onafhankelijke door een magneetveld beïnvloedde processen onderscheiden worden. Deze processen vinden hun oorsprong in enerzijds de ladingsrecombinatie in het reactiecentrum en anderzijds de tripletvorming in de antenne.
(Dit proefschrift, hoofdstuk IV en V)

II

De magneetveldafhankelijkheid van de vorming van het antenna-caroteentriplet en de bacteriochlorofylemissie onder oxiderende omstandigheden in de purperbacteriën Rhodospirillum rubrum en Rhodopseudomonas sphaeroides kan verklaard worden door splitsing van de energie van de eerste aangeslagen singulet toestand van het antenna caroteen molecuul, waarbij een triplet-paar gevormd wordt bestaande uit de triplet toestand van twee gelijksoortige caroteenmoleculen.
(Dit proefschrift, hoofdstuk IV en V)

III

In de purperbacterie Rhodopseudomonas sphaeroides veroorzaakt een zwak magneetveld (250 gauss) een afname van de emissie en een sterker veld (1000 gauss) een toename van de emissie. De conclusies van Frank en McGann dat dit verschijnsel veroorzaakt wordt door processen in het reactiecentrum en niet plaatsvindt in de sphaeroideen houdende stammen van Rhodopseudomonas sphaeroides, zijn onjuist.
Frank,H.A. en McGann,W.J.(1983), Proc.VIth Int. Congr. Photosynth. Brussels, in the press.

IV

De energieoverdracht tussen de verschillende fotosynthetische units in de purperbacterie Rhodospirillum rubrum kan beschreven worden door een matrixmodel met ondiepe "traps". Bij bacteriochlorofyl-excitatie gaat slechts een klein deel van de excitatieenergie verloren in de antenne, ongeacht de redoxtoestand van het reactiecentrum.
(Dit proefschrift, hoofdstuk VI)

V

Aan de hand van de met het reactiecentrum geassocieerde en door een magneetveld gestimuleerde bacteriochlorofylemissie kunnen de fracties van de reactiecentra in de redoxtoestanden $PQ_1$, $P^+Q_1$ en $PQ_1^-$ in continu licht bepaald worden.
(Dit proefschrift, hoofdstuk VI)

VI

De temperatuursafhankelijkheid van de bacteriochlorofylemissie en de reactiecentrumtripletopbrengst in de purperbacterie Rhodospirillum rubrum kan in samenhang met de magneetveldeffekten niet verklaard worden met behulp van een eenvoudig model met de ladingsrecombinatie als enige temperatuursafhankelijke reactie, in tegenstelling tot eerdere conclusies.
R.van Grondelle (1978), proefschrift Universiteit van Leiden.
Dit proefschrift, hoofdstuk VII

VII

Het rendement voor energieconversie in bladeren kan met grote nauwkeurigheid en op eenvoudige wijze bepaald worden uit directe of indirecte (bijvoorbeeld fotoacoustische) metingen van de oppervlaktetemperatuur in gemoduleerd licht.
Bults,G., Horwitz,B.A., Malkin,S. and Cahen,D. (1981)
FEBS letters, Vol. 129-1, 44-46

VIII

Modellen voor het cyclisch electronentransport in de purperbacterie Rhodopseudomonas sphaeroides via het zogenaamde cytochroom b - cytochroom c - quinol oxidoreductase, die gebaseerd zijn op een "Q-cyclus" - mechanisme, kunnen de waargenomen kinetiek van de reductie en oxidatie van cytochroom b na een korte flits na een korte donkerperiode niet verklaren.
Crofts,A.R. and Wraight,C.A. (1983)
Biochim. Biophys. Acta 726, 149-185.
Dutton,P.L. and Prince,R.C. (1978)
in Photosynthetic Bacteria, Plenum press, New York, 525-570 (R.K. Clayton and W.R.Sistrom, Eds.).

IX

Een van de bezwaren tegen het confessionalisme in de politiek is dat de neiging bestaat op geloof berustende voorschriften betreffende bepaalde zaken, zoals bijvoorbeeld de anti-conceptie en de zondagsrust, ook op te leggen aan andersdenkenden.

X

De betrekkelijkheid van de vrijheid van mensen in Nederland wordt uitstekend geïllustreerd door het feit dat vrije huisvestiging slechts in beperkte mate mogelijk is.

XI

Het bespelen en het gebruik van dubbelbladige rietinstrumenten, zoals de hobo of de fagot, zou aanmerkelijk gemakkelijker en beter zijn, als het tijdrovende en slecht reproduceerbare "rieten-snijden" zou komen te vervallen door het ontwikkelen van kunststofrieten van goede kwaliteit en duurzaamheid.

XII

Het toepassen van rood als kleur voor signaallichten in het verkeer en foto- en detectie-apparatuur (bijvoorbeeld met licht emitterende dioden), moet zo mogelijk vermeden worden gezien de relatief lage roodgevoeligheid van het visuele systeem van de mens.

XIII

Vervang in de komende jaren de in de diverse instituten en laboratoria aanwezige minicomputers door talrijke microcomputers met een verplaatsbaar veelzijdig multilasting, multiuser operating system (bijvoorbeeld Unix), met als beschikbare talen C, Basic, Fortran en Pascal.